NASA/
SP-20230004376
Version 1.0.3
June 2024

NASA Methodology for Physics of Failure-Based Reliability Assessments Handbook

OSMA Reliability & Maintainability
Washington, D.C. 20546

https://sma.nasa.gov

NASA/
SP-20230004376
Version 1.0.3

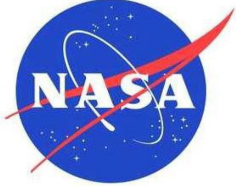

NASA Methodology for Physics of Failure-Based Reliability Assessments Handbook

National Aeronautics and Space Administration
NASA Headquarters

Washington, D.C. 20546

June 2024

NASA STI Program ... in Profile

Since its founding, NASA has been dedicated to the advancement of aeronautics and space science. The NASA scientific and technical information (STI) program plays a key part in helping NASA maintain this important role.

The NASA STI program operates under the auspices of the Agency Chief Information Officer. It collects, organizes, provides for archiving, and disseminates NASA's STI. The NASA STI program provides access to the NASA Aeronautics and Space Database and its public interface, the NASA Technical Report Server, thus providing one of the largest collections of aeronautical and space science STI in the world. Results are published in both non-NASA channels and by NASA in the NASA STI Report Series, which includes the following report types:

TECHNICAL PUBLICATION. Reports of completed research or a major significant phase of research that present the results of NASA Programs and include extensive data or theoretical analysis. Includes compilations of significant scientific and technical data and information deemed to be of continuing reference value. NASA counterpart of peer-reviewed formal professional papers but has less stringent limitations on manuscript length and extent of graphic presentations.

TECHNICAL MEMORANDUM. Scientific and technical findings that are preliminary or of specialized interest, e.g., quick release reports, working papers, and bibliographies that contain minimal annotation. Does not contain extensive analysis.

CONTRACTOR REPORT. Scientific and technical findings by NASA-sponsored contractors and grantees.

CONFERENCE PUBLICATION. Collected papers from scientific and technical conferences, symposia, seminars, or other meetings sponsored or co-sponsored by NASA.

SPECIAL PUBLICATION. Scientific, technical, or historical information from NASA programs, projects, and missions, often concerned with subjects having substantial public interest.

TECHNICAL TRANSLATION. English-language translations of foreign scientific and technical material pertinent to NASA's mission.

Specialized services also include creating custom thesauri, building customized databases, and organizing and publishing research results.

For more information about the NASA STI program, see the following:

Access the NASA STI program home page at *http://www.sti.nasa.gov*

E-mail your question via the Internet to help@sti.nasa.gov

Fax your question to the NASA STI Help Desk at 443-757-5803

Phone the NASA STI Help Desk at 443-757-5802

Write to:

NASA STI Help Desk
NASA Center for Aerospace Information
7115 Standard Drive
Hanover, MD 21076-1320

Acknowledgements

This document would not have been developed without the sponsorship and support of NASA OSMA Reliability & Maintainability Technical Fellow and the expertise and insights of the development team and NASA PoF handbook contributors. Therefore, the following individuals are acknowledged and are extend NASA's appreciation:

Sponsor:

Anthony DiVenti (NASA-OSMA)

Development Team:

Nancy J Lindsey (NASA-OSMA/GSFC)
Jeffrey Dawson (NASA- GSFC)
Hallie Marsh (NASA-GRC)
Douglas Sheldon (JPL)
Lionel-Nobel Sindjui (NASA- GSFC)

Contributors and reviewers from across NASA, JPL, and Aerospace:

Robert Abelson (JPL)
Jonathan Barth (NASA-GSFC)
Michael J. Campola (NASA-GSFC)
Milton C. Davis (NASA-GSFC)
Brendon J. Foran (Aerospace)
Mathew Forsbacka (NASA-OSMA)
David G. Gilmore (Aerospace)
Eric W. Grob (NASA-GSFC)
Matt Humberstone (NRC)
Ray Ladbury (NASA-GSFC)
John Lane (NRC)
Henning W. Leidecker (NASA-GSFC)
Jung Moon (JPL)
Daniel S. Mcguinness (NASA-GSFC)
Ching Ng (NRC)
David J. Petrick (NASA-GSFC)
Todd Paulos (JPL)
Jeannette Plante (NASA-OSMA)
John Ratliff (JPL)
Steven Rickman (NASA-JSC)
Kaitlyn Ryder (NASA-GSFC)
Bhanu Sood (NASA-GSFC)
John Welch (Aerospace)
Edward J. Wyrwas (NASA-GSFC)

Document History Log

Status	Document Revision	Change Number	Approval Date	Description
Baseline				Initial Release

Table of Contents

Section Page

1. Introduction ... 7
1.1 Scope ... 7
1.2 Background ... 7
1.3 Physics of Failure Foundations ... 10

2. Handbook Application Guide ... 11

3. Empirical Methods ... 13
3.1 Empirical Reliability Approach ... 13
3.2 Statistical Modeling Analysis (Bayesian, etc.) ... 13
3.2.1 Exponential ... 14
3.2.2 Weibull ... 15
3.2.3 Normal ... 17
3.2.4 Lognormal ... 18
3.2.5 Binomial ... 19
3.2.6 Bayesian Statistical Inference for Updating Failure Rates ... 20
3.3 Peck's Temperature-Humidity Relationship Prediction ... 21
3.4 Accelerated Performance Analysis ... 22
3.4.1 Arrhenius ... 22
3.4.2 Inverse Power ... 24
3.4.3 Coffin-Manson ... 26
3.4.4 Zhurkov Equation ... 28
3.4.5 Palmgren ... 28
3.4.6 Eyring Modeling ... 29

4. Deterministic Methods ... 30
4.1 What are Deterministic Methods? ... 30
4.2 Electromigration in Electrical and Electronic Components ... 31
4.2.1 Metals ... 31
4.2.2 Migration ... 32
4.2.3 The Fluctuation-Dissipation Theorem ... 33
4.2.5 Electromigration in Interconnection Traces and Vias in Integrated Circuits ... 35
4.3 Thermal Physics of Failure ... 36
4.3.1 Thermal Failure Mechanisms ... 37
4.3.2 Thermally Induced Failure Likelihood ... 40
4.3.3 Thermal Failure Uncertainties ... 41
4.4 Fluid (Pipe Flow) ... 42
4.5 Electromagnetics (Wave Optics, Ray Optics, AC/DC) ... 42
4.6 Structural Analysis Modeling ... 42
4.6.1 Fatigue Analysis ... 42
4.6.2 Damage Tolerance (Fracture) Analysis ... 44

4.6.3 Creep 46
4.7 Acoustics 46
4.8 Chemical (Batteries and Fuel Cells, Electrodeposition, Chemical Reactions) 46
4.9 Radiation Physics of Failure in Semiconductors 47
4.9.1 Total Ionizing Dose (TID) 47
4.9.2 Total Non-Ionizing Dose (TNID)/Displacement Damage Dose (DDD) 49
4.9.3 Single Event Effects (SEE) 50
4.9.4 Analysing Radiation-Induced Failure Modes 53
4.9.5 Instantaneous Radiation Failures (Single Event Effects) 58
4.9.6 Likelihood of Radiation Induced Failure Summary 62

5. Formulating Comprehensive Results from Individual Pof Findings 64

5.1 Aggregation Approach 64
5.2 Inclusive Relationship Finding Aggregation 65
5.3 Complementary Relationship Finding Aggregation 67
5.4 Interrelated Relationship Finding Aggregation 68
5.5 Aggregation Assistance 68

6. The Evolution of the Physics of Failure 69

6.1 NASA Path Forward 69
6.2 Technology Support 69
6.3 Advanced Technology Infusion 70
6.3.1 Artificial Intelligence (AI), Machine Learning (ML) 70
6.3.2 Data Monitoring/Analytics 71
6.4 Methodology Innovation Infusion 72
6.4.1 Remaining Useful Life (RUL) 72
6.4.2 Digital Twin Usage 75

Appendix A. Definitions 76

Appendix B. Case Study Chart 78

Appendix C. References 85

Appendix D. Acronyms 90

List of Figures

Figure 1. PoF Application Across the NASA Life Cycle……………………………………………...9
Figure 2. PoF Handbook Analysis Guide Use Cases……..…………………………………………12
Figure 3. Weibull Distribution Probability Density…………………………………….…………...16
Figure 4. Normal Distribution Probability Density………..……………………………………...17
Figure 5. Lognormal Distribution Probability Density…………………………….…………...18
Figure 6. Binomial Probability……………...……..…………………………………….………......19
Figure 7. Bayes' Theorem…………………………………………………………….………………20
Figure 8. Arrhenius Acceleration Factors………………………...…………………….………………23
Figure 9. Operational Life Versus Stress………………...…………………………….…………..25
Figure 10. Stress Versus Lifetime………………………………………………….……….................26
Figure 11. Stress Versus Number of Cycles…………………………………….………...........29
Figure 12. Process of TID Damage Occurring in MOS Structures……………….……………….48
Figure 13. Potential Isolated Defects in Silicon Induced by Incident Particle…….…...…………..49
Figure 14. Ion Entering the Depletion Region of a Biased P-N Junction…..…..………………....51
Figure 15. Piece-Part RHA Methodology..……………………………………………...………54
Figure 16. TID Probability Distributions……………………………..……………………...….56
Figure 17. TID Failure Distribution for SFT2907A Bipolar Transistor…..……………………......56
Figure 18. Failure Probabilities for the SFT2907A Transistor…..…………………………………57
Figure 19. Example of a SEE Severity Flow Diagram.……………………………………...…59
Figure 20. LET Spectra for the ISS Orbit at Solar Min (black) and Solar Max (red).…………...60
Figure 21. Calculating Single Event Rates.…………………………………………………......61
Figure 22. Determination of TID/TNID/DDD Failure Likelihood.……………………………......62
Figure 23. Determination of DSEE Failure Likelihood.……………………………………..…....63
Figure 24. Determination of NDSEE Failure Likelihood.………………….………………….....63
Figure 25. Potential Probability Relationship States for Aggregate Findings...……...…………...65
Figure 26. Potential Probability Combination Methods....……………………………….……...66
Figure 27. Conceptual Definition of RUL.....………………………………………………….......73
Figure 28. Remaining Useful Life (RUL) Systems Modeling Approaches…………...….……......74
Figure 29. Probabilistic Parameters of a Hidden Markov....…………………………….……....74

List of Tables

Table 1. Statistical Modeling Tools 13
Table 2. Weibull Probability Density Function Characteristics 16
Table 3. Failures Seen in Electronic Box Parts for Different Thermal Test Failure Mechanisms38

Introduction

1.1 Scope

The scope of the book is to introduce basic Physics of Failure (PoF) concepts and give example case studies of their application to all systems and materials at NASA. It presents the foundations of PoF approaches to reliability applications at NASA. This book is intended to be a living document, with updates as time progresses.

1.2 Background

Since an item's reliability or longevity is dependent not only on its design but also on how it is used, manufactured, and tested, and the stresses it has or will experience, all these factors must be considered in failure likelihood assessments. While an item's design will introduce susceptibilities (e.g., radiation tolerance, stress) to internal or external failure mechanisms, how well it is made (its inherent or assured/screened quality or compliance with accepted standards) and age will also affect its reliability. A high-quality part may have fewer inherent susceptibilities to use or stresses (e.g., thermal, voltage, current, age exposure, mechanical, environmental), but manufacturing or installation issues may increase susceptibility or exacerbate existing weaknesses. Therefore, in reliability analysis, it is essential to consider all contributions to failure, and their underlying physics, to accurately formulate failure rates and assess probabilities.

Reliability assessments based on the underlying physics are more effective at contributing to the following than reference failure rates/probabilities, and may be applied across the life cycle of a NASA project, as shown in Figure 1 [Diventi, 2020]:

- Defining the environmental conditions or controls that components or assemblies will experience or need to function, by simulating the actual hardware operation in its assumed and refined stress states. For example, if the proposed thermal or radiation stress an item will experience is applied to it in a model/digital twin PoF analysis (or in test) and it induces failure, then the final design or operations concept, or Fault-Detection- Isolation-and-Recovery (FDIR), can be adjusted to prevent or mitigate the potential for that failure mechanism.

- Optimizing environmental/qualification or stress tests to excite susceptibilities or verify susceptibilities are mitigated. For example, if a model/digital twin and analytical physics methods are used to identify an item's susceptibilities to certain stresses, these can be the focus of testing.

- Enabling better design tradeoffs via enhanced sensitivity studies, where design parameters such as materials, geometries, configurations, and stresses may be easily manipulated in computational models and optimized prior to fabrication and use. For example, if the analysis shows that there will be a thermal distortion leading to a connection loss then the

material or item planned can be revised before acquired or fabricated.

- Improving hardware life and reliability estimations with failure mechanism or mode likelihood accuracy by applying simulated stress conditions to physics-based failure models. For example, the reliability of an item may decrease if the stresses proposed show any of its failure mechanism or mode's likelihood increasing with in situ conditions and planned exposures.

- Prompting the definition of operational monitoring and diagnostics, operational and contingency procedures, and FDIR designs to mitigate effects of failure potentials/likelihoods.

- Informing production acceptance and operations decision-making by providing failure risk/likelihood updates based on modelled/simulated nonconformance or failure conditions. For example, if a product is found to be noncompliant with defined optimal manufacturing standards, its reliability should be reassessed using this new in situ knowledge. The PoF risk/likelihood results in this case would then be able to be factored into use-as-is or replacement decisions and to target updates to operational and contingency procedures.

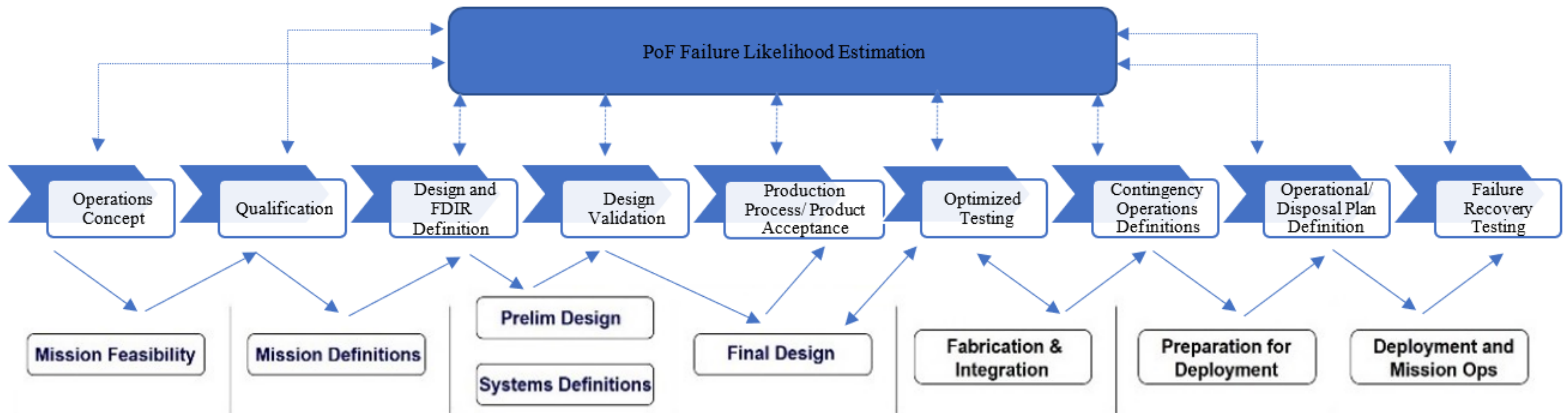

Figure 1. PoF Application Across the NASA Life Cycle

1.3 Physics of Failure Foundations

Applying physics to failure likelihood assessment is called Physics of Failure (PoF). PoF is a reliability technique that leverages the knowledge of an in-situ design or condition of an item with an understanding of the stresses, processes and mechanisms that induce its failure to predict its reliability. Those predictions can be given as a point estimate or as a number within statistical confidence bounds. However, it cannot be assumed that any single PoF model will represent an item's full likelihood of failure. Therefore, it is essential that all failure mechanisms or modes that are possible be characterized through the application of experimental or theoretical physics principles to develop a full understanding of the reliability or life of any item or system.

Characterization of failure rates using experimental physics is an empirical approach to PoF. Empirical PoF (Chapter 3) uses an item's/system's degradation and failure data from experiencing physics, during field studies, operations, and lab tests, and statistical methods to predict the reliability. These statistics use mathematical models to describe (or approximately match) the observed physical behavior to develop a probability density function that can be used to extrapolate further performance or like-system performance. Not all systems have this type of data, therefore PoF also includes characterization of failure probabilities with theoretical physics or a deterministic approach to PoF (Chapter 4). Deterministic PoF uses modeling to analyze the dominant failure mechanisms due to accumulated damage from stress, erosion, diffusion, and corrosion leading to sudden or eventual failure. To develop a valid forecast of an item or system's reliability or performance risks, the reliability analyst must select the best PoF method or methods for deriving or updating failure rates.

This may mean that a single method or multiple methods would be utilized or should be used concurrently with, or in lieu of, reference rates (e.g., handbook data) to capture a complete reliability forecast. When multiple likelihoods are derived or available for an item or system with, or in lieu of, reference rates, it will be necessary to combine those findings. Considering this, it is important for the analyst to evaluate the magnitude, independence, and dependence of each likelihood result on a case-by-case basis so that an aggregated or all-inclusive failure likelihood can be attained. Independence or dependence can be assessed using the cause-and-effect relationship established in a Failure Mode Effects and Criticality Analysis (FMECA), Fault Trees, or similar method [Fischer, 2016]; (Chapter 5).

2. Handbook Application Guide

This handbook can be used to inform reliability analysts on PoF methods, determine data needs for deriving failure rates using physics, guide analyses, and to further the PoF methods. It explains PoF methods, with supporting case study references, across three sections: Empirical (based on historical data or experimental physics), Deterministic (based on theoretical physics or physical modeling of failure mechanisms), and Aggregation (deterministic and empirical estimation combination methods). This means that users can concentrate on any of the experimental or theoretical physics application methods for reliability individually, research data needs to define tests or experiments that support PoF-based failure rate development, or review sections and select the best PoF method or methods for deriving or updating failure rates based on system physics and data available.

Readers can concentrate on any of the many experimental or theoretical physics application methods for reliability individually since each method is explained in an independent section and supported with case study references. In the Empirical section, the reader will be able to discover the data needs and usefulness of statistical models (Exponential, Weibull, Normal, Lognormal, and Binomial) and parametric modeling approaches (Bayesian Inference) to convert the physics experienced (test or operational physical phenomena/experiences) by a system into a forecast of reliability. In the Deterministic Methods section, the reader will see how predicted stresses and theoretical physics relationships can be used to forecast reliability or system-usage risks (or usage changes).

Analysts and data creators can research or define tests/experiments to acquire the data needed to develop PoF-based likelihoods of failure by referring to the Empirical and Deterministic sections of this handbook. For example, use/failure data will be needed for Bayesian Inference; material fatigue properties will be needed for fatigue/structural analysis; and Total Ionizing Dose and Radiation Susceptibility will be needed for radiation-induced failure probabilities.

PoF analysts can use this handbook to review and select the best PoF method or methods for deriving or updating failure rates based on the data available, until all failure mechanisms or modes that are possible for the scenario of interest are characterized through physics (see figure 2). This will mean the analyst will need to fully define the analysis goal and data available first, then test or use differing methods with that data and system/stress modelling to develop likelihood estimates. These results will then need to be validated as plausible and that they fully capture the scenario of interest and aggregated (Chapter 5) as warranted.

While the physics underpinning of the PoF practices are well defined, the methodologies and supporting infrastructures to determine the likelihood of failure are continually being refined and advanced (Chapter 6). Therefore, readers are encouraged to provide the team with updates, modifications, and case studies that may extend or enhance the concepts discussed in this handbook and advance the community of practice.

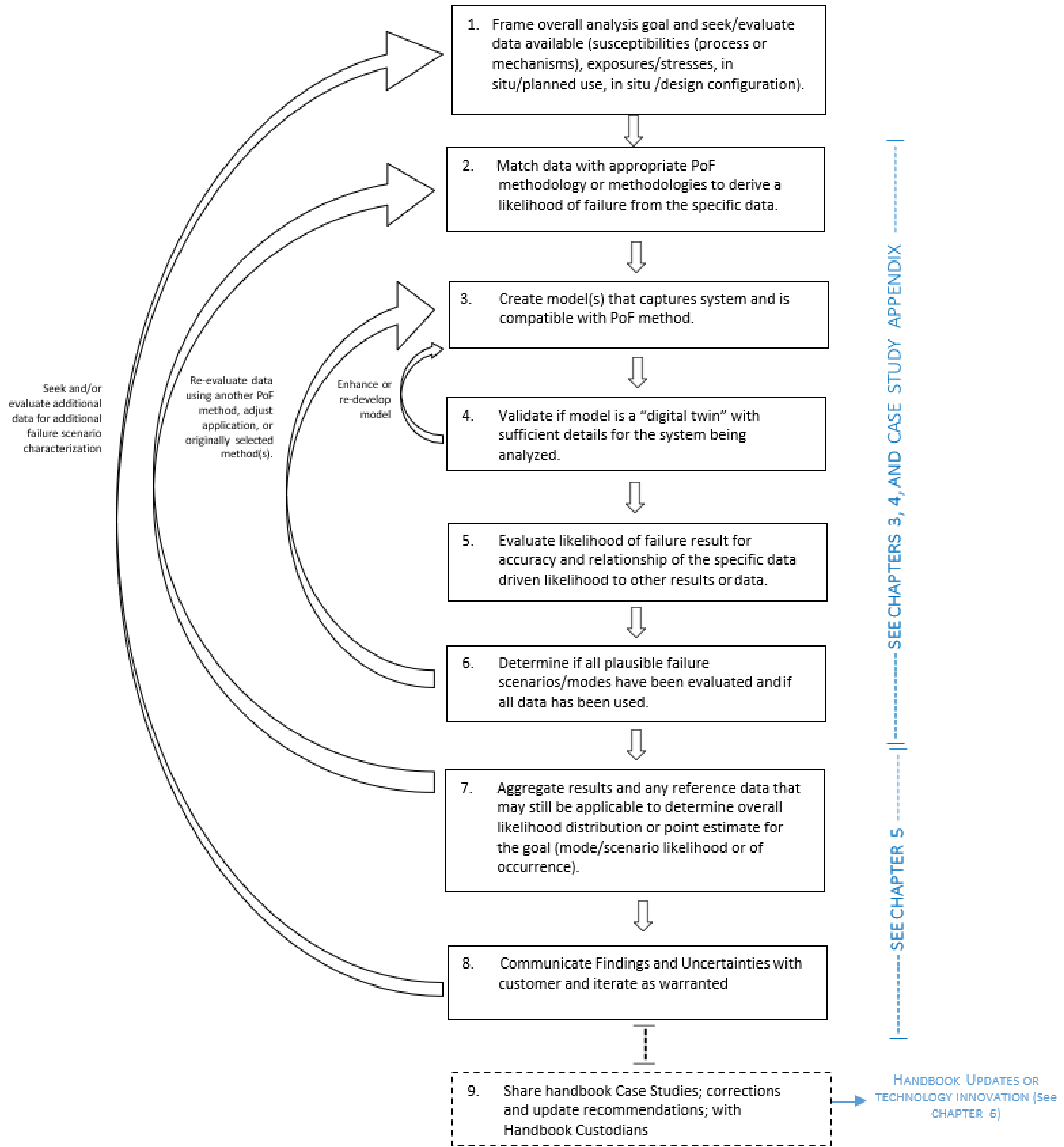

Figure 2. PoF Handbook Analysis Guide Use Cases

3. Empirical Methods

3.1 Empirical Reliability Approach

Failure rate empirical estimation methods used in science and engineering are often based on past data. Using component failure data from field studies, warranty claims, and lab tests, reliability engineers have developed techniques to predict the reliability of systems. Statistical modeling (empirical methods) has at its foundation experimental physics processes and are discussed in these sections.

For additional insights and guidance, see case studies digitally linked here.

3.2 Statistical Modeling Analysis (Exponential, Weibull, Lognormal, Normal, Binomial, Bayesian)

Statistical modeling analysis is the discipline of using statistical models to describe the physical behavior of components and systems. These items range from piece parts (e.g., Electrical, Electronic and Electromechanical Parts), components (e.g., reaction wheels), subsystems (e.g., spacecraft avionics systems), or systems (e.g., spacecraft and instruments). Statistical analysis is particularly useful when deterministic models (e.g., Force = Mass x Acceleration), further described in chapter 4, that can adequately describe the relationship between variables or inputs and corresponding outputs of the items under evaluation do not exist.

This chapter addresses five fundamental statistical models (Exponential, Weibull, Normal, Lognormal, and Binomial) and one more-advanced parametric modeling approach (Bayesian Inference), which enables physical data to be combined with engineering knowledge about the item of interest. Each of these primary statistical modeling and analysis techniques is described below:

Table 1. Statistical Modeling Methods

Section	Title and Description	Application Examples
3.2.1	Exponential	Describing end-item characteristics such as reliability or lifetime estimates associated with constant failure rates
3.2.2	Weibull	Describing end-item characteristics such as reliability or lifetime estimates associated with increasing, constant, or decreasing failure rates
3.2.3	Normal	Characterizing the capability or quality of manufacturing processes in meeting defined upper and lower end item specification limits

Section	Title and Description	Application Examples
3.2.4	Lognormal	Characterizing knowledge or epistemic uncertainty associated with likelihood estimates Describing the likelihood of extreme or rare event occurrences
3.2.5	Binomial	Describing end-item characteristics such as reliability or lifetime estimates associated with only two end states (success/failure).
3.2.6	Bayesian Inference	Describing end-item characteristics such as reliability or likelihood estimates when the availability of corresponding physical system data is extremely limited at the onset of analysis activities

For additional insights and guidance, see case studies digitally linked here.

3.2.1 Exponential

The exponential distribution is often used in reliability analysis to model both the failure rates of individual components and of complete systems. The exponential distribution is a special case of the gamma distribution. It is also related to the Poisson distribution (a property which is useful in queuing theory) since the occurrence of failures in the exponential distribution is a Poisson process. The exponential distribution has a constant failure rate over time; as time increases, the probability of failure during a given time interval increases.

While theoretical discussions of the statistical characteristics of the exponential distribution and the theoretical basis for how it is used to model the reliability of systems involve complex mathematical derivations, in reliability practice use of the exponential distribution is simple. Given a component with a constant failure rate (under given conditions) of λ failures per unit of time, the probability of successful operation for a given time t is:

$$p(\text{success}) = e^{-\lambda t}.$$

For a simple reliability model of a series of components, any one of which if failed would result in system failure, an exponential model can be used (even when some of the individual components have failure rates determined by other distributions). In this case, the equation for n components is:

$$R_S(t) = \prod_{i=1}^{n} R_i(t) = \prod_{i=1}^{n} e^{-\lambda_i t}$$

where λ_i is the failure rate of the ith component.

For individual components, use of the exponential distribution is justified when infant failures have been eliminated and the wear-out phase of time is not expected to be encountered during the usage lifetime of the item. For components that degrade over the usage time, the Weibull (or another) distribution is more appropriate.

For additional insights and guidance, see case studies digitally linked here.

3.2.2 Weibull

NASA uses Weibull analysis to estimate reliability when there is sufficient relevant failure data available for an item that might not have a constant failure rate, i.e., an item that might have an increasing failure rate (wear out) or a decreasing failure rate (infant mortality). Analysis is performed in two steps; estimation of Weibull parameters based on failure (and success) data and probability calculation based on those parameters.

Developing a Weibull-based model to replace handbook data can have multiple benefits. Weibull can specifically model different stages of the hardware life (i.e., infant mortality, constant failure rate, and wear out). And if the reliability data used is specific to (or just more similar to) the hardware and/or environment being analyzed than handbook/manufacturer data, then a more accurate calculation can be achieved. However, misapplication of Weibull analysis can result in misleading estimations. Reliability data that includes insufficient data (particularly very few failures) is difficult to accurately analyze with Weibull, leading to very little confidence in the calculations. Similarly, mixing reliability data from across multiple hardware life stages can affect calculation accuracy and confidence.

The Probability Density Function (PDF) for a two-parameter Weibull distribution is

$$f(t) = \theta\beta t^{\beta-1} e^{-\theta t^{\beta}}$$

where $t > 0$, $\theta > 0$, $\beta > 0$. Below is a graph of the probability density as a function of time, *t,* for different values of β and θ. β is the shape parameter. In reliability analysis, θ is the characteristic life, the time when 0.632 of items in a lot will have failed. When $\beta = 1$, the Weibull distribution reduces to the exponential distribution.

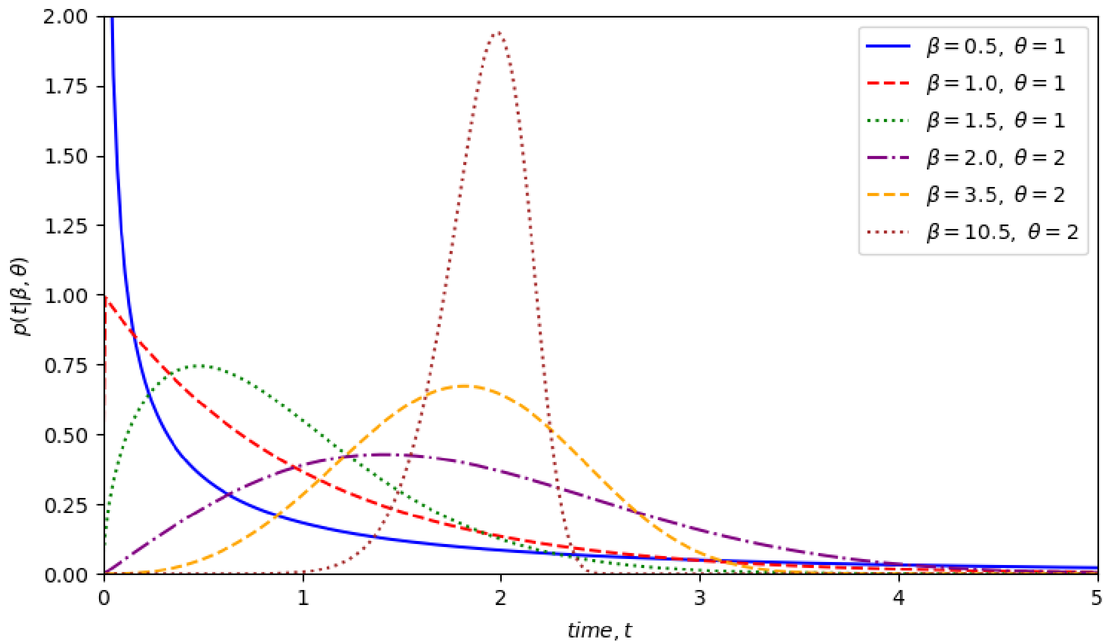

Figure 3. Weibull Distribution Probability Density

Weibull PDF characteristics are summarized in this table (adapted from table 4.2, Tobias & Trindade, 1995, p. 87).

Table 2. Weibull Probability Density Function Characteristics

Shape, β	pdf characteristic	Failure rate
$0 < \beta < 1$	exponentially decreasing from infinity	decreasing
$\beta = 1$	exponential distribution	constant
$\beta > 1$	rises to peak then decreases	increasing
$\beta = 2$	Rayleigh distribution	linearly increasing
$3 \leq \beta \leq 4$	has normal (Gaussian) distribution shape	rapidly increasing
$\beta > 10$	similar to Type I extreme value distribution	very rapidly increasing

For individual components, the Weibull is best used when empirical data appear to indicate variability in failure rates over the usage lifetime of the item. In support of NASA missions, this method normally focuses on wear out or increasing failure rates since preoperational component testing and part screening tend to mitigate instances of infant mortality or improving failure rates.

For additional insights and guidance, see case studies digitally linked here.

3.2.3 Normal

The normal (Gaussian) distribution is used in statistical quality control and in analyzing measurement and statistical modeling errors. The measurements of outputs of random industrial processes often follow a normal distribution. For example, the fill levels in bottles of liquids for sale follow a normal distribution, reflecting random variations in the filling process. Standard plus or minus three-sigma quality control limits, used to assess process stability, are based on the normal distribution. In addition, the normal distribution has numerous properties that make it useful in statistical analysis. It is not generally used for the modeling of failure times in reliability. However, as noted in the next section, it is used to calculate lognormal distribution probability values. The normal distribution is symmetrical and characterized by is mean, μ, and standard deviation, σ.

The equation for the normal distribution is

$$f(x) = \frac{1}{\sigma\sqrt{2\pi}} e^{-\frac{(x-\mu)^2}{2\sigma^2}}$$

Below is a graph of the normal PDF for various values of μ and σ.

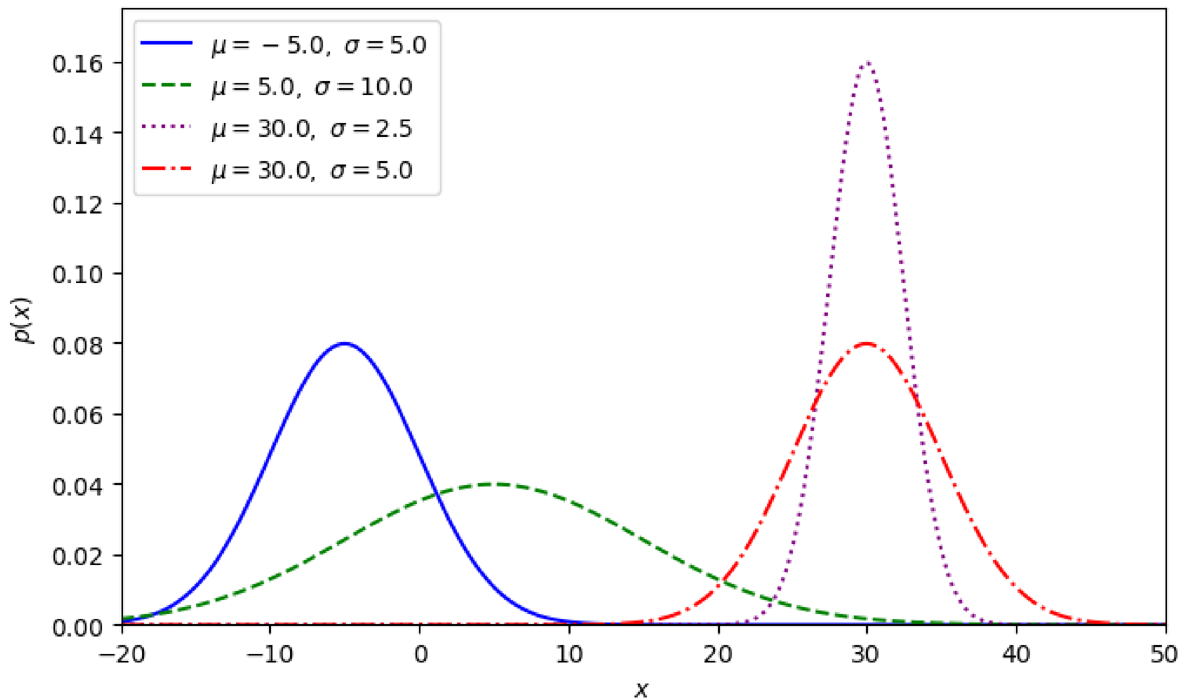

Figure 4. Normal Distribution Probability Density

For additional insights and guidance, see case studies digitally linked here.

3.2.4 Lognormal

The lognormal distribution is often used in reliability to model components whose failure is due to stresses over time. The PDF for the lognormal distribution is

$$f(t) = \frac{1}{\sigma t\sqrt{2\pi}} e^{\left[-\frac{1}{2}\left(\frac{\ln t - \mu}{\sigma}\right)\right]^2}$$

with $\mu \geq 0$, $\sigma > 0$. σ is the standard deviation and shape parameter. μ is the location parameter. The lognormal cumulative density function (CDF) can be written in terms of the normal distribution CDF, so that normal CDF tables can be used in computations. Below is a graph of the lognormal PDF for various σ values when $\mu = 0$. Increasing μ shifts the PDF to the right along the t axis.

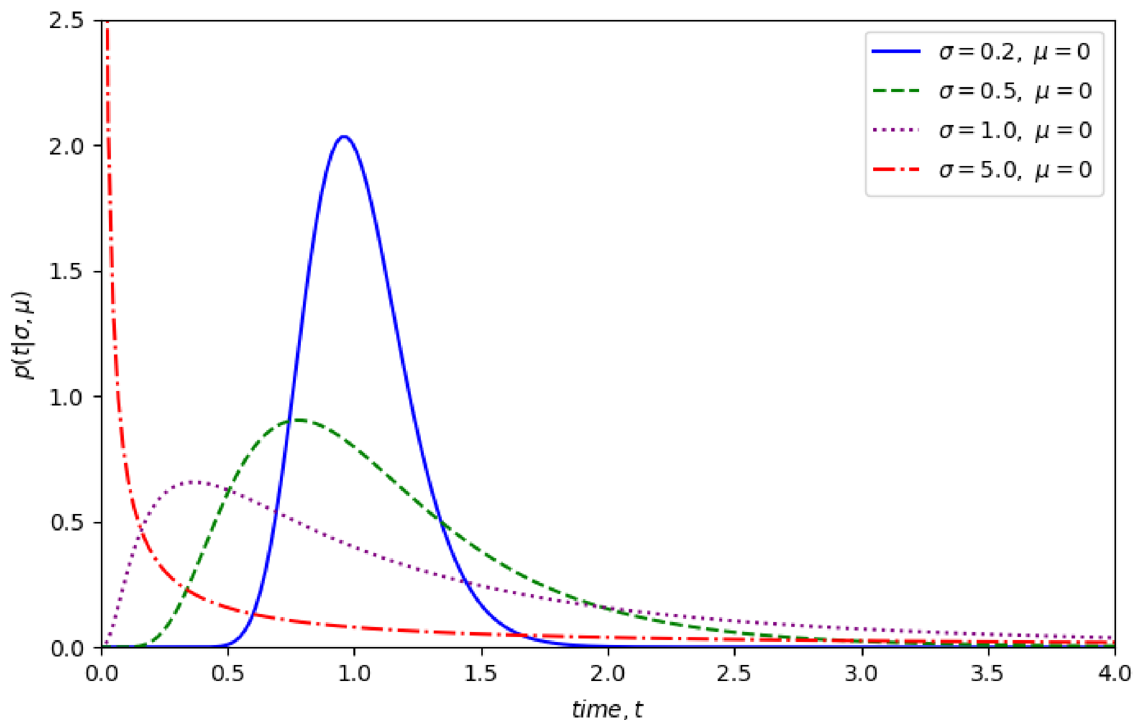

Figure 5. Lognormal Distribution Probability Density

Choosing between the Weibull and lognormal distributions to model failures due to stresses (such as mechanical fatigue or electromigration in electronics) can be based on experimental or field data. Tobias and Trindade summarize an approach for choosing:

> One trick that occasionally helps choose whether a lognormal or Weibull will work better for a given set of data is to look at a histogram of the logarithm of the data. If this is symmetrical and bell-shaped, the lognormal will fit the original data well. If, on the other

hand, the histogram now has a left skewed appearance, a Weibull fit to the original data might work better [Tobias and Trindade, 1995].

In support of NASA missions, this method normally applies to items that are showing symptoms of stress or stresses that are higher than forecast.

For additional insights and guidance, see case studies digitally linked here.

3.2.5 Binomial

The Binomial distribution is used to formulate a probability for failures in a set of components that have only two outcomes (success/failure or defect), and empirical data shows failure/defect events over time/demands. For this situation, the probability that x failures or less will occur in a random sample of n items is given by:

$$f(x) = \binom{n}{x} p^x q^{(n-x)}$$

where

$$F(r) = \sum_{x=0}^{r} \binom{n}{x} p^x q^{(n-x)}$$

Figure 6. Binomial Probability
[Reliability Analytics Corporation, 2010-2023]

F(r) is the probability of obtaining not more than r failures in a sample of n items where p is the probability of failure/defect and q (or 1 – p) is the probability of obtaining success or an unflawed item.

In support of NASA missions, this method is best applied to manufacturing lots or redundant item architectures or testing to assess the probability of a specific outcome (e.g., all redundant components fail, component selected is flawed).

For example, if manufacturing process creates defects at a rate of 2.5% (p=0.025) then sample of 20 would have:

The probability of finding exactly 1 defect in 20 samples is 0.3091.
The probability of finding 1 or fewer defects in 20 samples is 0.9118.
The probability of finding 2 or more defects in 20 samples is 0.0882.

For Example, if a system has 4 identical items/units the risk of having a common failure or unacceptable quantity of failures (2 or more out of 4) given a failure rate of 2.5% (p=0.025) would be:

The probability of having exactly 1 failure in 4 units is 0.0927 (or a success potential of 0.9073).
The probability of having 1 or fewer failures in 4 units is 0.9964.
The probability of having 2 or more failures in 4 units or system failure is 0.0036 (or 0.9964 probability of success).

For additional insights and guidance, see case studies digitally linked here.

3.2.6 Bayesian Statistical Inference for Updating Failure Rates

Bayesian inference is a method of continual statistical inference in which Bayes' Theorem is used to update the probability of a hypothesis or failure rate estimate, as more evidence or information about the system's responses to operational physical stresses become available. This process can be considered an applied physics method that takes a prior distribution and evidence to statistically infer a new probability distribution, known as the posterior distribution. In terms of reliability this method uses all of the (currently available) information or the effects of physics on a system and leads to superior parameter or failure rate estimates.

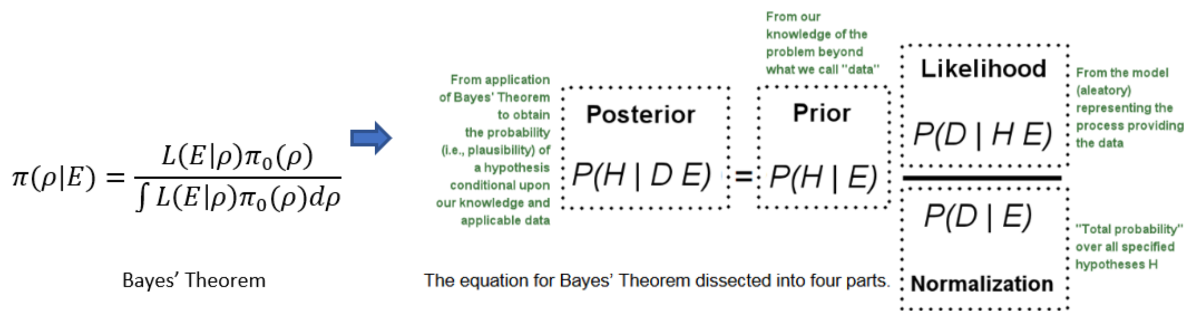

Figure 7. Bayes' Theorem [Dezfuli, 2009]

Since this method is dependent on both the evidence and the prior, it is important to scrutinize and be discriminatory in the data being applied and to validate that the prior distribution is consistent with what is known about the system. It is best used when there are components for which an accepted failure rate point estimate, or an established or previously derived/posterior failure distribution (informative prior) is known, and there is enough success and failure data to inform a new hypothesis, but not enough data to derive a new and statistically credible failure rate or distribution. All data applied should be weighted and validated in applicability to the system in question. This may mean certain data is not applied or is weighted differently than other data. Whereas the prior and its homogenous or nonhomogeneous distribution type (e.g., binomial for failures in n demands, Poisson for events in time, or gamma for n failures in time) should be selected and defined as accurately as possible to efficiently reach convergence (the

point where additional data will not significantly change the posterior). Any prior will reach convergence if enough data is applied [Clyde, 2021].

In support of NASA missions, this method can be continually used from design through in situ operations since Bayesian inference learns from data incrementally. Each update will better inform analyses and risk decisions and bring the new failure rate estimate closer to convergence. For example: If a Bayesian inference is begun with a prior failure rate from a handbook, it will be a constant value of n failures in time prior that may be conservative, but it will not be an elicited value or a complete prior distribution. Therefore, a gamma prior distribution should be developed with an elicited guess, agreed upon assumed standard deviation or coefficient of variation CoV(λ), such as 0.5, thereby making a subjective prior distribution (or an uninformative or weak prior [Zhu, 2004], or Jeffrey's prior [Glen, 2021] as considered by some) that can be used to generate a gamma posterior (new failure distribution), but will not overly bias results. To generate the posterior distribution, the prior should be combined with experience data (failures (r) and time (T), or Poisson data) or a point estimate at the assumed CoV:

$$\lambda_{\text{Bayesian}} = \frac{\delta'}{\rho'} = \frac{\delta + r}{\rho + T}$$

$$\text{given } \rho = \frac{\delta}{E(\lambda)} \text{ and } \delta = \frac{1}{[CoV(\lambda)]}$$

The results of this method are a posterior distribution or a point estimate, as noted above. The posterior distribution is best used for further system assessment since it is more precise over time than a selected point estimate. However, if the use of a distribution is not possible in a system assessment, a point estimate (i.e., mean) from that distribution can also be used with appropriate caveating or assumptions noted.

Note: Once a posterior is obtained using Bayesian inference, it should be updated when significant experience/failure data is available. This is done by using the generated posterior as the new prior and applying this additional data, so its failure rate distribution becomes more indicative of performance.

For additional insights and guidance, see case studies digitally linked here.

3.3 Peck's Temperature-Humidity Relationship Prediction

Empirical models used in reliability are not limited to those based on past field failure data. Peck's temperature-humidity model, based on test data, can be used to predict electronic semiconductor life.

As industries and products become much more sophisticated in terms of both design and materials selection, empirically based models that can provide a reasonable degree of coverage for a specific technology still enjoy significant use and support. One such model is the Peck model for degradation due to humidity [Peck, 1986]. The specific technology area of interest here was plastic packaged semiconductors. Initial integrated circuits were mostly sold in

hermetically sealed ceramic packages. The packages were quite heavy and expensive to make. Epoxy-based encapsulants were an important innovation in the late 1970s and early 1980s. Metallurgies of this era mostly involved aluminum interconnects that were quite sensitive to moisture. Peck provided a model relating life of semiconductor electronic components to humidity and temperature.

$$t_f = A(RH)^{-n}e^{\frac{Ea}{kT}}$$

Here RH = relative humidity.

The Peck formula can be put into the Eyring form using the inverse power law for humidity and the Arrhenius equation for the temperature. The Eyring model is discussed in section 3.4.6.

For additional insights and guidance, see case studies digitally linked here.

3.4 Accelerated Performance Analysis

The foundational concept of acceleration is based on the Arrhenius relationship, which is described in some detail. Then, a variety of practical accelerated relationships that are based on the Arrhenius expression are discussed. These include Inverse Power, Coffin-Manson, Zhurkov, and Palmgren. All these relationships have failure time expressed in an exponential relationship with one or more real world stressors on the system such as temperature or voltage. These relationships form the "physics" in the Physics of Failure expression.

For additional insights and guidance, see case studies digitally linked here.

3.4.1 Arrhenius

The fundamental principle of all modern PoF acceleration is the Arrhenius relationship. The Arrhenius relationship takes the following mathematical form:

$$t_f = Ae^{\frac{-E_a}{kT}}$$

Here, t_f is a time to fail, A is scaling constant, E_a = activation energy, k = Boltzmann's constant, and T is temperature. In the most practical and frequent applications, the Arrhenius equation is used to define acceleration factors (AF) between a lab or test temperature and the final use temperature of the device. This temperature acceleration factor (AF) is defined by

$$AF = \exp\left[\frac{E_a}{k}\left(\frac{1}{T_{use}} - \frac{1}{T_{test}}\right)\right]$$

The effect of the exponential nature of this relationship can be seen in the graph below. Here, acceleration factors for a variety of use temperatures are calculated for two different test temperatures, for a particular activation energy. Over a typical range of possible use temperatures, the acceleration factor changes by two orders of magnitude. This exponential

acceleration feature enables practical laboratory test times (hours to a few weeks) to be relatable to long term product use conditions (months and years).

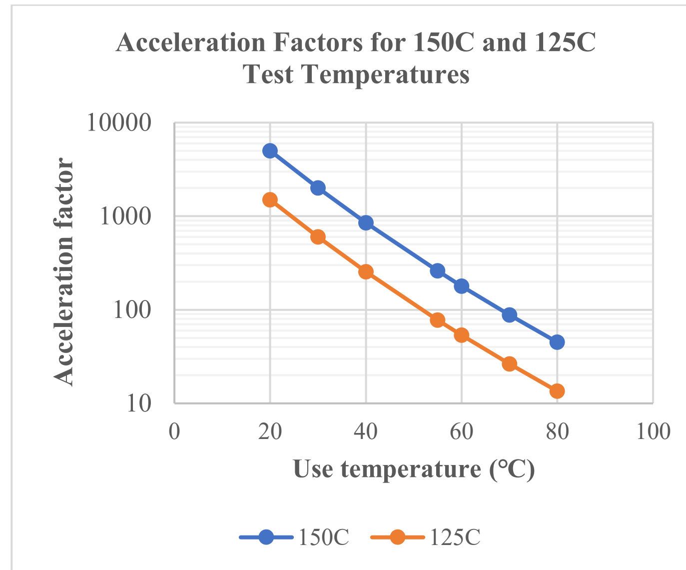

Figure 8. Arrhenius Acceleration Factors

A typical example of this is the 1,000 hr life test requirement of all modern semiconductor devices. Here a sample of usually 77 parts is stressed at high temperature, usually 125C to 150C. With an activation energy of 0.7 eV (as used in the above graph), one hour of stressing at 125C has an acceleration factor of (or is equivalent to) 77.8 hours of use at 55C. Hence 1,000 hours at 125C is equivalent to 77,800 hours at 55C or about 8.8 years.

The mathematics of the Arrhenius relationship are both very simple and very compelling. Proper use of the Arrhenius relationship however depends on understanding the underlying physics that the equation represents. Two key concepts are highlighted by the constants used in the Arrhenius acceleration expression:

- Activation energy
- Boltzmann's constant

Both constants open up the discussion of how materials change over time and the basics of thermodynamics that govern these processes.

Maxwell-Boltzmann statistics are used as the foundation of the kinetic theory of gases. This theory describes the interaction of particles in an idealized gas encompassed inside a given container. The particles move freely inside the container until they collide with each other. These collisions are described by the momentum and energy of the particles and the exchange of these quantities between particles and the existing thermal environment inside the container. The resulting Maxwell-Boltzmann statistics provide an expression for distribution of speeds of the particles.

$$\frac{dN}{N} = (\frac{m}{2\pi k_b T})^{\frac{1}{2}} e^{\frac{-mv^2}{2k_b T}} dv$$

dN/N is the fraction of molecules moving at velocity *v* to *v + dv.*

The exponential nature of the Arrhenius relationship can now be seen to have a formal thermodynamic basis. It can be seen that this exponential term can be interpreted as containing the kinetic energy of the particles. This allows for the beginning of formulating the activation energy as being a description of the detailed state of matter. This expression can be used to define the concept that the heat contained in a gas is a measure of the movement of the individual particles [Feynman, 1963]. Arrhenius' key contribution was to recognize that this expression not only describes the temperature dependence of physical processes but could be applied to chemical reactions as well [Arrhenius, 1903].

Arrhenius was addressing the problem of electrolytic dissociation of various inorganic salts and sulfates ($MgSO_4$, $BaCl_2$, etc.). Arrhenius described that a minimum amount of energy is needed for these various dissociative reactions to occur. This minimum amount of energy required for a chemical reaction and/or physical process to take place can now be seen to be the activation energy. Arrhenius also used the Boltzmann distribution to describe the kinetic energy of these molecules.

NASA Electronic Parts Assurance Group (NEPAG) Amendment to the Arrhenius model

The Arrhenius equation is widely followed for the burn-in and life test of semiconductor devices.[1] However, it gives no guidance on limitations for setting the test (stress) temperature. NEPAG would like to introduce the following amendment to the Arrhenius model: The stress temperature used should be the safe operating temperature; one that would not damage the device under test. It is recommended that the parts are characterized at the stress temperatures for DC, AC and functional operations to ensure there are no anomalies in the data (look for signs of damage to the device). The NASA and other users should exercise extreme caution in picking the stress temperature; one cannot just select a test temperature to shorten the test time/meet schedule constraints.

For additional insights and guidance, see case studies digitally linked here.

3.4.2 Inverse Power

The Arrhenius discussion now provides the bedrock for modern physics of failure topics and discussion. First up is the general concept of Inverse Power. The inverse nature of the relationship is evident from the Arrhenius expression where the logarithm of time is inversely proportional to temperature as shown below:

[1] Arrhenius modeling covers the whole spectrum of devices from discretes to monolithic/hybrid/2.5D and 3D microcircuits, and others. The up-screening of commercial-grade devices requires special attention.

$$\ln(t_f) \propto \frac{1}{kT}$$

This simple relationship implies that higher temperatures produce smaller lifetimes. It is important to recognize that the inverse relationship is between time and energy as kT has units of joules (energy). This is a much more profound result. Namely that lifetime is inversely related to the amount of energy "applied" to a system. Energy applied to a system can take on many practical engineering forms like temperature, voltage, etc. From a reliability physics of failure point of view, this energy can be considered as a "stress" upon the system.

Operational stresses on devices/boards are much less stressful than accelerated test conditions that can be applied in the laboratory. This embodies the inverse relationship of stress vs time. This is graphically shown in figure below:

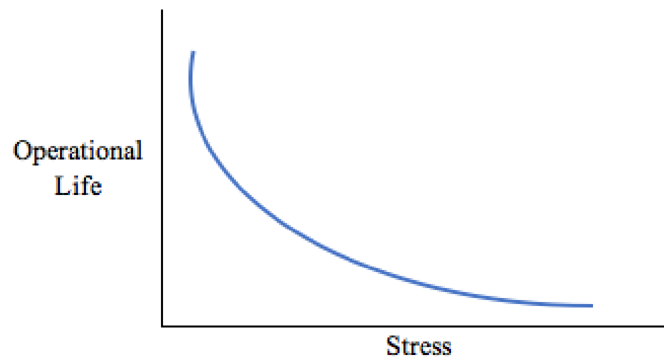

Figure 9. Operational Life Versus Stress

The graph highlights the basic inverse concept that significant stress has a corresponding significant reduction in operational life. The converse holds as well for very limited stress prolongs operational life. This relationship between stress and life is practically a very non-linear relationship as highlighted by the Arrhenius equation and its exponential relationship. The terms "stress' and 'Operational Life' have significant depth to each of them that need to be explored and discussed.

Stress can mean temperature, voltage, mechanical strain, vibration, corrosion, excess humidity, etc. And often these stressors occur in combinations, not just individually. So being able to precisely articulate the physical interactions with stressors is often one of the most important aspects of physics of failure work.

Operational time means time to when the devices stopped meeting requirements. A device can fail to meet requirements when it fails to function and can no longer be made to function, fails to function but can be repaired or restarted, or when the device's performance degrades past a level of acceptable performance or capability, but the device still functions.

Each of these definitions of life is acceptable, but each also needs to be formally tied to stress conditions to provide a meaningful expression of inverse relationship between stress and time.

An example would be where a transistor's subthreshold leakage current degrades enough due to buildup of oxide traps over time to make the transistor too leaky (pass too much current) for a memory cell to function. The transistor however still operates in terms of being able to turn off and on a conducting channel between a source and drain. Once the oxide traps build up, and there is a dielectric breakdown and the gate oxide is compromised, then at that point in time the transistor has ceased to function and can no longer be made to work.

At a more basic level the discussion of time being inversely related to stress (energy) provides an opportunity to define reliability in true thermodynamic terms. In their key 1996 paper, "Connecting Parametric Aging to Catastrophic Failure Through Thermodynamics. "Feinberg and Windom, the authors start with the same Maxwell-Boltzmann statistics mentioned above and define ageing as a fractional rate of change parameter:

$$\text{Damage} = \frac{\sum W_{\text{actual}}(t)}{W_{\text{actual-failure}}}$$

The inverse power relationship discussion also assumes a mathematical and hence physical continuity in stressors [Feinberg and Windom, 1996]. This must be carefully understood in real life as too much stress may change the failure mechanism of the device and result in an inaccurate prediction of life. This is where statistical life testing needs to be undertaken to ensure that there is indeed a predictable and justifiable continuity. A graphical example of a statistical life test is shown below:

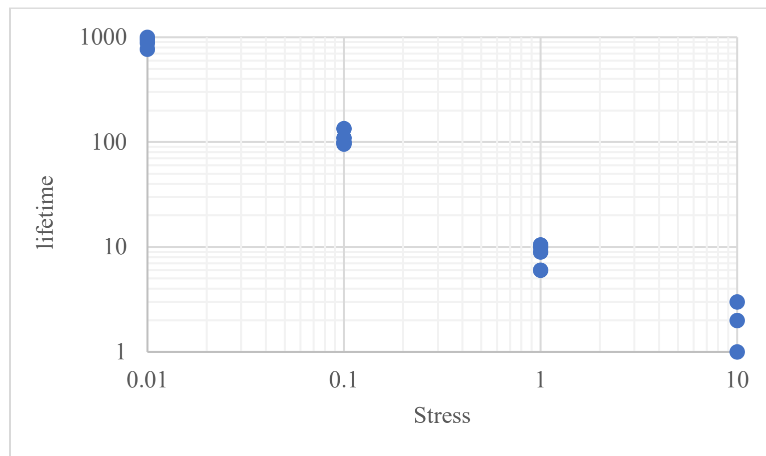

Figure 10. Stress Versus Lifetime

For additional insights and guidance, see case studies digitally linked here.

3.4.3 Coffin-Manson

Another method for accelerating life is temperature cycling a component or system to induce thermal fatigue. However, when choosing the test conditions, it is important that the upper and lower temperatures selected do not exceed the item's temperature limits or erroneous failures

could be observed. It is also important not to remain at the dwell temperatures for too long since this can also induce erroneous results from failure induced by non-operational mechanisms (e.g., melting solder, crossing the glass transition temperature of a polymer, etc.).

The amount of acceleration induced by thermal cycling is defined by the Coffin-Manson equation, which describes the relationship between temperate range and thermal cycles as shown below:

$$\varepsilon_{a,t} = \varepsilon_{a,e} + \varepsilon_{a,p} = \frac{\sigma'_f}{E}(2N_f)^b + \varepsilon'_f(2N_f)^c$$

where the ε and c are material-specific fatigue coefficients that are determined experimentally, N is the fatigue life of the material, E is the Young's modulus, and was the result of Coffin and Manson, materials research scientists, in the 1950's [Coffin, 1954]. Simplified this equation becomes:

$$AF = (\Delta T_{test} / \Delta T_{use})^m$$

where AF is the acceleration factor, ΔT is temperature difference (°C), and m is the Coffin-Manson exponent [Delsero Engineering Solutions, 2015]. Where m is typically found to lie in one of three relatively narrow ranges: m for ductile metal fatigue is 1-3, m for commonly used integrated circuit metal alloys and intermetallics is 3-5, while m for brittle fracture (e.g., ceramics) is 6-8. Knowing the acceleration factor of a test or exposure allows use-case life expectancy to be estimated (Life-exp = AF*Exposure-cycles/Use-case cycles per time unit). This relationship can also be used to estimate unexpected life usage from anomalous thermal use conditions that can be used to estimate remaining life by subtracting the anomalous exposure life estimate from the baseline life expectancy estimate. Further, any life expectancy, with appropriate statistical analysis, can also translated to a MTTF or failure distribution for reliability use.

However, if temperature cycling profile parameters (e.g., dwell, time, dwell temperature, ramp rates/frequency, cycle length) are known, then the Coffin-Manson equation evolution of Norris and Landzberg (1969) shown below, can be used to resolve the limitations of the simplified Coffin-Manson equation only taking into account the physical effects of temperature changes:

$$\text{Acceleration Factor (AF)} = \left(\frac{\Delta T_A}{\Delta T_B}\right)^{\alpha} \left(\frac{f_B}{f_A}\right)^{\beta} \exp\left(\frac{E_a}{k}\left[\frac{1}{T_B} - \frac{1}{T_A}\right]\right)$$

where N is fatigue life, ΔT is the temperature range, f is frequency, T is temperature, E_a is the activation energy, K is the Boltzmann constant, and α and β are experimentally defined parameters (e.g., with β=0.33, α=1.9, and E_a/k=1414 for lead free solder [Vasudevan and Fan, 2008]. The inclusion of frequency of cycling gives the Norris-Landzberg expression very practical and relatable means to accelerate life between applications and laboratory settings, that Reliability can use to derive a MTTF or failure distribution from life expectancies results and appropriate statistical analysis like with Coffin-Mason shown above. Also, the JEDEC has adopted the above expression in both the JESD47I, Stress-Test-Driven Qualification of

Integrated Circuits and JESD94A, Application Specific Qualification Using Knowledge Based Test Methodology over Engelmaier and Darveaux expressions that are less accurate. Whereas tools like Sherlock Automated Design Analysis and CALCE use the Blattau stress/strain expression.

For additional insights and guidance, see case studies digitally linked here.

3.4.4 Zhurkov Equation

Following directly from the Coffin-Manson discussion of materials, specific failure mechanisms is another materials-focused relationship, the Zhurkov equation. The Zhurkov equation is used to predict the durability of polymers and general large macromolecules based on replicated substructures. In its most general form, the Zhurkov equation is

$$\tau = \tau_o \exp\{\frac{U - \nu\sigma}{k_B T}\}$$

Where τ is the lifetime of a specimen under tensile load σ at temperature T, k_B is Boltzmann's constant, U, τ_0 and ν constants. Zhurkov originally proposed this model in 1965 [Zhurkov, 1965]. The core concept of the theory is thermofluctuation of fracture. The fracture process of a given solid is determined by mechanical stress and temperature. Uniaxial tensile stress on a wide range of material was used as the experimental basis for the equation. The physical details of the constants listed in the equation above can be defined as τ_0 = the natural oscillation frequency of the atoms in the sold, U = the binding energy, and ν as the proportionality constant related to molecular disorientation. The importance of the Zhurkov approach is that it defines the kinetic concept of the fracture process proceeding in three separate stages:

1. Excitation of the bonds broken as a result of tension-related stresses
2. Breakage of the above excited bonds due to thermal fluctuations
3. Continual accumulation of broken and ruptured bonds that finally precipitate loss of material stability resulting final breakdown

These three processes define the concept of thermofluctuation of fracture. While focused on the details of the solid materials studied, the Zhurkov expression continues to reenforce the validity of the fundamental Arrhenius expression and its thermodynamic foundation, namely that the inverse exponential relationship of lifetime as a function of stress condition continues to hold true.

For additional insights and guidance, see case studies digitally linked here.

3.4.5 Palmgren

The Palmgren equation for lifetime is sometimes called the Palmgren-Miner equation [Palmgren, 1924; Miner, 1945]. This is another equation that expresses the lifetime of solid material based on its materials properties. The Palmgren-Miner equation provide a linear damage accumulation approach where failure (or end of life) is usually defined as the appearance of a crack in the material. The accumulation approach allows for a variety of stresses to occur and then be

compared, each individually, to an existing stress life (SN) curve. Such a life-stress life curve is empirically derived and conceptually looks like the following:

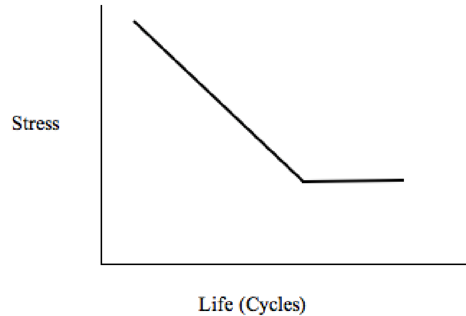

Figure 11. Stress Versus Number of Cycles

The decreasing stress as a function of life cycles can be either a linear-linear or linear-log relationship. The flat (zero-slope) portion of the curve defines a condition of "infinite life." This means at stress levels at or below this level, the lifetime of the material no longer degrades. The Palmgren-Miner equation is:

$$\sum_{i=1}^{k} \frac{n_i}{N_i} = C$$

Where n_i = number of cycles accumulated at stress S_i and N_i = average number of cycles to failure at that stress, S_i. C is a constant and usually assumed to be 1. The linear summation approach enables superposition of different numbers of stress cycles to accumulate over time until the end of lifetime is calculated at C = 1. The Palmgren-Miner expression is simple to comprehend and introduces a key concept. It does not correctly account for sequencing effects where different combinations of stress levels are assumed to be independent when in fact they are not. High/low versus low/high stressing has been shown to have different results.

For additional insights and guidance, see case studies digitally linked here.

3.4.6 Eyring Modeling

The Eyring model [Eyring, 1935] is a very powerful tool that is important both empirically as well as from a theoretical first principals' point of view. At first the Eyring model resembles a seemingly straightforward generalization of the Arrhenius expression, i.e.

$$t_f = AT^{\alpha}\left[\frac{\Delta H}{kT} + \left(B + \frac{C}{T}\right) * f(V, T, \ldots)\right]$$

For example, with B = 0 and C = 1, the Eyring expression becomes a special form of the exponential life stress model with a typical term for an inverse temperature behavior. However, the Eyring model can be derived directly from transition state theory. This is different from the Arrhenius model, which started out as a heuristic explanation of empirical results. Because the Eyring model has a formal mathematical basis, it has extensibility across broad areas of chemistry and physics. The Eyring model can rightly be considered as the penultimate theoretical

justification of the work initially pioneered by Arrhenius. Transition state theory (TST) was needed to formally describe the activation energy and pre-exponential factors of the Arrhenius expression. Because of this TST is widely used to determine the rate coefficients of chemical reactions. TST is rigorously based on the assumption that transition state is a hypersurface in phase space that divides reactants and products. This allows for both a classical as well as a quantum approach to TST.

From a practical point of view the flexibility and power of the Eyring model is often quoted in semiconductor literature to express acceleration factors with variety of environmental stresses besides temperature.

$$K = a\frac{kT}{h}e^{\frac{-Ea}{kT}}S^{\alpha}$$

Here S can represent voltage, humidity or mechanical stress. The Eyring model features prominently in JEDEC JEP122F (2010), which discusses hot carrier injection for NMOS devices, time to failure modes for surface inversion, and a back end of line (BEOL) mechanical time to failure model. JEP122F actually provides a general table of failure mechanisms and model parameters with the statement that "*All models are inherently Eyring; so take product of Arrhenius and other functions.*" This is an indication of how important and all-encompassing the Eyring model truly is.

For additional insights and guidance, see case studies digitally linked here.

4. Deterministic Methods

4.1 What are Deterministic Methods?

Deterministic models analyze the dominate failure mechanisms behind a failure and how they limit the functional capability of the component [Varde, 2001]. Failure mechanisms described by deterministic models include degradation (due to accumulated damage from stress), erosion, diffusion, and corrosion phenomenon leading to sudden or eventual failure [Schenkelberg, 2020]. The model incorporates the component load profiles, material specifications, and environmental stresses to recreate the life conditions a component or system experiences as a means to predict the reliability. Often this approach is based on the utilization of software applications which has advantages such a predefined or tailorable load profile and the ability to define geometric and electrical properties of the component under analysis. Over the years modeling precision and accuracy have increased, which has led to a deeper understanding of failure mechanisms and more realistic predictions [Matic and Sruk, 2008].

For additional insights and guidance, see case studies digitally linked here.

4.2 Electromigration in Electrical and Electronic Components

Electromigration is the process in which metal ions move under the influence of an electrical field E, which is the gradient of the electrical potential V: $\mathrm{E} = -\nabla\mathrm{V}$; this has caused the failure of many components. Migration can also be induced by gradients of concentration (diffusion), gradients of temperature (Soret effect), and gradients of mechanical stress; these processes have also caused failures.

4.2.1 Metals

Metals are the chemical elements in the periodic table that form a metallic bond with other metal atoms when in a condensed aggregate (phase); a metallic bond forms when the outermost electrons of the atoms detach from the atoms, which then become ions; these detached electrons move throughout the entire condensed phase, becoming a "sea" of conduction electrons. The metallic bond is strong and directionless, pulling the ions in the condensed phase into a close-packed crystal, such that each atom usually has 12 touching neighbors; this results in a (usually) high melting point and a high boiling point. Metallic bonds cause many of the traits of metals, such as strength, malleability, ductility, luster, and a facile conduction of both heat and electricity. An alloy is a solution of metals.

As typically formed, the crystal structure of a metal is not perfect over greatly extended distances; rather, a typical metal is made of many "crystal grains," which are regions of crystalline regularity. These grains are joined at grain boundaries where there are misalignments across the joining region. Grain size is typically log-normally distributed, with a median grain size ranging from fractions of a micrometer to several micrometers for the metals typically used in components.

There are a variety of imperfections within, and between, grains. Since the mechanisms of ion migration, and of metal deformation, are controlled by these crystal imperfections, these play an *essential* role in these processes.

There are three conventional types of crystal imperfections: point defects, line defects, and planar defects:

- Point defects:
  - Vacancy: missing ion at a certain crystal lattice position
  - Interstitial impurity ion: extra impurity ion in an interstitial position
  - Self-interstitial ion: extra ion in an interstitial position
  - Substitution impurity ion: impurity ion, substituting an ion in crystal lattice
  - Frenkel defect: extra self-interstitial ion, responsible for the vacancy nearby
- Line defects:
  - An edge dislocation is an extra half plane of ions inserted into the crystal lattice. Due to edge dislocations and their mobility, metals possess a characteristic high

plasticity, including ductility and malleability.
  - A screw dislocation is formed when one part of a crystal lattice is shifted (through shear) relative to the other crystal part. It is called a 'screw' since atomic planes form a spiral surface around the dislocation line.

- Planar defects – an imperfection in form of a plane between uniform parts of the material. The most important planar defect is a grain boundary. Formation of a boundary between two grains may be imagined as a result of rotation of the crystal lattice of one of them about a specific axis. Depending on the rotation axis direction, two ideal types of a grain boundary are possible:

  - Tilt boundary: rotation axis is parallel to the boundary plane
  - Twist boundary: rotation axis is perpendicular to the boundary plane: An actual boundary is a mixture of these two ideal types.

The density of point defects of a crystal in equilibrium at an absolute temperature T is their number per volume, and this cannot be zero, no matter how carefully the condensate is formed. As Yakov (or Jacov) Frenkel noted in his *Kinetic Theory of Liquids* [Frenkel, 1946], written in WWII, a crystal in equilibrium will have a number of vacancies (missing ions) determined by the Boltzmann factor exp $[-E^I/k_B T]$, where E^I is the binding energy of the ion in the lattice, and k_B is Boltzmann's constant. In practice, the actual number of vacancies can be substantially higher. Vacancy density is critical for migration processes: ions can only migrate thru crystal imperfections.

The density of edge dislocations is the total length of edge dislocations in a unit crystal volume. The edge dislocation density of annealed metals is about $10^{10}/m^2$ to $10^{12}/m^2$. After work hardening, the dislocation density increases up to $10^{15}/m^2$ to $10^{16}/m^2$. Further increases of edge dislocation density causes cracking, and then fracture.

Grain boundaries accumulate crystal lattice defects (vacancies, dislocations) and other imperfections, therefore they effect metallurgical processes. Diffusion along grain boundaries is much faster than throughout the grains.

Segregation of impurities in form of precipitating phases in the boundary regions causes a form of corrosion, associated with chemical attack of grain boundaries. This corrosion is called Inter-Granular corrosion.

For additional insights and guidance, see case studies digitally linked here.

4.2.2 Migration

Migration is movement from one place to another. The ions within a metal at a temperature T are in perpetual motion. In the absence of any biasing forces, this motion is random: an ion will vibrate around its average lattice position with a range of frequencies up to about 10^{12} Hz, and very occasionally jump to a neighboring vacancy, if one is available. So, a steady,

nondirected migration happens and ions slowly move at random throughout the condensed phase.

Various situations can install a biasing force and impose an average direction to the migration. These include:

- An electrical field $E = -\nabla V$, where V is the electrical potential. In a metal with an electrical conductivity σ, an electrical field induces an electrical current density $J = \sigma E$. (This is Ohm's law, expressed using the fields J and E.) The conduction of the current by the mobile electrons involves these electrons losing momentum p to the ions – this is related to σ – and conservation of momentum implies that there is a steady force applied to these ions: $F_{wind} = dp/dt$; this is usually called the force of the "electron wind."

  There is a second effect: the ions are electrically charged, and so the electrical field acts directly on the ions; however, the conduction electrons distribute themselves around each ion to partially shield it, so it is the force on the shielded ion, with effective charge Q_{shield}, that matters: $F_{ion} = Q_{shield}E$. Usually, this is a substantially smaller effect than the "wind." This biases the ion's jumps to be in the direction of the net force: $F = F_{wind}+Q_{shield}E$.
- A concentration gradient of ions. This introduces a ion-flux $J = -D\nabla c$ where c is the concentration of the ions, and D is the diffusion parameter (also called the diffusivity): this is 'Fick's First Law.'

For additional insights and guidance, see case studies digitally linked here.

4.2.3 The Fluctuation-Dissipation Theorem

The Fluctuation-Dissipation Theorem says that when there is a force-driven process that dissipates energy, turning it into heat, there is a related process describing thermal fluctuations when the system is in thermal equilibrium. This is best understood by considering examples.

For additional insights and guidance, see case studies digitally linked here.

4.2.4 Viscous Drag and Brownian Motion

An object experiences viscous drag when it is moved through a fluid, and this generates heat. A measure of this viscous drag is the mobility μ of the particle, which is the ratio of the particle's terminal drift speed under the applied force. The corresponding fluctuation in thermal equilibrium is the Brownian Motion that the object exhibits in the fluid, while in thermal equilibrium.

Albert Einstein developed a precise treatment of this in his doctoral dissertation (1905). He considered the sequence of displacements in successive time-intervals, each of duration τ, of a small particle, $\Delta_1(\tau), \Delta_2(\tau), \cdots$, in a fluid in equilibrium, and showed that the mean of the

squared displacements in equilibrium $\overline{\Delta(\tau)^2}$ was related to the mobility μ of the particle, which is measured out of thermal equilibrium, when the particle is moving under an applied force:

$$\frac{\overline{\Delta(\tau)^2}}{\tau} = 2\mu k_B T \, .$$

Where k_B is Boltzmann's constant, and T is the absolute temperature.

For additional insights and guidance, see case studies digitally linked here.

4.2.4.1 Electrical Resistance and Johnson-Nyquist Noise

The electrical current passing thru an electrical resistor experiences a drag that causes a drop in the electrical potential across the resistor and generates Joule heat. In equilibrium (i. e., when the average current passing thru the resistor and the average voltage across the resistor both vanish), the instantaneous current thru the resistor fluctuates in time: this is called the Johnson-Nyquist noise.

This type of noise was discovered and first measured by John B. Johnson at Bell Labs in 1926. He described his findings to Harry Nyquist, also at Bell Labs, who was able to explain the results, and derive the relation:

$$\frac{\overline{V^2}}{\Delta\nu} = 4Rk_B T$$

where V^2 is the mean of the squared voltages within the frequency bandwidth $\Delta\nu$ (that is, the "noise"), R is the resistance, k_B is Boltzmann's constant, and T is the absolute temperature.

For additional insights and guidance, see case studies digitally linked here.

4.2.4.2 Generalization by Callen, Welton, and by Kubo

The Fluctuation-Dissipation Theorem was proven by Herbert Callen and Theodore Welton in 1951 and expanded by Ryogo Kubo in the mid-1960s. There are antecedents to the general theorem, including Einstein's explanation of Brownian motion during his *annus mirabilis* and Harry Nyquist's explanation in 1928 of Johnson noise in electrical resistors.

One way to exhibit the Fluctuation-Dissipation Theorem is the following. Let $X(t)$ be an observable quantity of a system that can be in thermal equilibrium, and therefore has thermal fluctuations around the mean value X_0. The Fourier transform is $X(\omega)$ where $\omega = 2\pi f$ is the angular frequency and f is the conventional frequency.

The power spectrum of these fluctuations is $S(\omega) = \overline{X(\omega)^* X(\omega)}$.

Switch on a stimulus $f(t)$. To first order, the response of the system is characterized by the (linear) susceptibility $x(t)$:

$$\overline{X(t)} = \overline{X}_0 + \int_{-\infty}^{t} \chi(t - t')f(t')\,dt'.$$

The Fluctuation-Dissipation Theorem states

$$S(\omega) = \left[\frac{2k_B T}{\omega}\right] \cdot I[\chi(\omega)] \qquad (4)$$

Where I[·] means the imaginary part, and $\chi(\omega)$ is the Fourier transform of $\chi(t)$. The left-hand side measures fluctuations in X in equilibrium, while the right-hand side measures the (energy) dissipation generated in first order while driving the system out of equilibrium.

For additional insights and guidance, see case studies digitally linked here.

4.2.5 Electromigration in Interconnection Traces and Vias in Integrated Circuits

In one class of electromigration phenomena, an interconnecting trace or via in an integrated circuit deforms under the influence of electrical currents: one class of deformations induces voids, and these have caused an open circuit that has destroyed the proper functioning of the circuit; another class induces extrusions of metal, some of which have caused short circuits that have destroyed proper functioning. The median lifetime L_{med} for both classes have been usefully described by Black's Law

$$L_{med} = \left[\frac{A}{J^n}\right] \cdot \exp\left[-\frac{E^*}{k_B T}\right], \qquad (5)$$

where J is the electrical current density flowing thru the interconnection, k_B is Boltzmann's constant, and T is the absolute temperature. The activation energy E^* and the parameters A and n are empirically determined for the particular materials and geometry of the interconnection.

At the time of first widespread introduction of integrated circuits in the early 1960s, electromigration-driven voiding of interconnects was a common failure mode. Most designers learned by the mid-1970s to choose sizes for interconnects to limit current densities thru them, to give a nominal decade of median lifetime at the design currents and temperatures. However, there has remained a drizzle of design mistakes and manufacturing blenders that has caused some electromigration-induced failures. The failure in 2008 of Side A of the Scientific Instrument Command & Data Handling (SI-C&DH) system in the Hubble Space Telescope was caused by electromigration of the power traces of a microcontroller integrated circuit, as was determined when the system was returned from orbit and studied in GSFC's Parts Lab.

Advances in the technology of integrated circuits, including the widespread movement from interconnecting traces made of aluminum to traces of copper, and the continuing shrinkage

of scale, indicate that the median lifetimes caused by electromigration will decrease to less than five years by the mid-2020s: this has ominous implications for spacecraft missions with planed durations of five years or longer. This is treated in detail in the book *Fundamentals of Electromigration-Aware Integrated Circuit Design* [Lienig and Thiele, 2018].

For additional insights and guidance, see case studies digitally linked here.

Examples of Electromigration

- Electromigration in hot filaments, as are used (for example) in incandescent lamps, electron sources, and the filaments of electrical fuses. This was the cause of premature failures of incandescent lamps in the early Geostationary Operational Environmental Satellite (GOES) series of weather satellites, resulting in several congressional investigations. It has caused the premature failure of calibration lamps in examples of the Moderate Resolution Imaging Spectroradiometer (MODIS) instruments. And it was a life limiting mechanism for the early versions of the electron sources in the Planetary Instrument for X-ray Lithochemistry (PIXL) for the Perseverance Rover, until this mechanism was addressed.

- Electromigration along moist surfaces. This is a recurring mechanism for the failure of electrical parts; for example, it was the cause of the failure of one of the six Battery Charge/Discharge Units in International Space Station (ISS). (These are essential for the operation of ISS.) It is also a common mechanism for the development of electrical short circuits in Multi-Layer Ceramic Capacitors (MLCC) that have one or more cracks between the capacitors outside at the eternal electrodes of the capacitor.

- Electromigration over dry surfaces. This is a mechanism for the development of electrical short circuits in Multi-Layer Ceramic Capacitors (MLCC) that have internal cracks bridging between alternate electrodes.

- Electromigration thru the porous membrane separating the electrodes in an electro-chemical cell (e. g. a battery).

For additional insights and guidance, see case studies digitally linked here.

4.3 Thermal Physics of Failure

The “thermal mechanisms” that cause failure may be classified as absolute temperature effects, relative temperature (gradient) effects, or thermal cycling effects. In some cases, specific failure modes may result from both absolute and gradient temperature effects.

Failure mechanisms may be generalized as falling within three categories that are all affected by temperature:

1. Structural effects resulting from physical forces generated by temperature-driven deformations, including cyclical mechanical loading. As motion (towards the atomic scale) is directly related to heat, there is a direct connection between most failure modes and thermal conditions.
2. Chemical effects resulting from the reaction of materials with elements across interfaces and/or decomposition of metastable material phases. The chemical reactions may be exothermic (release heat) or endothermic (absorbing heat) related to the enthalpy and entropy of starting materials and reaction end products.
3. Electrical/Optical stressors, including electrical fields (voltage) and power (current flow or optical density absorbed). Heat plays a role where it changes the distribution of electronic states of atoms in materials, carrier densities, and scattering physics affecting absorption and emission characteristics.

Absolute temperature is especially important in thermal diffusion and chemical reaction-based failures, where temperatures can induce changes in local chemistry affecting material properties. Differences in coefficients of thermal expansion for dissimilar materials that are in contact is a particularly important factor in reliability. This is because differing expansion in adjacent materials creates stress, voiding, and cracking.

For additional insights and guidance, see case studies digitally linked here.

4.3.1 Thermal Failure Mechanisms

Temperature-related failure modes for most hardware found on NASA projects involve multi-physics processes. Temperatures are traditionally assessed using single-physics thermal models that provide temperature information based on the physics of heat transfer only. The temperature information is then used in other types of analysis programs to assess failure modes via other physical processes, such as fatigue stress, distortion, etc.

Thermal engineers deal with the “movement” of heat, or heat transfer, governed by the First Law of Thermodynamics (Conservation of Energy), via different heat transport mechanisms[2]:

Conduction (Fourier):

$$\frac{\dot{Q}}{A} = \dot{q} = -k\frac{dT}{dx}.$$

Convection (Newton’s Law of Cooling):

$$\frac{\dot{Q}}{A} = \dot{q} = h(T_w - T_\infty)$$

Radiation (Stefan-Boltzmann):

$$\frac{\dot{Q}}{A} = \dot{q} = \sigma \epsilon T^4$$

Thermal models are constructed from corresponding CAD models to simulate the conduction, radiation, and sometimes convective or evaporative heat transfer processes. Appropriate thermo-physical and thermo-optical properties are added for materials and surfaces, as required, to

[2] All of the four classical heat transport mechanisms – conduction, convection, radiation, and evaporative cooling – may be represented in spacecraft thermal models, although conduction and radiation are the predominant modes of heat transport in most space applications. Convection heat transfer is usually of greater importance in ground-based systems, launch vehicles, or human spaceflight missions such as ISS. Fluid transport systems, such as those used in pumped cooling loops, also include convection heat transfer. Evaporative cooling is sometime encountered on human spaceflight systems where cooling is required for short time periods.

generate a node and conductor network. Some software platforms combine heat transport and fluid transport within a single package.

The purpose of thermal analysis is twofold—to provide sufficiently detailed temperature predictions to allow an assessment of the impact of the temperature on the many constituent parts and materials of the assembly being analyzed, and to determine any heater power needed to maintain minimum temperatures. The temperature predictions are compared to the various known material/part temperature limits and can also allow a mechanical assessment of the physical/mechanical stress and strain on the system caused by material expansion and contraction with temperature. This latter analysis requires a mapping of the temperature over a structural Finite Element model.

Failures of electronic units are a major cause of mission degradation or failure. Electronics boxes consist of many piece-parts of different types, most of which are sensitive to thermal environmental conditions. Electronic units therefor receive considerable attention in reliability calculations and thermal testing. The thermal environment failure mechanisms for these different parts can vary and include hot and cold temperatures, temperature gradients, thermal shock, time-at-temperature, and thermal cycling. Table 3 provides common thermal failure mechanisms for different types of electronic box parts and the associated failures seen for these mechanisms.

Table 3. Predominant Failures Seen in Electronic Box Parts for Different Thermal Test Failure Mechanisms

Part Type	Thermal Test Failure Mechanism	Failure
Semiconductor devices and integrated circuits	Temperature cycling	Cracking of die, delamination at chip-resin interface, Hillock formation
	Temperature cycling, thermal shock	Die-bond defect, package-seal defect, CTE mismatch, substrate defect
	Thermal shock	Cracking of resin
	High temperature, thermal shock	Thermomigration/electromigration, Dielectric breakdown, Cracking of encapsulation
	High storage temperature	Metallization defect, corrosion, bulk-silicon defects
	High temperature in accelerated test	Electromigration
	Low temperature	Increase in leakage current, hot-electron effects
Printed wire boards	High temperature, thermal shock	Discoloration, cracking, warping, delamination, "measling"
Conformal coatings	High temperature, thermal shock	Cracking of coating (lack of protection)
Resistors	Temperature cycling, thermal shock, high temperature	Discoloration, charring, change in resistance, open circuits, melting
Inductors / transformers	Temperature cycling, thermal shock, high temperature	Open circuit; short circuit between windings
Capacitors	Elevated temperature life test	Changes in capacitance, dielectric strength, insulation resistance; surface cracking
Electrolytic capacitors	High temperature, thermal shock	Damage to hermetic seal, drying or leakage of electrolyte
Chip capacitors	Temperature cycling, elevated temperature	Cracks in body/attachment joints; oxygen vacancy migration
Crystal oscillators	Temperature change	Drift in oscillation frequency
All electronic parts (& cables/connectors)	High temperature, thermal shock	Damage to mechanical joints, loosening of terminations, softening of insulation, solder grain coarsening, opening of solder joints, change in electrical characteristics, cracking of part cases and wires
	Low temperature	Cracking on bonds and wires, CTE mismatches, deformation and hardening of materials at glass transition temperatures
	Thermal gradient	Creep-induced strain, creep-fatigue in solder joints, thermomigration/electromigration

For additional insights and guidance, see case studies digitally linked here.

4.3.1.1 Absolute Temperature Effects

Absolute temperature is responsible for changes in material characteristics including strength, ductility, and hardness, but also optical and electrical properties.

In physical chemistry, the Arrhenius equation is a formula based on empirical assessments for the temperature dependence of reaction rates and has an important application in determining rate of chemical reactions and for calculation of energy of activation. It can be used to model the temperature variation of diffusion coefficients, population of crystal vacancies, creep rates, and many other thermally induced processes/reactions. Mostly a consideration in the realm of micro-electronics, an Arrhenius model uses steady-state temperature to model the mean time-to-failure for each failure mechanism, as applicable [White, Bernstein, 2008]. (Refer to section 3.4.1 Arrhenius equation usage.)

For additional insights and guidance, see case studies digitally linked here.

4.3.1.2 Relative Temperature Effects

In addition to absolute temperature, stresses due to temperature changes, temperature rates of change, and spatial temperature gradients must be considered for hardware design, reliability predictions, and testing. The traditional thermal model will provide temperatures for the many parts of a component, assembly, or system by analyzing the sources of heat within a structure (which may be considered as static or changing in time) and by calculation of thermal diffusion rates to predict how heat will move through different materials and across interfaces. The relative temperature of parts can be used to determine physical distortions of the parts by "mapping" the temperatures over a corresponding structural model of the part being analyzed. Temperature gradients can significantly impact failure modes related to strain and diffusion along or across materials and interfaces. Further, the time scale of cyclical stresses, including heating and cooling, can impact failure modes.

When a material is heated or cooled, it will expand or contract, respectively. If the material is physically unrestrained, the material can expand or contract freely without generating internal stresses. The change is physical dimensions can be computed using the material's coefficient of thermal expansion,

$$\Delta L = L\alpha\Delta T$$

where ΔL is the change in length, L is the original length, α is the thermal expansion coefficient, and ΔT is the temperature difference between the final and initial states. If the material is restrained, such as being attached to a rigid surface, it cannot expand or contract, and internal stresses develop within the material. Under such thermal gradients, the internal stress produced can be computed from

$$\sigma = E\alpha\Delta T$$

where σ is the thermal stress and E is Young's modulus. The material's stress-strain curve will indicate the yield and ultimate stress at which point the material begins to fail. Thermal gradient

stresses of concern in hardware design include those within solder joints, composite-material booms, and booms and struts at the interfaces of dissimilar materials. For rapid heating or cooling, the surface of the material responds to the changing environment quicker than internal locations. The extreme case of thermal expansion stresses is thermal shock, where the heating and cooling is very rapid.

Temperature cycling induces stresses within an assembly. This occurs due to differences in the coefficient of thermal expansion of the various materials of which the hardware is constructed and the changing temperature gradients within the assembly being temperature cycled.

Thermal analyses may be conducted to predict temperatures and temperature gradients within a part or assembly and those temperatures may be mapped onto a structural model to predict resultant deformations and stresses. By modelling both absolute and relative temperature effects, material properties such as strength, ductility, and hardness may thus be assessed with respect to physics of failure modes. In some cases, other physical properties affecting failure can be predicted. These may range from availability and behavior of charge carriers (electrical) to changes in optical absorption or emission.

For additional insights and guidance, see case studies digitally linked here.

4.3.2 Thermally Induced Failure Likelihood

The probability of failure due to thermal effects (or other stressors) can be estimated by combining the Arrhenius (section 3.4.1) statistical mode with other relationships of relating stress to a life parameter relating operating time to probability of failure.

In the simplest case, the life parameter of interest is the mean time-to-failure (MTTF), or equivalently a failure rate $\lambda = \frac{1}{\mathrm{MTTF}}$, and the statistical model is the exponential distribution. This combined Arrhenius-exponential model can be found within MIL-HDBK-217F where the method of predicting failure rates is generally of the form

$$\lambda_p = \lambda_b \pi_T \prod \pi_{\mathrm{various}}$$

where λ_b is the base failure rate for the component in question, and λ_p is the predicted failure rate, derived by the multiplication of λ_b by π_T and various other π-factors describing the characteristics and operating conditions of the component [Defense, U. S. D. o., 1991]. π_T is notable as it describes the impact of junction temperature, T_j, on the predicted failure rate. It can be seen from the equation specified to derive π_T,

$$\pi_T = \exp\left[-C\left(\frac{1}{T_j + 273} - \frac{1}{298}\right)\right]$$

where C is a constant, that π_T is equivalent to $\frac{1}{AF}$, where AF is the acceleration factor described in section 3.4.1, if $C = \frac{E_a}{k}$, T_j is the use temperature, and 25°C is the test temperature used to establish λ_b.

Once a temperature-dependent life parameter, e.g. λ_p, is computed, it is straightforward to estimate the probability of failure for a given operating time as follows:

$$P(\text{failure in time t}) = 1 - e^{-\lambda_p t}$$

This approach can be generalized to any statistical model where one or more parameters are surmised to exhibit a temperature dependence. While the exponential-Arrhenius formulation is common due to its simplicity and indeed foundational to reliability models utilizing MIL-HDBK-217F or similar frameworks, other statistical models, such as the Weibull or lognormal distributions are generally more appropriate when assessing temperature dependence on probability of failure [Defense, U. S. D. o., 1991]. For Weibull-distributed data, the scale parameter θ (also known as characteristic life) is dependent upon temperature according to an Arrhenius relationship, while the shape parameter β is generally considered independent of temperature.

Substituting the Arrhenius relationship for θ in the Weibull cumulative distribution function results in:

$$P(\text{failure in time t, temperature T °K}) = 1 - e^{-\left(\frac{t}{Ae^{-\frac{E_a}{kT}}}\right)^{\beta}}$$

with k Boltzmann's constant and each of parameters A, E_a, and β either assumed known or estimated from data (e.g., via maximum-likelihood estimation).

A similar formulation can be used to adapt the lognormal or other location-scale family distribution to a temperature-dependent time-to-failure model. Where appropriate, other equations relating various stressors to life parameters can be combined with statistical models to estimate probability of failure in a similar fashion.

While the Arrhenius relationship is widely used in many applications, it does not apply to all temperature-acceleration problems, notably thermal cycling and transients, where the activation energy can change with the cycle count and cyclic extremes. The Arrhenius relationship is only adequate over only a limited temperature range [Meeker, 1998]. Furthermore, when estimating parameters for statistical models to predict probability of failure as a function of time and temperature, care should be taken to account for estimation uncertainty, as such uncertainty can be magnified when extrapolating from test to use conditions. Additionally, the choice of statistical model and stress-life relationship should be rigorously evaluated against all available data.

For additional insights and guidance, see case studies digitally linked here.

4.3.3 Thermal Failure Uncertainties

Thermal margins must be applied to cover the uncertainties inherent in predicted temperatures and to ensure a design is not allowed to operate at a temperature that is too close to a failure

threshold. These margins are part of the overall strategy for minimizing the probability of operational failures. To account for analysis and design uncertainties, temperature margin, or control authority margin on active thermal control systems like heaters or pumped cooling loops, must be maintained between temperatures predicted by a thermal model and the temperatures to which an operational unit is acceptance tested. To ensure design robustness, additional qualification margin is generally required and demonstrated by test. The quantitative values for these margins vary somewhat between various government and commercial organizations, but the concept of using margin as a failure mitigation strategy is common among them.

For additional insights and guidance, see case studies digitally linked here.

4.4 Fluid (Pipe Flow)

Fluid flow failure-inducing mechanisms (vibration/turbulence, impact, erosion/corrosion, and viscosity changes) can impact NASA systems in a multi-physics manner. These mechanisms can be evaluated via these TBD PoF techniques.

For additional insights and guidance, see case studies digitally linked here.

4.5 Electromagnetics (Wave Optics, Ray Optics, AC/DC)

Electromagnetic conditions internal and external to a space-system can cause failure in the form of interference, optical disruptions/aging, and short-circuits. These mechanisms can be evaluated via these TBD PoF techniques.

For additional insights and guidance, see case studies digitally linked here.

4.6 Structural Analysis Modeling

The purpose of structural analysis is to assess the likelihood of failure due to the physical/ mechanical stress and strain on the system. In general, there are two classes for these types of analyses. They are the inherent/nominal tolerance of the design to planned loads, Fatigue Analysis, and the residual/resultant tolerance after impairment or including nonconformances, Fracture or Damage Tolerance Analysis. The methodology applied to each analysis class is similar but has distinct variations as described below.

For additional insights and guidance, see case studies digitally linked here.

4.6.1 Fatigue Analysis

Fatigue or structural failure under cyclic loading analysis, in general, establishes the potential for fatigue or damage leading to failure under the loading conditions. Fatigue is the weakening of a material under periodic or cyclical mechanical loading events that result in failure or progressive structural damage, the formation of minute cracks, which can lead to eventual failure. Evaluation of fatigue involves determination of the mean (i.e., non-cyclic) and alternating (i.e., cyclic) stress

applied based on the geometry and loading, and the system's susceptibility to that loading and results in a determination of the failure risk based on a cumulative damage assessment. Various methods can be employed to make these stress or load spectra determinations:

a. Use of closed-form hand calculations when using simple geometry, such as those found in *Roark's Formulas for Stress and Strain* [Young and Budynus, 2002].
b. Measured test data from a component under appropriate loading (both cyclical and non-cyclical). Examples of an approach for random vibration, sine vibration and acoustic cyclic loading can be found in a legacy document prepared at NASA/GSFC: *General Fracture Control Plan for Payloads Using the STS* [Cooper, 1988].
c. Finite Element Modeling or other validated mathematical analysis tools. Examples include MSC and NX NASTRAN, Ansys, ABAQUS, and COMSOL.

When general stress results are obtained, they can be recalculated into the following forms for use in both Fatigue and Damage Tolerance analysis:

$$\sigma_m = \frac{1}{2}(\sigma_{\max} + \sigma_{\min}) \qquad \sigma_a = \frac{1}{2}(\sigma_{\max} - \sigma_{\min})$$

σ_m = mean stress $\quad$ σ_a = alternating stress

σ_{max} = maximum stress = $\sigma_m + \sigma_a$ $\quad$ σ_{min} = minimum stress = $\sigma_m - \sigma_a$

Material-based fatigue data, or the susceptibility of the material used, in the design to loading is determined by the S-N curve [Young and Budynus, 2002]. This is a plot of the magnitude of alternating stress versus the number of cycles to failure for a particular material. Typically, S-N curves for common materials are obtained through general literature searches. One common document used by NASA is *Metallic Materials Properties Development and Standardization* [Battelle Memorial Institute, 2020], where S-N curves are available for various metallic materials. Updated versions the document are produced yearly, the latest being *MMPDS-15* [Battelle Memorial Institute, 2020]. S-N curves can also be developed through specific fatigue testing, using various ASTM standards such as *Standard Practice for Conducting Force Controlled Constant Amplitude Axial Fatigue Tests for Metallic Materials* (ASTM-E466) and *Standard Test Method for Strain-Controlled Fatigue Testing* (ASTM-E606) [ASTM, 2015, ASTM, 2019].

Note: Before direct application of the alternating stress values to the S-N curve, one must also consider adjusting these values for the presence of the mean stress (i.e., the S-N curves are normally assessed assuming fully-reversed or $R = \sigma_{min}/\sigma_{max} = -1$ data, which by definition means $\sigma_m = 0$). To do this, the modified Goodman approach can be used, viz.,

$$\frac{\sigma_a}{\sigma_e} + \frac{\sigma_m}{\sigma_{ut}} = \frac{1}{FS}$$

where FS is the applied factor of safety, and the other variables are as described above [Shigley and Mischke, 1989]. Solving this equation for σ_e and equating this value to an updated alternating stress (call it σ_e'), allows one to then use this directly for S-N application in determining a corresponding number of fatigue life cycles.

Ultimately a cumulative damage assessment or the potential for failure determination is performed using the mean and alternating stress estimates (and associated number of cycles) and the correspondingly adjusted material S-N curve described above, using Miner's Rule [Shigley and Mischke, 1989]. In this method a total summation of these corresponding life cycles compared against the stress-inducing cycles determined allows one to perform a cumulative damage assessment for fatigue,

$$\sum_{i=1}^{k} \frac{n_i}{N_i} = C$$

where n_i = number of applied stress cycles at each stress level and N_i = allowable fatigue life at each corresponding stress level. The approach is then to compare the summation of these ratios to that of an experimentally determined failure factor, which is normally set to 1.0. If the summation is shown to be less than 1.0, additional fatigue life is present with the component under the mission loading, and it will withstand the life of the mission. If the summation is shown to be greater than or equal to 1.0, no additional fatigue life is present for the component, which will likely fail under cumulative mission loading.

For additional insights and guidance, see case studies digitally linked here.

4.6.2 Damage Tolerance (Fracture) Analysis

A damage tolerance analysis involves many of the same evaluations of the mean (i.e., non-cyclic) and alternating (i.e., cyclic) stresses applied based on the particular geometry and loading and the system’s susceptibility to that loading, as described above. This results in a determination of crack growth potential versus a cumulative damage assessment.

In a damage tolerance assessment, material-based crack growth (or propagation) data is utilized versus S-N fatigue data to establish the system’s susceptibility with existing flaw size and critical crack size or geometric case to make its determination. For material-based crack growth (or propagation) data, specific testing is performed to measure the change in the characteristic length of a predetermined crack (“a”) versus the number of cycles under cyclic loading (at a particular R value). As part of this testing, a parameter called the stress intensity factor (K) is also calculated, which describes the stress state near the crack tip caused by the cyclic load. In general, this is written as

$$K = \sigma \sqrt{\pi a}\, f(a/W),$$

where σ is the stress, and f (a/W) is a geometry-dependent function of the crack length, a, and the specimen width, W. With knowledge of the K-value at each cycle, a crack propagation curve can be developed for use in the damage tolerance assessment. This shows the relationship between the change in the crack size with number of cycles versus the change in the stress intensity factor K, or a da/dN versus ΔK relation. A general crack growth equation is then fit to this third-order polynomial function and used in the crack propagation prediction (see below). This takes the general form of the Paris' Law, where C and m are fit parameters:

$$\frac{da}{dN} = C(\Delta K)^{m}$$

Further, from the available test data, the material-dependent property fracture toughness (K_c) is typically established to define the stress intensity factor above which unstable crack propagation occurs. Testing for this intrinsic property is also performed explicitly; see *Standard Test Method for Measurement of Fracture Toughness* and *Standard Test Method for Measurement of Initiation Toughness on Surface Cracks Under Tension and Bending* for examples [ASTM, 2020].

Flaw size, a measurable crack size (a_o), is established by using one of various nondestructive evaluation (NDE) techniques for each piece of assessed hardware. NASA-STD-5009, *Nondestructive Evaluation Requirements for Fracture-Critical Metallic Components* [NASA, 2019], details the NDE methods such as magnetic resonance, ultrasonic, and dye-penetrant inspection. Due to the resolution of each method, minimum detectable crack (or flaw) sizes are established based on a 90/95 % probability of detection (90% probability of detection with 95% lower confidence bound). Depending on the NDE method and geometry type, these minimum sizes are then used as the initial crack size for the damage tolerance assessment.

Critical crack size, a_c should be determined using the appropriate shape function assumption to determine when cracks will grow with added stress or spontaneously. For example, the Griffith's crack growth equation can be used with the material's fracture toughness, K_{IC}, if a shape factor of 1 is appropriate:

$$a_c = \frac{1}{\pi}\left(\frac{K_{IC}}{\sigma_{max}}\right)^2$$

Note: If the size of the crack at any time, a_n, reaches a_c, there will be spontaneous catastrophic crack growth through the material.

Using the parameters above and the fatigue crack propagation law (below) the crack growth rate (da/dN) and fatigue life (Failure cycles, N_f) can be estimated:

$$N_f = \int_{a0}^{af} \frac{da}{C(\Delta K)^m}$$

As with a fatigue assessment, the large uncertainty associated with the crack propagation data necessitates the use of a 4x multiplier on the loading spectra (i.e., mission life cycles). Results from the analysis indicate if the crack case geometry under the applied loading spectra shows an unstable crack growth from the initial flaw (a_0 will exceed the critical crack size during the mission). If not, the part is deemed damage tolerant to the mission-specific cyclic loading (cycles to failure (N_f) < mission cycles).

Typically, though, a crack growth prediction tool, like NASGRO®, is used for the assessment and enables (i) crack-case and initial flaw size, (ii) appropriate material data, (iii) loading spectra, (iv) analysis parameters, and (v) output data requests.

For additional insights and guidance, see case studies digitally linked here

4.6.3 Creep

Creep (also referred to as cold flow) phenomenon of a solid material to dimensionally changing via slow deformations while subject to persistent stress which can lead to failure-inducing mechanisms (solder joint breakage, mechanical inference, fracture, diffusion) that can impact NASA systems in a multi-physics manner. These mechanisms can be evaluated via these TBD PoF techniques.

For additional insights and guidance, see case studies digitally linked here.

4.7 Acoustics

Sound exposure from a system itself or its exposure from other sources can cause failure by such multiphysical processes as exciting harmonics, inducing structural damage, initiating vibration damage to hardware that can cause software faults, and more. These mechanisms can be evaluated via these TBD PoF techniques.

For additional insights and guidance, see case studies digitally linked here.

4.8 Chemical (Batteries and Fuel Cells, Electrodeposition, Chemical Reactions)

Chemicals inherent in designs can limit design life due to the nature of the chemical reaction being used (e.g., battery degradation), while the exposure to certain chemicals in the operational space environments can cause irreparable damage or degradation to optics, structures, and electronics. These mechanisms can be evaluated via these TBD PoF techniques.

For additional insights and guidance, see case studies digitally linked here.

4.9 Radiation Physics of Failure in Semiconductors

Radiation effects on semiconductor devices and Integrated Circuits (ICs) generally fall into two types of physics of failure models – non-stochastic (wear-out events like parametric shifts) and stochastic (random events like bit flips). Total Ionizing Dose (TID) and Total Non-Ionizing Dose (TNID) are cumulative, which make them fundamentally different from the instantaneous Single Event Effects (SEE) caused by a single random particle strike. Radiation environment predictions and susceptibility analyses are empirically driven, and therefore call upon a number of methodologies to assess mission risks. The contents that follow provide an explanation of physical mechanisms that are the root cause of these different families of effects as they are understood in susceptible technologies. This section's content and more are covered in *Avionics Radiation Hardness Assurance (RHA) Guidelines* [NASA, 2021]. In that document, further categorization of irreversible processes vs. reversible state changes are covered in detail, and guidance on how to carry these responses and failure modes into analysis of higher-level system failures is suggested. This document section seeks to define the types of failures and, when applicable, how deeper analysis using physics of failure can be done to understand system impacts.

4.9.1 Total Ionizing Dose (TID)

TID is the absorbed dose in a target material caused by energy deposition of ionizing radiation, i.e., charged particles in the natural space radiation environment. The absorbed energy results in the creation of electron-hole pairs within the semiconductor and insulating materials (e.g., oxides). TID amounts are communicated by energy deposited per unit mass of medium, which can be measured via the SI unit, Gray (1 Gy = 1 J/kg), or more commonly in the US radiation community, as rad (1 rad = 100 erg/g). The absorbed dose depends not only on the incident radiation but also on the absorbing material, so absorbed dose must be reported as a function of target material (e.g., rad(SiO_2) or Gy(Si)). Dependence on target material is one complicating factor that can make TID more difficult to assess for an entire system. In the space environment, TID usually results from exposure to protons, x-rays, and electrons over the entire mission duration from both trapped radiation in planetary magnetic fields and Solar Particle Events (SPEs). Bremsstrahlung (energetic photons), secondary radiation produced when primary radiation is slowed or stopped, can dominate the TID exposure in heavily shielded environments.

<u>How TID Mechanisms Manifest</u>

An energetic particle incident on a material can ionize target atoms, producing electron-hole pairs within the semiconductor and insulating materials (e.g., oxides). Some of this charge is trapped in insulators or leads to the formation of interface traps at the semiconductor-insulator surface. TID mechanisms are an accumulation of many electron-hole pair creation and charge trapping which typically occur gradually over mission lifetime. TID exposure is always time-dependant, and conditions at which devices start to behave anomalously may have an abrupt onset or appear gradually depending on the trapped charge locations and device functions. Figure 10 shows how charge creation leads to charge migration and eventually permanent trapping in metal oxide semiconductor (MOS) structures.

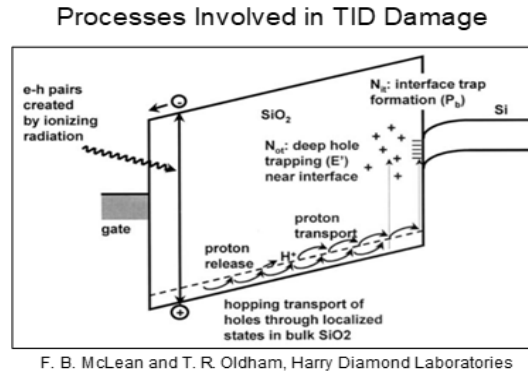

Figure 12. Process of TID damage occurring in MOS structures

Examples

The following (non-exhaustive) list contains some of the ways devices are affected by TID which may result in unexpected or erroneous operating conditions or failures:

- In complimentary metal-oxide-semiconductor (CMOS) structures, TID creates trapped charge in the oxide or near the oxide semiconductor interface which causes a shift in the gate threshold voltage, resulting in a reduction in threshold voltage for N-type MOS devices, or an increase in voltage threshold for P-type MOS devices.

- In isolation oxides, TID can create leakage pathways, resulting in parasitic power consumption which may result in other functional complications.

- In bipolar devices, trapped charges along isolation or passivation from TID can increase surface recombination, decreasing the gain of bipolar transistors. If the trapped charge density is high enough, an inversion layer can be created in p-doped regions that increase the surface area of the junction. This also affects transistor gain and can cause substantial increases in leakage current.

- Bipolar and bipolar-CMOS (BiCMOS) technologies can also suffer from enhanced low dose-rate sensitivity (ELDRS), where device electrical parameters can degrade more under low-dose-rate conditions (e.g., the natural space environment) than under high-dose-rate conditions (this is important for consideration of accelerated/standard TID testing).

TID is a cumulative effect that will often look like ageing or wear out of parametric outputs of the device that depend on oxides, interfaces, passivation, etc. Most high reliability devices show graceful degradation that is predictable and repeatable, therefore past data can be useful if there are no changes to the manufacturing process, while other devices may show more lot-to-lot or part-to-part variability. As IC complexity goes up parametric shifts on chip can result in devices that stop operating completely without external connections to measure the parametric degradation that leads to failure.

For additional insights and guidance, see case studies digitally linked here.

4.9.2 Total Non-Ionizing Dose (TNID)/Displacement Damage Dose (DDD)

An energetic particle can also cause damage within materials via the creation of phonons (vibrational energy) as well as the displacement of atoms within a crystalline lattice. The introduction of defects through displaced atoms (i.e., termed displacement damage) can significantly impact fundamental material properties such as recombination lifetime. TNID or DDD (D_d) has units of MeV/g, energy per unit mass. It is typically given in terms of the product of total particle fluence (ϕ) and the Non-Ionizing Energy Loss (NIEL) factor, representing the nonionizing energy loss via displacement damage and resulting in the $D_d = \phi \times NIEL$. NIEL factor is typically expressed as (MeV-cm^2/mg) representing the rate at which nonionizing energy is lost to the production of atomic displacements in a given material. Like TID, the NIEL factor (and thus overall TNID damage) is dependent on the incident particle and energy, and the absorbing material.

<u>How TNID/DDD Damage Mechanisms Manifest</u>

When atoms are dislodged from within a lattice, a pair of defects is created, whereby the absence of the atom within the lattice is referred to as a vacancy and the dislodged atom within a non-lattice position is referred to as an interstitial. Depending on the amount of energy transferred to the original displaced atom known as the Primary Knock-on Atom (PKA), the PKA can in turn displace additional atoms, creating a cascade of the defects that form localized clusters of disorder. Therefore, defects created from TNID can create either isolated defects or a combination of isolated and clustered defects, which will vary in stability as well as the impact to material characteristics. Following generation, these defects can anneal to form stable configurations, which are temperature and excess carrier dependent. Like TID, TNID is a exposure/time-dependent phenomena, which can also depend on temperature during irradiation and subsequent storage. Figure 11 demonstrates the potential defects created in a crystal lattice via TNID.

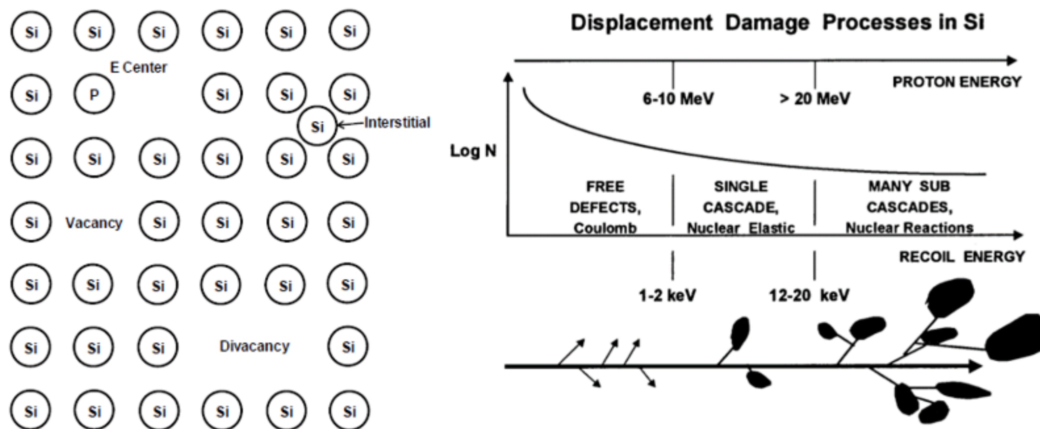

Figure 13. Potential Isolated Defects in Silicon induced by Incident Particle

Examples

The following (non-exhaustive) list contains some of the ways devices are affected by TNID which may result in unexpected or erroneous operating conditions or failures:

- In Charge Coupled Devices (CCDs), TNID damage can result in degradation in Charge Transfer Efficiency (CTE) as trapped charges are released as time constant depending on the energy state of the trap. Increased dark current resulting effectively in increased "noise" within a device, Hot Spots, which manifest as "bad pixels" or bright spots on imaging devices.

- TNID induces damage in CMOS Image Sensors (CIS) where damage can manifest as dark current, increased hot spots, as well degradation in responsivity.

- TNID damage in Photodiodes can act as recombination/generation centers, which can result in degradation of the photocurrent or a generation of excess current, which can appear as dark current.

- Within Laser Diodes, TNID creates increases in non-radiative recombination centers, which results in decreased output power, typically drawing higher to maintain consistent power.

Special attention should be called to the susceptibility of opto-electronic devices to TNID. Phototransistors, photodiode detectors, and light-emitting diodes all degrade due to introduction of generation and recombination centers. The light output of LEDs is reduced, the optical responsivity of photodiodes and phototransistors is degraded, the leakage current increases in diodes and transistors, and the phototransistor gain is reduced. In some devices, cumulative damage due to TNID far outstrips damage due to TID. Devices that inherently depend on material properties (e.g., recombination lifetime, carrier concentrations) will typically be more susceptible to DDD effects.

TNID is a cumulative effect that will often look like ageing or wear out of material properties within the device that depend on lattice structure. Most high reliability devices show graceful degradation that is predictable and repeatable when there aren't manufacturing changes, while others show lot-to-lot or part-to-part variability. Due to sensitivity and operation some devices or portions of the device may stop operating completely.

For additional insights and guidance, see case studies digitally linked here.

4.9.3 Single Event Effects (SEE)

SEEs are memoryless stochastic (i.e., Markov) processes; their probability in the mission depends on the specific component's susceptibility and the local/temporal radiation environment, but not previous (mission) history. SEEs are caused by interaction of a single primary or secondary ionizing particle (e.g., proton, neutron, or heavy ion) within a semiconductor part. All semiconductor parts containing p-n junctions (referred to as "active electronics."), with natural or

applied electric fields are potentially susceptible to SEE [Petersen, 2011]. SEE can be destructive or non-destructive. Destructive effects are typically instantaneous catastrophic failures to short or open and are non-recoverable. Non-destructive effects are typically recoverable, where parts or components will regain functionality or operability naturally or through user-intervention (e.g., power-cycling). However, non-destructive effects can potentially cause non-recoverable system-level effects if not accounted for in designs.

SEEs are usually discussed with reference to the susceptibility to the incident ionizing particle using the term Linear Energy Transfer (LET). LET is the measure of the ionizing energy deposited per unit length as an energetic particle travels through a material, while accounting for the energy and mass of the incident particle and the material properties of the target material, and has units of MeV/cm^2-mg. LET can be expressed as the incoming particle stopping power normalized to the target material density. Many SEE types only occur above a certain LET threshold (LET_{th}), which dependent on several factors including individual device, and SEE type, and operating conditions (e.g., operating temperature, input voltages or current). For example, most RHA standards will require that destructive SEEs must have an LET_{th} > 75 MeV/cm^2-mg.

How SEE Mechanisms Manifest

Ionizing particles passing through a semiconductor lattice lose energy through Coulombic and nuclear processes. This lost energy generates excess electron-hole pairs in the semiconductor, inducing a current if the charge is generated in or near electric fields and changes the nominal electric fields. While some of the electron-hole pairs will recombine, the remaining charge can get swept into the junction contacts. If the resulting charge generated exceeds the critical charge of the device, it can result in immediate observable effects in device operation (SEE). The observed effect from SEE depends on device type, operating conditions, and circuit configuration. Figure 12 shows a p-n junction and an ion strike that creates a charge funnel (i.e., liberated charge or electron-hole pairs) that propagates as an SEE disturbing nominal operations.

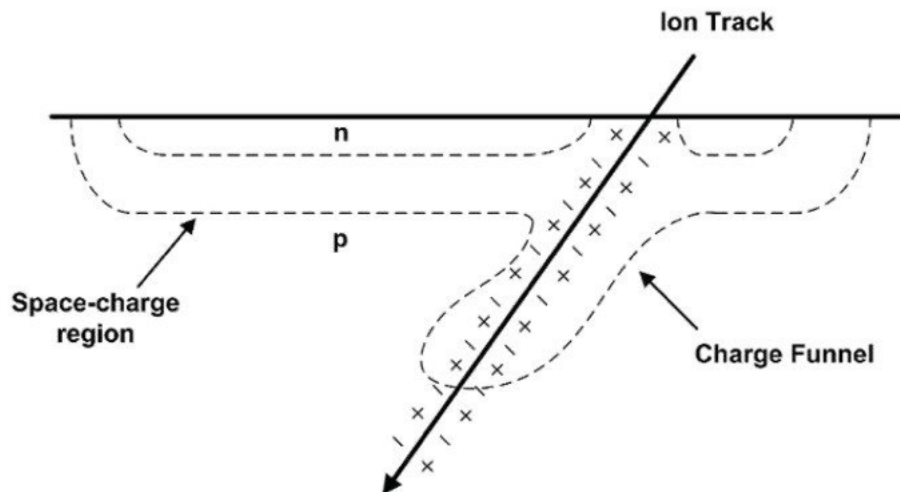

Figure 14. Ion entering the depletion region of a biased p-n junction resulting in a charge funnel.

Destructive Examples

Destructive SEE types include Single-Event Latchup (SEL), Single-Event Dielectric Rupture (SEDR), Single-Event Gate Rupture (SEGR), Single-Event Burnout (SEB), and permanently stuck bits. The following (non-exhaustive) list contains some of the ways devices are affected by SEE which may result in unexpected or erroneous operating conditions or failures:

- CMOS-based devices can experience SEL, which results in a sustained high current state that can cause thermal runaway and can damage the affected device as well as other devices in the current path. The high current state caused by SEL can be recovered from by power cycling the affected device.

- Power devices can experience SEB and SEGR, which result in permanent loss of device functionality.

- On chip capacitors can suffer arcing or SEDR.

Non-Destructive Examples

Non-destructive SEE types include Single-Event Transient (SET); Single-Event Upset (SEU), including Single-Bit Upset (SBU) and Multiple-Cell Upset (MCU); and Single-Event Functional Interrupts (SEFI). Multiple-Bit Upset (MBU) refers to single event upset of multiple cells in the same logical word or frame occurring from one particle [JEDEC, 2017]. The following (non-exhaustive) list contains some of the ways devices are affected by SEE which may result in unexpected or erroneous operating conditions or failures:

- Bits in memory devices can be flipped by SBU or MBU. Error Detection and Correction (EDAC) software can sometimes be used to fix flipped bits effectively.

- When an SEU occurs in registers, or control circuitry has an unexpected change of state, Single-Event Functional Interrupts (SEFI) can occur, rendering the device unresponsive, causing a reset, changing the operating mode, adding offset Analog-Digital Converters, etc. SEFIs can typically be recovered from by power cycling or reloading the device's programming. If not planned for, power cycling at a higher architectural level may not be able to fully power cycle or remove the SEFI.

- SET are deviations from expected outputs or nominal outputs on devices that are temporal. They are typically short-lived (lasting nanoseconds to milliseconds) and may be small or large excursions from nominal, however, extreme or long-lived excursions may exceed downstream circuit limitations and can therefore be destructive (e.g., tight tolerance applications such as FPGA cores).

SEE is an evolving field that encompasses a wide range of failure mechanisms and anomalous behaviors in EEEE parts. As new devices are developed and tested existing taxonomies, classifications, acronyms, and terminology are not always consistent. As a reference, SEE type

definitions exist within standards and literature [ASTM, 2018; JEDEC, 2017; ESCIES, 2014; Petersen, 2011; JEDEC, 2013].

For additional insights and guidance, see case studies digitally linked here.

4.9.4 Analysing Radiation-Induced Failure Modes

Semiconductor and IC failures induced by radiation can manifest very differently for cumulative effects and SEE. The responses not only depend on the type of radiation the part has been subjected to, but also the technology and its materials within. Some radiation effects may cause physical damage, but not immediate failure, however the integrity and reliability of the device operation may be hindered afterwards. Both cumulative and instantaneous effects will be explored in the following sections, with discussions on how effects can propagate through a system or component and how risk and radiation hardness assurance are evaluated. In all cases, the assessment of potential failures must look at the design implementation and requirements to determine if radiation induced changes to device operation (reversible or non-reversible) are considered a failure. There exist many applications and mitigation techniques that provide system tolerance to reversible effects. The design architecture plays a crucial role, and the criticality of the device operation and function will determine the fidelity or extent of analysis required. Through radiation hardness assurance practices, an iterative approach of looking at a system's sensitivity to possible failure modes in the selected technologies will reduce the number of tests and increase reliability overall.

For additional insights and guidance, see case studies digitally linked here.

4.9.4.1 Cumulative Radiation Effects Failures

Cumulative radiation effects are first addressed as a deterministic problem of expected environment doses and inherent shielding profiles. Statistically bounding estimates of dose are made with simple geometries and predictive environment models. The environment models are built and updated from in-situ measurements by a growing number of science instruments, allowing for confidence levels on the expectations. In some cases, devices (e.g., rad-hard components show guaranteed hardness on their datasheet) have sufficient margin such that more analysis is not necessary. If the parts are well shielded or the environment is benign with respect to the performance of a technology/family of devices, deeper analysis is typically not required. First principles of parametric shifts (threshold voltages, leakage currents, etc.) and what they mean to the system can further help to identify where more analysis is needed (e.g., transistors used as a switch with a gain of 1 will not care about gain degradation from 400 to 300 over the mission dose). Where deterministic evaluations are insufficient (i.e., lack of margin), probabilistic methods can be used, however applicable test data must be available.

In cases where the margin between part survivability and failure is tight for cumulative effects, high-fidelity modelling and ray-tracing methods can be used to obtain a clearer understanding of the dose on specific parts and components. Theses modelling efforts can account for complex shielding geometry within spacecraft, providing a much more precise dose estimate and reducing the bounding estimate for expected failure. This high-level modelling is relatively time-

consuming compared to models obtained via simple spherical geometry but is often far more cost-effective than pursuing probabilistic methods (i.e., testing).

When the mechanisms or physics of failure are not understood (e.g., new technologies, new applications), subject matter expertise and testing may be made necessary. This is especially true for cumulative effects, where results tend to be more lot specific: small changes in the manufacturing process can result in large radiation response changes (e.g., oxide thickness, interface imperfections, passivation layer materials).

4.9.4.2 Cumulative Radiation Effects Failures in a System

At the system level, TID/TNID hardness assurance is based on understanding degradations at the piece-part level and how they may impact system operation. This is a methodology to assure that microelectronic piece-parts meet specified requirements for system operation with sufficient margin, such that further analysis is not required. The requirement for system operation allows for a failure definition that is determined by the application of all parts in the system. The requirement to meet functional requirements at a specified radiation level allows a deterministic approach to approving a total system that has margin in its operation constraints.

In the methodology described in Figure 13, based on MIL-HDBK-814, all the microelectronic piece parts are categorized for each system application and localized radiation environment. For any system's piece-part hardness assurance program, designers and RHA engineers must start with the application of the part in the system and its necessary functions. The application will determine the failure level of the part that has the potential to propagate to a system level.

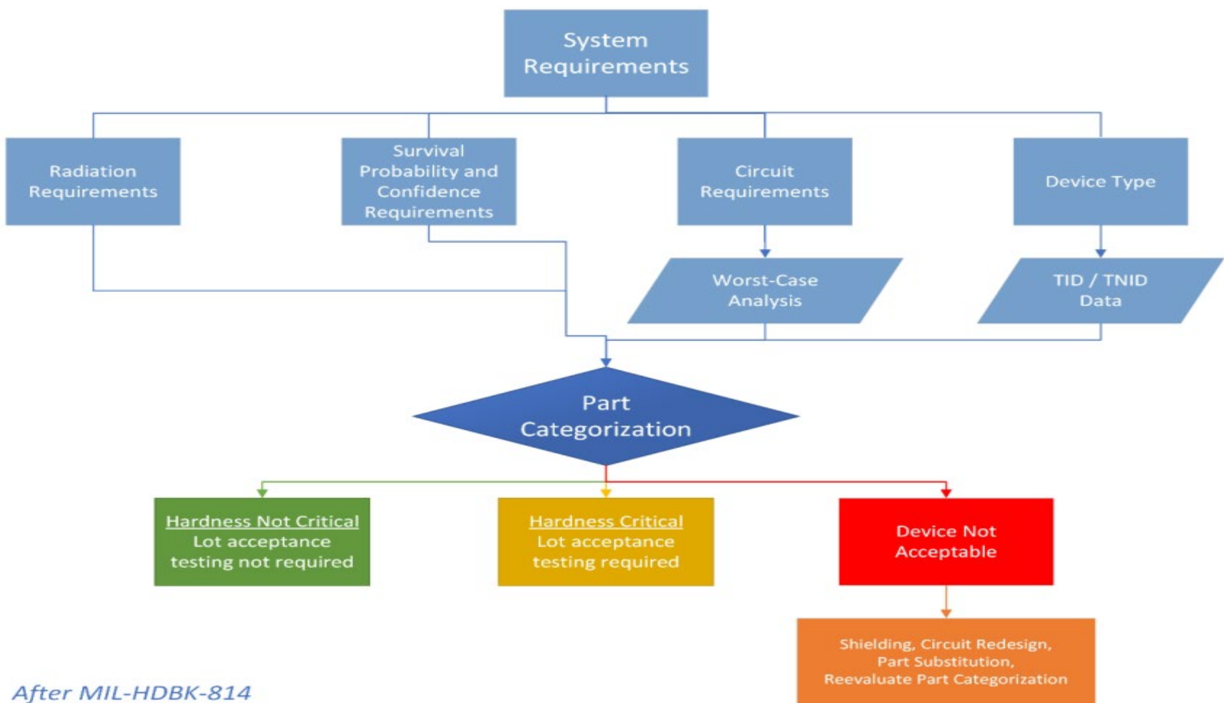

Figure 15. Piece-Part RHA Methodology (adapted from Poivey, 2017)

There are three categories in which a part may be placed: (1) Hardness Non-Critical (HNC), (2) unacceptable, and (3) hardness critical. This can be determined at different

(1) For parts that are categorized as HNC, no further testing or analysis is required.

(2) For parts that are categorized as unacceptable then either a different part must be used in the application or mitigation factors must change. The factors that may be changed include:

- Radiation specification level using shielding and/or more detailed radiation transport analysis (i.e., ray-tracing).
- Failure definition through application circuit redesign.
- Radiation failure level through part substitution, application condition, hardening of the part, or specific lot selection.

(3) For parts that are categorized as hardness critical analysis may require more detailed analysis for both radiation transport and performance predictions. When it does come to needing higher fidelity or detailed analysis there exist probabilistic methodologies to ensure hardness assurance at the piece-part level in the following section.

4.9.4.3 Cumulative Radiation Effects Failures in a Part or Component

For components or parts categorized as hardness critical, their mission environment application and lifetime will all play a role in their predicted performance. As previously discussed, cumulative degradation through TID/TNID are time-dependent phenomena. In select circumstances, hardness assurance will call for ground-based testing or test data. It should be clearly understood that cumulative radiation degradation effects cannot be mitigated by redundancy between devices, as multiple devices will still experience the same degradation over time (this is true for biased and unbiased devices). The most used mitigation strategy for cumulative radiation degradation effects is varying shielding, which will be discussed further. Determination of the probability of failure can be understood as product of the expected probability distribution lifetime mission dose (either TID or TNID) and the expected probability of parametric failure of a device.

During mission planning (i.e., pre-phase A), an environment must be defined for radiation analysis to proceed. Radiation environments are typically defined by the orbital parameters and mission duration, although additional factors also affect the radiation analysis, such a mission featuring direct insertion, phasing loops, or variations on transfer method. Any changes in these mission parameters will also incur a change in the radiation environment. Once a radiation environment is defined, a probability function for dose can be generated. As an example, figure 14 shows the probability distribution function for a 1-year GEO mission with varying levels of shielding and confidence levels ranging from 1% to 99%. This probability distribution function for the radiation environment can be referred to as H(x). The probability that a device exceeds this dose can be seen as 1-H(x). Shielding levels from right to left, are 10, 50, 100, 200, 500 and 1000 mils Al.

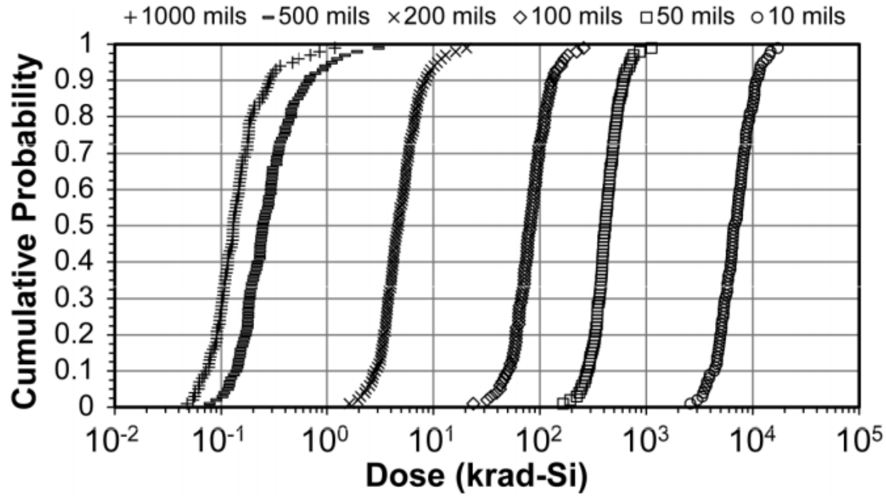

Figure 16. TID Probability Distributions

After a radiation environment is defined, devices are reviewed, selected, and tested based on expected mission dose and parametric failure concerns. Although parts are usually screened for failure prior to selection, some devices may be tested if part behavior in the radiation environment is not thoroughly understood. Through lot testing, the parametric failure distribution of a device can be determined. Figure 17 displays the parametric failure distribution of the SFT2907A bipolar transistor, based on test of ten devices. A lognormal fit of the data can then be taken as the Cumulative Density Function (CDF) of the parametric device failure. This Total Dose device failure distribution can be referred to as g(x). The line is a lognormal fit to the data

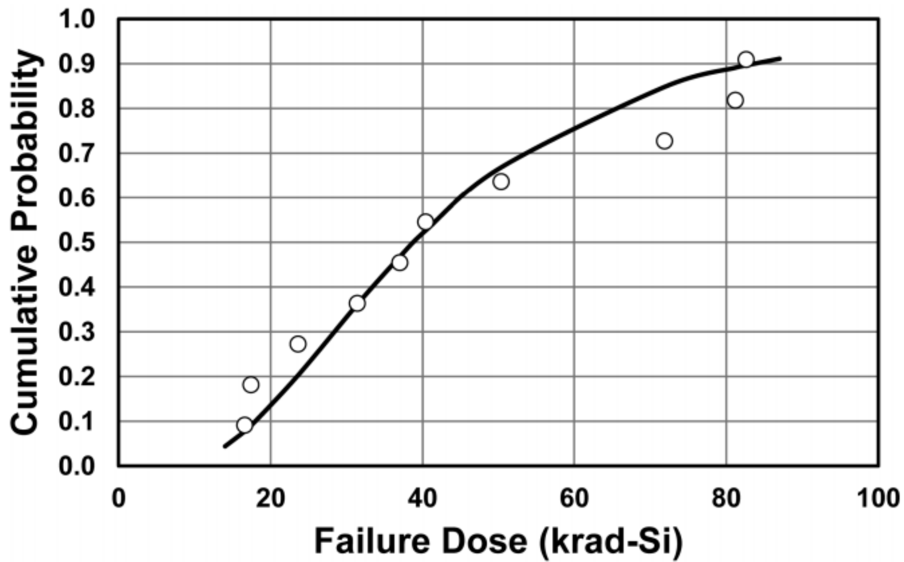

Figure 17. TID Failure Distribution for SFT2907A Bipolar Transistor

Once both distributions have been determined, the distributions can be combined to obtain the probability for device failure during the mission for a dose interval of x to x + dx, as given by the equation:

$$[1 - H(x)] \cdot g(x)\,dx$$

Integrating over all possible dose values gives the total dose failure probability, P_{fail}, during the mission:

$$P_{fail} = \int [1 - H(x)] \cdot g(x)\,dx$$

It should be noted that in cases where parametric failure distribution is much higher than expected mission dose, P_{fail} will be close to 0, and, conversely, where parametric failure distribution is much lower than expected dose, P_{fail} will be close to 1. In cases where the distributions overlap, P_{fail} will between 0 and 1. An example of probability of failure distribution with respect to device shielding can be seen in figure 16, where device failure is shown for multiple orbits of the bipolar transistor example from figure 15.

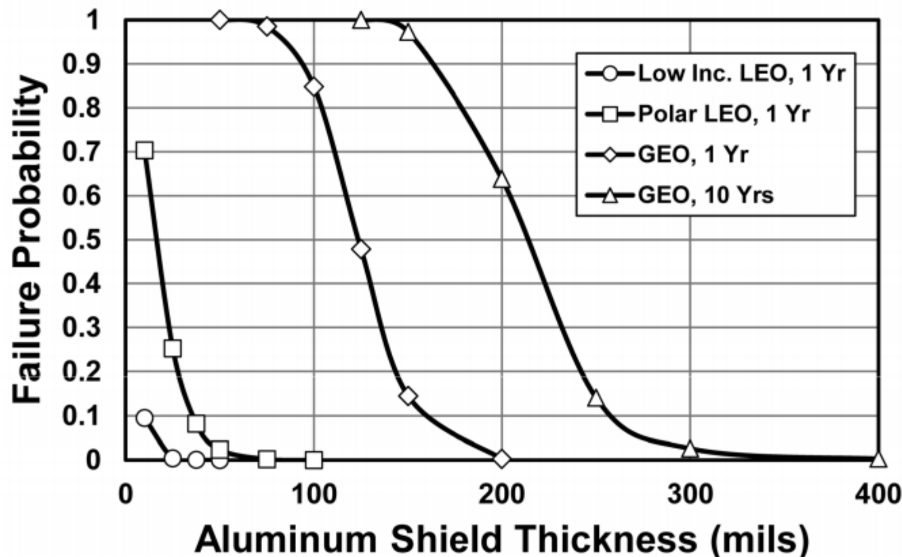

Figure 18. Failure Probabilities for the SFT2907A Bipolar Transistor as a Function of Shield Thickness for Different Orbits and Mission Durations

The example of the transistor used, is a simplified case, but shows how failure distributions of parts and the confidence levels on the environment can be used to determine the probability of success for any given device parameter or sensitive application if ground-based data exist for TID/TNID/DDD.

For additional insights and guidance, see case studies digitally linked here.

4.9.5 Instantaneous Radiation Failures (Single Event Effects)

Instantaneous radiation effects are handled differently than the cumulative counterpart. Due to the permanent loss of device function caused by destructive SEE, the typical focus of SEE hardness assurance is selection of parts insensitive to destructive SEE and system tolerance of non-destructive effects where they are unavoidable. Failure likelihood of recoverable and non-recoverable effects are different to one another. Categorization of failure depends on a part's response in its application, and the effect it has on system availability/operability; it depends on the function required of the part and the mode of failure/disruption to mission goals.

The deterministic approach is to establish a LET_{th} requirement structure for types of events such that anticipated likelihoods are low enough to accept the risk of the response (e.g., no destructive thresholds less than 75 $MeVcm^2/mg$). Where this approach is insufficient for risk posture (or parts lack data), further mitigation, analysis and/or testing may need to be done. Often misinterpreted, shielding has limited effectiveness as a mitigation for single-event effects, which can be induced by deeply-penetrating, high-energy particles (e.g., Galactic Cosmic Rays). SEE analysis begins with device application and function within the system, and whether or not propagation of effects has an impact. If a given application is not susceptible to a device response or failure, having mitigation for the effect, or some level of redundancy, no further analysis is necessary. System tolerance and/or mitigation takes the form of fault isolation, detection, and recovery; EDACs; filtering circuitry; power-cycling; current limiting; and other techniques to mitigate or eliminate any effect on broader system operation. Where the application cannot be deemed acceptable or the response impact on propagation cannot be explained piece-part testing for the application may be necessary.

For additional insights and guidance, see case studies digitally linked here.

4.9.5.1 Instantaneous Radiation Effect Failures in a System

Understanding the ability of a SEE response/failure to propagate from a device level through to the system level allows for the categorization of "criticality classes" that can express the unintended operation or part failure at a functional level. By categorizing the functions and addressing which components play a role in providing that function, a lot of SEE concerns can be addressed at the system level without further analysis.

- Error-Critical: functions where SEEs are unacceptable. Part failure in this system would endanger the mission irrevocably:
    - Power management parts/ICs throughout the mission: no destructive effects allowed, due to the dependence on sub-system functions across system.
    - Guidance, navigation, and control electronics during critical maneuvers (e.g., docking; entry, descent, and landing; touch-and-go; orbit changes, etc.): no allowable interruptions to availability during these windows.
    - Environmental control and life support systems throughout the mission.
- Error-Vulnerable: functions where low probability for SEE is required, response with mitigation or risk of SEE is permissible.
    - Power management parts/ICs: single event transient of sufficient magnitude may reset a box or card at the wrong time.

  - Data transmission: SEFI impact on availability during downlink over ground station.
  - Mission Processor (embedded or standalone) with known error rate may be vulnerable at specific times during the mission.
- Error-Functional: functions may be unaffected by SEE; large probability of events may be acceptable.
  - Data retention: memory storage can reliably detect and correct errors without loss of information.
  - Data transmission: transient effects or loss of packets acceptable for telemetry having continued measurements.

Gathering the system susceptibilities in an analysis such as a SEE Criticality Analysis (SEECA), will capture failures for a mixture of non-destructive and destructive effects, using system level functions to identify and categorize impact of SEE. Figure 19 shows a decision tree for the categorization of criticality/severity of SEE response:

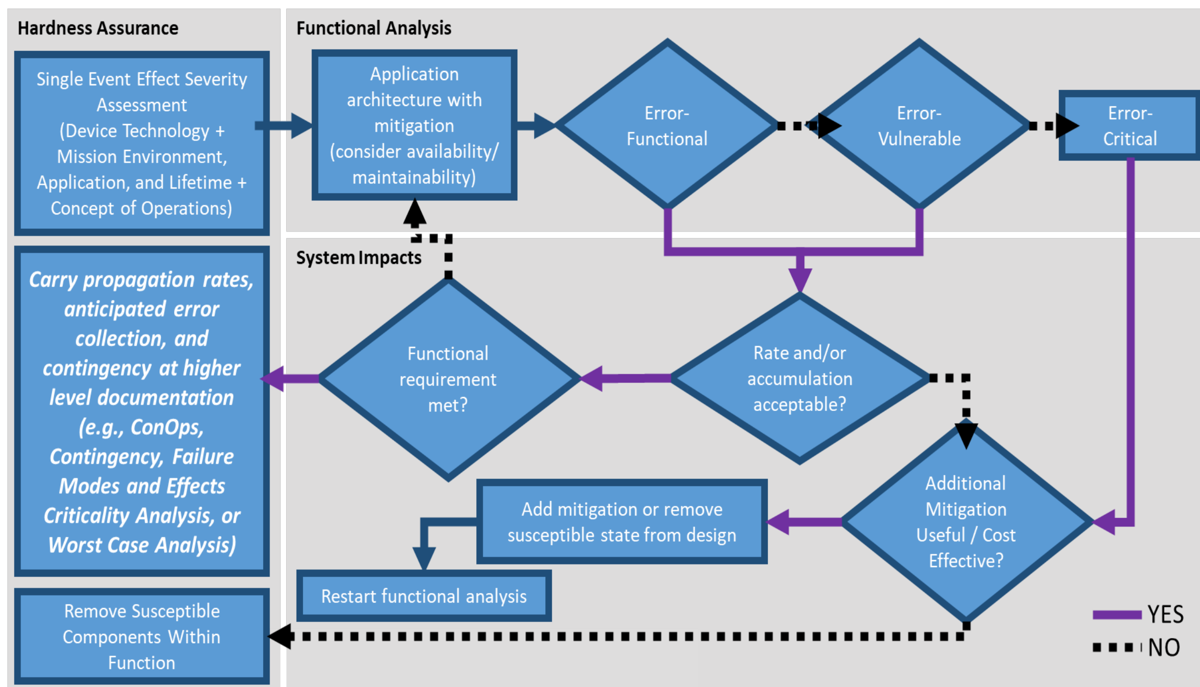

Figure 19. Example of a SEE Severity Flow Diagram

Likelihood calculations can then be reduced to the susceptibilities within the system that propagate, and the rate of upsets for the single event signatures that are impactful can be calculated and compared to required availability for success.

4.9.5.2 Instantaneous Radiation Effect Failures in a Part or Component

As previously discussed, failures from SEE are modeled as memoryless stochastic (i.e., Markov) processes, whose probabilities depend on the specific device and the local radiation environment, but not previous (mission) history. As such, the probability of an SEE occurring is constant

throughout the entire mission (notwithstanding changes in environment and/or device operating conditions). Failure from SEEs is typically defined based on the function of the devices and if the SEE is a soft or hard error. Failure definitions for soft errors include that the probability of outage/downtime during a particular window of time is less than a critical value or that the rate of bit-flips is sufficiently low. Failure definitions for hard errors include that the probability of a hard error occurring over the entire mission be sufficiently low. SEEs can be mitigated against through careful part selection, deliberate choice of operating conditions, or by using redundancy between devices, boards, and subsystems.

The mission radiation environment is typically defined at the outset of mission planning. Factors including orbital parameters, mission duration, and others are used to simulate the expected radiation environment. Changes in these factors can cause changes in the radiation environment. For SEEs the most important aspects of the radiation environment are Galactic Cosmic Rays (GCRs), Solar Energetic Particles (SEP), trapped protons, and solar protons. These radiation sources are condensed into LET spectra, which show the expected flux for all particles based on their LET. Figure 18 shows some LET spectra for a near-Earth interplanetary orbit. LET spectra is affected by the solar cycle, so spectra at both solar maximum and solar minimum is shown. Spectra is also shown for Solar Particle Events, with spectra prediction for the worst possible day and 5-minute period of a solar particle event. As can be seen, LET spectra is several orders of magnitude higher during solar particle events than during nominal periods of activity, when GCR contribution dominates. As such, care must be given when evaluating rate calculations whether device operability and availability is required, i.e., if the device is required to operate during the worst periods of a solar storm.

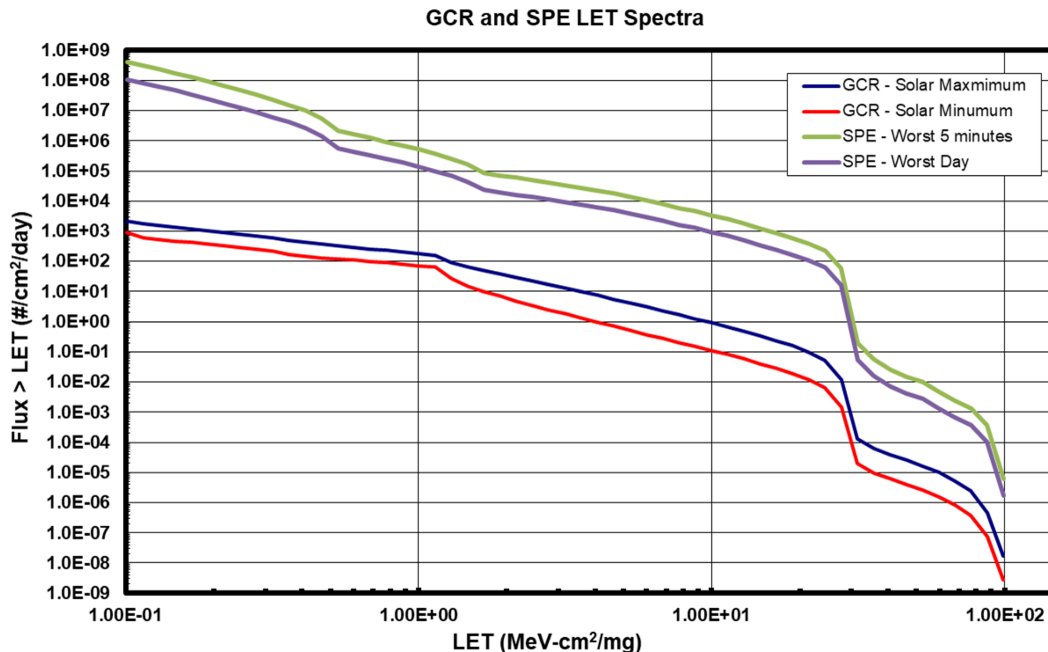

Figure 6. LET Spectra for the ISS Orbit at Solar Min (black) and Solar Max (red).

Fundamentally, calculating SEE error rates requires calculating the rate at which the radiation environment deposits the minimum amount of energy necessary into a device to produce an SEE.

One common SEE error rate calculation method involves integration assuming an active region of a rectangular parallelepiped which can be done using publicly available CRÈME96. CRÈME96 calculates SEE error rates by integrating the LET spectrum over the chord length distribution for the device's sensitive volume. Sensitive volumes can be defined by either a rectangular parallelepiped (RPP) and a critical charge, or through a Weibull distribution of SEE cross-sections; in either case, sensitive volumes are generally experimentally derived. This methodology is useful typically only when device response is well understood and characterized, typically via testing.

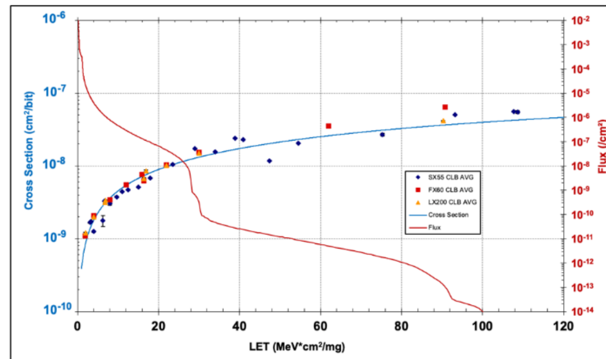

$$Rate = \int \frac{dflux(LET, \theta)}{dLET} \cdot \sigma(LET, \theta)\, d\theta\, dLET$$

environment

device response

Figure 21. Calculating Single Event Rates

Alternative methods for rate calculations exist that are built from empirical data to estimate bounds of upsets for a given environment condition, such as SEE Figure of Merit (FOM). The FOM also uses the Weibull distributions of SEE cross-sections, and is defined:

$$FOM = \frac{\theta_{HL}}{L_{0.25}^2}\left[\frac{\left(MeV \cdot \frac{cm^2}{mg}\right)^2}{cm^2}\right]$$

where is the limiting heavy ion cross-section at large LETs, and is the LET at 25% of the limiting cross-section. if the heavy ion cross-section has been fit to a cumulative Weibull distribution, can be calculated using the Weibull parameters (threshold LET), (width), and (shape parameter):

$$L_{0.25} = L_0 + w \times 0.288^{\frac{1}{s}}.$$

The SEE rate can then be calculated from the FOM by:

$$R = C \times FOM$$

where is the SEE error rate and is an orbit specific rate coefficient.

FOM calculations can be useful for making an initial determination as to potential likelihood of failure. For instance, a calculation may reveal of a SEFI to be less than once per 1,000 years, therefore further consideration may not be required as to part susceptibility. However, FOM is not always accurate for rate-calculations of low-Z particles and should be used with some precaution.

Both methods for calculating SEE error rates result is an error rate of SEEs per unit time, which can be used to calculate the probability of SEEs occurring over a particular time period.

For additional insights and guidance, see case studies digitally linked here.

4.9.6 Likelihood of Radiation Induced Failure Summary

When screening, mitigation, or system-level masking are not sufficient, analysis and/or testing are required to determine the likelihood of failure. For any radiation likelihood, no matter the physical mechanism, the determination must be done for the specific mission environment, application, and lifetime.

Cumulative Effects

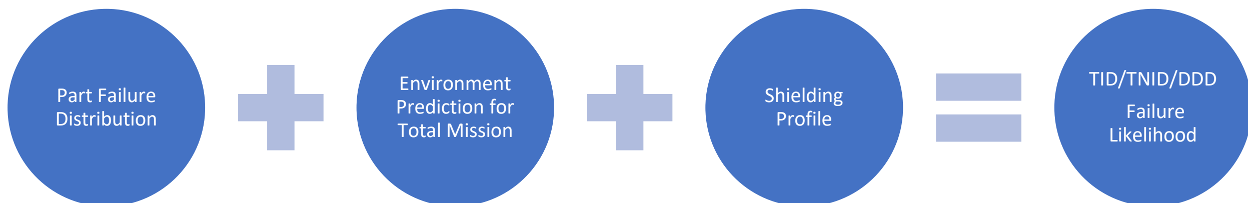

Figure 7. Determination of TID/TNID/DDD Failure Likelihood

Cumulative effects are permanent changes in the device operation. Figure 22 shows the basic information necessary to calculate the likelihood or probability of failure for a given part in each application on a spaceflight mission. See also the figure 16 on cumulative failure modes. Crudely put,

$$P_{fail} = \int \text{probability of mission dose} \cdot \text{ part failure distribution}$$

Cold sparing or redundancy is not an effective mitigation because cumulative effects can accrue even in the off state for semiconductor devices. The only system masking would be tolerance to degradation or drift of parametric values, or some sort of diverse redundancy that provides functional backup through a different design performing the same function containing different semiconductor parts.

Destructive Single Event Effects

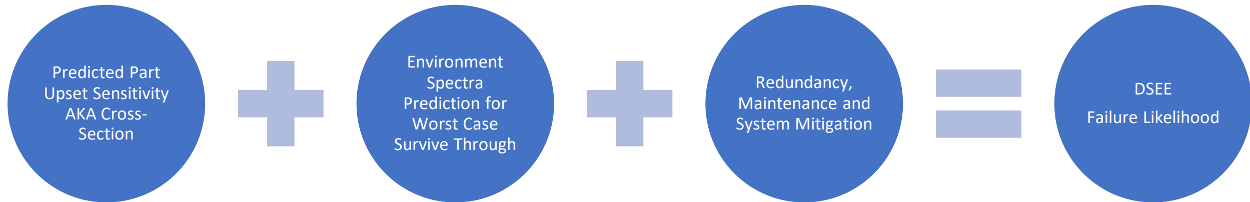

Figure 23. Determination of DSEE Failure Likelihood

Destructive SEE are irreversible failures at the part level. Figure 23 shows the basic information necessary to determine a likelihood of permanent failure for a given part. A device's application cross-section and the worst-case environment that it will have to operate in can be used to calculate a predicted likelihood for a given mission phase, but the failure likelihood must also take into account nominal operations and availability required for the entire mission. The overall failure likelihood is the combined failure rate for every device in each application in each operational mode for the mission duration. Crudely put,

$$P_{fail} = \int \text{predicted rate} \cdot \text{ duration}$$

Systems may use mitigation, maintenance, or redundancy (cold sparing) in some instances to reduce likelihoods. The ability of DSEE to propagate are determined in a criticality analysis.

Non-Destructive Single Event Effects

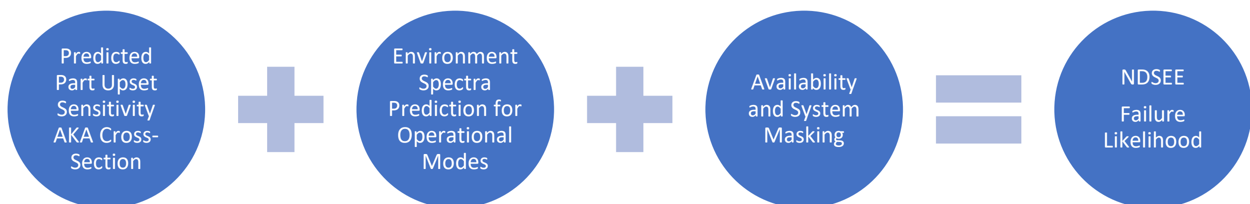

Figure 8. Determination of NDSEE Failure Likelihood

Non-destructive SEE can lead to failure if they happen so frequently that operation is overwhelmed, or if they produce a device output that exceed limitations of downstream devices. Figure 24 shows the basic information necessary to determine a likelihood of DSEE failures. A rate calculation is done for a given part in each application, this uses the part's cross-section and the environments predicted spectra of particle energies. If the effects can propagate and are too frequent such that availability is impacted; system masking such as error detection and correction are overwhelmed; or requirements are unable to be met; a failure mode and its likelihood are determined from the rate for duration of operation in that critical mode. Crudely put -

$$P_{fail} = \int \text{predicted rate} \cdot \text{ duration}$$

The ability for N to propagate are assessed through a criticality analysis.

For additional insights and guidance, see case studies digitally linked here.

Formulating Comprehensive Results from Individual Pof Findings

5.1 Aggregation Approach

Each PoF analysis or method will result in deriving or updating the failure rate or likelihood for each failure mechanism or mode. Reliability analysts will need to combine individual findings to formulate a comprehensive result that fully captures all failure susceptibilities of a system or scenario of interest unless the likelihood of only one failure mechanism is the result of interest. This may be an iterative process or singular event depending on the quantity of findings and their relationships.

In developing a comprehensive result, aggregated likelihood of failure, the relationship between each of the individual findings must be determined to avoid over or underestimating failure probabilities. The relationship between any two or more findings can be described in one of three ways, and each has its own precepts for accurate aggregation:

1. Inclusive - Findings are considered inclusive when any likelihood covers the same failure scenarios or is part of another likelihood or a working aggregated likelihood (figure 25.A).
2. Complementary - The findings are considered independent/disjointed when two or more likelihoods (individual or aggregated) do not cover the same failure scenarios (figure 25.B), making them independent of each other.
3. Interrelated – Findings where likelihoods have intersecting failure scenarios (figure 25.C) are considered interrelated.

Each of these relationship states is supported by specific reliability and statistical techniques, such as fault trees, Bayesian networks, or conditional probability (see figure 26), which may be applied once or multiple times until all applicable likelihoods are combined or considered. Underlying analyses will dictate the amount of aggregation needed on a case-by-case basis. If

individual findings are not aggregated properly, the likelihood of any one or more mechanisms may be omitted or applied repeatedly causing erroneous results.

For additional insights and guidance, see case studies digitally linked here.

5.2 Inclusive Relationship Finding Aggregation

If likelihoods are inclusive, then the failure distributions or PoF finding estimations are for the same failure contributors and there will be dominate and nondominant contributions (figure 25.A). If this is not the case then this type of aggregation would not be appropriate, since picking only one contributor's failure rate would mean omitting the others and could create an underestimated failure probability prediction. For example, if a handbook parts count derived rate (1.33 failures per million hours 1.33 x 10^{-6} failures per hour (the blue circle in 25.A.2)) is known to include the failure contributions of thermal (Section 4.3) and electrical stresses (Section 4.6), it may be more accurate to assume that likelihood than a thermal-only likelihood PoF finding (the hypothetical yellow circle in 25.A.2). Conversely, if the nondominant likelihood does include all the failure contributors of the dominant one, or is a working aggregated finding, then the analyst can use performance experiences to determine which is most indicative the actual failure potential (figure 25.A.1 or 25A.2 or 25A.3) and use that as the comprehensive result.

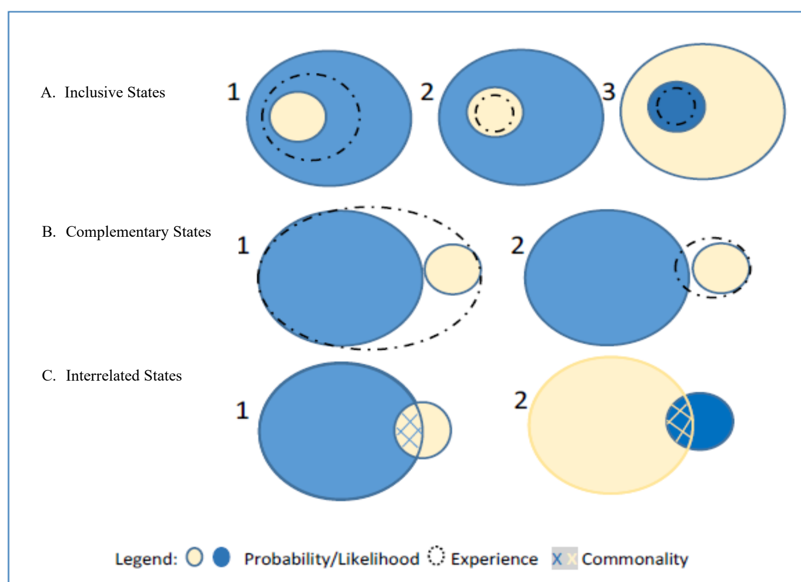

Figure 25. Potential Probability Relationship States for Aggregating Findings

(Aggregation of only two findings is shown in this figure, but in an actual aggregation there may be many more than two findings to aggregate and each combination will have its own one of these relationship states to consider.)

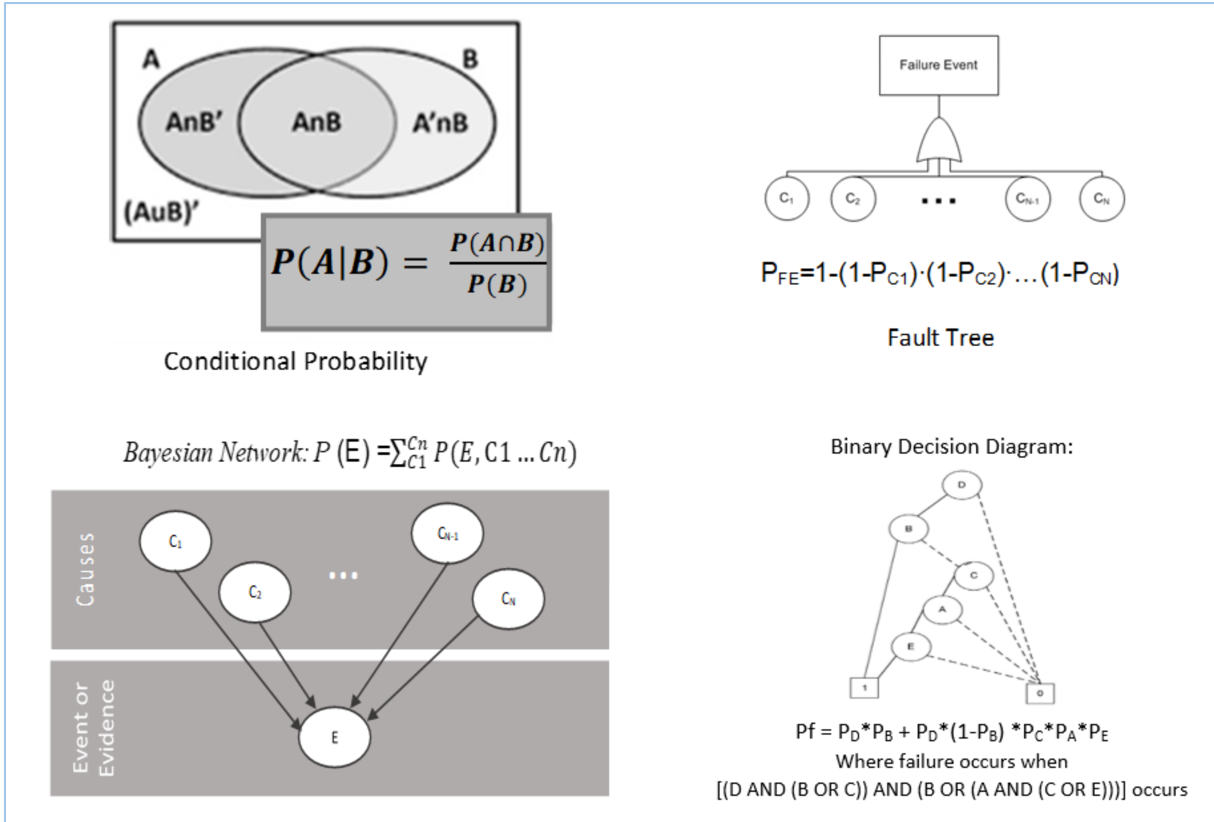

Figure 26. Potential Probability Combination Methods

For example, if a reference or handbook derived parts-count rate (1.33 failures per million hours (1.33 x 10^{-6} failures per hour, the blue circle in 25.A.2) and a Bayesian updated rate (0.395 per million hours (3.95 x 10^{-7} failures per hour, yellow circle in 25.A.2), as described in section 3.2.6, are being considered for aggregation, it is highly likely that they cover the same failure modes. Further, if the analyst knows that usage experience shows a 9.725 x 10^{-8} failures per hour metric (dotted circle in 25.A.2), then the analyst would choose the Bayesian finding since it is more similar to the observed performance. Given that choosing one failure likelihood over another is possibly subjective, it may be beneficial for a reliability analyst to provide to risk-informed decision makers a range of probabilities, with uncertainties, that includes the alternate and the chosen likelihoods for better decision making.

For additional insights and guidance, see case studies digitally linked here.

5.3 Complementary Relationship Finding Aggregation

If the likelihoods are complementary, then the failure distributions or PoF finding estimations must be for different failure contributors or fully independent of each other (figure 25.B). This would be when the probability of a failure given one likelihood is not affected by the probability of another likelihood finding (e.g., P(Finding-A|Finding-B) = P(Finding-A) Under this circumstance, the analyst will need to combine them, via fault trees or Bayesian networks with the appropriate weightings, given experience or engineering judgment, to formulate a complete likelihood estimation [Heard and Rubin-Delanchy, 2017]. Conversely, if there is contribution overlap of some kind or probabilities are affected by each other, then interrelated or inclusive aggregation should be used.

When using the fault tree method to perform a complementary aggregation, it is constructed with the envisioned aggregated result as the top-level event and the independent PoF probability findings as the subordinate failure events combined logically with the OR function (figure 26). The fault tree can then be solved using Boolean algebra (e.g., P(A or B) = P(A) + P(B) – ($P(A_{AND}B)$) or a binary decision diagram (BDD) to compute the aggregate failure likelihood as shown in figure 26 [Márquez, 2008]. Whereas a Bayesian network of independent cause probabilities would be evaluated by multiplying the probabilities of each independent cause initiating the failure event (P(E|C)) with the probability of the cause (C) in existence (P(C)) and the probability of the non-existence causes ($1-P_{c,d,e,f\,...}$) and summing the results of each permutation or

$$P\,(\mathrm{E}) = \sum_{C1}^{Cn} \mathrm{P(E, C1, \ldots Cn)}$$

Where n is the total number of causes including plausible combinations or

$$P\,(\mathrm{E}) = \sum_{i=1}^{n} \mathrm{P(E|Ci)} * \mathrm{P(Ci)} * [1 - \mathrm{P(Ci's\ above\ i)}] * [1 - \mathrm{P(Ci's\ below\ i)}] \text{ or}$$

$$\mathrm{P\,(E)} = \sum_{i=1}^{n} \mathrm{P(E|Ci)} * \mathrm{P(Ci)} * [(1 - \mathrm{P(Ci+1)}) \ldots * (1 - \mathrm{P(Cn)})] * [((1 - \mathrm{P(Ci - (i-1))} * (1 - \mathrm{P(Ci - (i-2))} \ldots (1 - \mathrm{P(Ci-1)})].$$

For example, a system is planning to use a proven and well-known terrestrial component (Ps = 0.8 at the mission duration) in a space application, and it has been determined via radiation susceptibility testing, that the probability of failure from radiation, Pf, equals 0.7. In this case the analyst would be able to assume that the terrestrial and radiation failure mechanisms are independent or disjointed, and would use a fault tree to calculate the probability of failure as:

$$(1-Ps_T) + Pf_R - Pf_{TANDR} = 0.2 + 0.7- (0.7*0.2) = 0.76$$

or a Bayesian network to find:

$$\sum (P(F|T, R) = (P(F|R)*Pf_R *1-Pf_T) + (P(F|T)* Pf_T * 1-Pf_R) +(P(F|(R|T))*(Pf_R *Pf_T)*(1-Pf_{others}))$$
$$\sum (P(F|T, R) = 1*0.7*0.8 + 1*0.2*0.3)+ (1*(0.7*0.2)*1) = 0.76$$

For additional insights and guidance, see case studies digitally linked here.

5.4 Interrelated Relationship Finding Aggregation

Most often, failure distributions or PoF finding estimations will have or can be assumed to have likelihoods that have interrelated or intersecting failure scenarios (figure 25.C). This would be when failure contributors overlap or are dependent on another contributor occurring to occur. This will require the reliability analyst to evaluate and compensate for the contributions of common scenarios to avoid over counting the likelihood of any scenario. This is best done using fault trees, conditional probability, Bayesian networks, or Binary Decision Diagrams (BDD) with appropriate handling of intersecting probabilities (figure 26).

When fault trees are used to combine interrelated PoF probabilities, they are constructed with the envisioned aggregated result as the top-level event and the PoF probability findings as the subordinate events, as described earlier. However, in the interrelated cases these subordinate events or probabilities are combined with AND and OR logic-gates that capture their interdependencies and conditional probabilities (probability of event A occurring given the occurrence of event B or $P(A|B) = P(A_{AND}B)/P(B) = P(A)*P(B)/P(B))$ as needed. The fault tree can then be solved using Boolean algebra (e.g., $P(A \text{ or } B) = P(A) + P(B) – (P(A_{AND}B))$ and $P(A_{AND}B)= P(A)*P(B))$ or by capturing its characteristics in a Bayesian network of causes, as long as the analyst has calculated any conditional probabilities so that each cause-value is unique as shown in figure 22. Alternatively, the systems interdependencies can be modeled with a BDD (using summations of the multiplicative chains of failure scenarios) to compute the aggregate failure likelihood value as shown in figure 26.

For example, if a project is considering a “Use-As-Is (UAI)” decision, a reliability analyst would be looking at a dependent assessment to inform this decision. Both the nominal (reference or derived, (nom)) failure potential (Pf = 0.2, the blue circle in 25.C.1) and the non-conforming failure potential (Pf = 0.12, the yellow circle in 25.C.1) would need to be combined with the commonality or duplicity eliminated. In a Fault Tree this would be captured by a three-parameter-OR $((0.2\text{-}0.024)_{nom} + (0.12\text{-}0.024)_{uai} + (0.024)_{nom.AND.uai} = 0.296)$, or Bayesian network (1*0.2*0.88 + 1*0.2*0.12+ 1*0.12*0.8 = 0.296) or Boolean algebra (0.2 + 0.12 -0.024) can also be used.

For additional insights and guidance, see case studies digitally linked here.

5.5 Aggregation Assistance

Given the complexity of these dependency determinations and, in some cases, the cumbersome summations, it is best to employ statistical modeling tools to ensure an appropriate comprehensive result is attained.

In some cases, multiphysics simulation and analysis tools (See Section 6.1) can assist with the challenge of creating and aggregating PoF results. However, users of such tools need to know if

the tool applies all appropriate failure models based on a comprehensive set of physics processes, as described herein, or just a limited set of these, such as static and dynamic mechanical stress and fatigue only; thermal stresses and fatigue only; or thermal acceleration only [Nikfarjam, 2020].

Based on this knowledge, the analyst will be able to use the tool's results appropriately as a comprehensive likelihood or working-aggregated likelihood that will then need to be further aggregated with other PoF findings, as shown above.

For additional insights and guidance, see case studies digitally linked here.

6. The Evolution of the Physics of Failure

6.1 NASA Path Forward

While the physics underpinnings of the PoF practices are well defined, the methodologies, technology, and supporting infrastructures to determine the likelihood of failure are constantly being refined and advanced. NASA's intention is that this NASA PoF handbook continues to evolve based on community lessons learned and the introduction of new assessment methodologies. Therefore, reliability engineers, physicists, designers, and operations/research teams are asked to provide additions, updates, modifications, and case studies that may extend or enhance the concepts discussed in the handbook. The desire for continued growth in PoF is an indication of a very fruitful and rewarding set of opportunities for new study and future investment.

For additional insights and guidance, see case studies digitally linked here.

6.2 Technology Support

Technology support of PoF is a dynamic and fast-growing field. Ubiquitous and low-cost, high-performance computing resources have revolutionized the ability to use sophisticated and highly accurate physics models. Currently, technology for PoF analysis is limited to statistical analysis and multiphysics simulation tools but can already assist with some of the aggregation methods and challenges presented in section 5. Statistical analysis tools (e.g., R, Weibull++, BlockSim, ITEM ToolKit, Excel, MATLAB, R-DAT, Mathematica. OpenBUGS, BlockSim) are rooted in data analysis and fitting observed physics to mathematical expressions. Multiphysics simulations packages (e.g., COMSOL, MATLAB, Windchill, Ansys Sherlock, Cadence, and Altair) are also rapidly advancing with complex and sophisticated use of Artificial Intelligence (AI) or Machine Learning (ML) techniques. However, current multiphysics tools still generally use a limited set of coupled physics equations and Monte Carlo simulations that give damage accumulation estimates, time-to-failure forecasts, or fatigue life predictions, and statistical tools that still rely on curve fitting.

For additional insights and guidance, see case studies digitally linked here.

6.3 Advanced Technology Infusion

Historically, supervised learning approaches have had the limitations of time-consuming data processes, and non-physics-based extrapolation and error generation have been replaced with a variety of neural network solvers. For example, neural network forward solvers can be supervised based on governing physical laws only and do not require any extrapolated training data [Hennigh, 2021]. The constantly evolving capabilities of High-Performance Computing and technology have now allowed data analysis and empirical fitting to be commoditized with extensive AI-based visualization and data aggregation scripts that operate as simple drop-down menus. For PoF, this could take the form of AI and ML concepts, and real-time data/prognostics monitoring/analytics.

For additional insights and guidance, see case studies digitally linked here.

6.3.1 Artificial Intelligence (AI), Machine Learning (ML)

The fields of AI, ML, and data science have expanded exponentially over the past 10 years to encompass every technical field, from theoretical physics to manufacturing engineering. By way of defining terms, AI is the overarching concept of trying to create intelligent machines that can mimic human thinking processes and behaviors. AI is usually divided into two general areas, Weak AI and Strong AI. The former is an AI that can perform a narrowly defined set of tasks or just one task. The latter is an AI that is capable of applying intelligence to a problem and even showing consciousness [IBM, 2023]. ML on the other hand is usually defined as a subset of AI focusing on training machines to learn from various data sources without specific and explicit software instructions [Wikipedia-MIL, 2023]. ML systems that learn and predict outcomes without manually programming a computer are also known as predictive analytics or statistical learning. These statistical learning techniques can be based on pattern recognition concepts and include supervised and unsupervised learning methods.

AI and ML in a PoF context can be rephrased as Physics-Based Modeling with ML and can be implemented empirically or deterministically or both. Empirically, ML would monitor performance and utilize advanced pattern recognition capabilities to identify new signatures or modes of failure from the experienced physics of system operations. These new failure mode signatures could then be used to prevent failure with enhanced monitoring and contingency action planning. Further, these new modes would each have an observed or predictable occurrence rate that with appropriated statical analyses could be converted to a likelihood of failure for each mode and aggerated with existing likelihood values to develop a new and more accurate system PoF-based failure rate.

Deterministically, this would be physics modeling with ML that begins with previously existing physical theories and related laws. Often these expressions are mathematical approximations that are needed for both clarity of description as well as ease of computation. ML modeling provides a new direction in modeling both physical processes that are not completely described or understood, as well as exploring other areas of incomplete knowledge very effectively. The complementary nature of heritage physics approaches mixed together with rapidly evolving ML

techniques has resulted in a fast and very active area of growing research, both at the scientific and the engineering level. [Willard, 2020]

This mix of approaches is sometimes referred to as the white box (versus black box) approach. The white box approach incorporates the known physics as a fundamental model to produce a casual change in state variable(s) as a function of environmental stress. The black box model is the data-driven model. Modern black box models are usually characterized by high computational complexity with an emphasis on speed and quality of prediction. The combination of the two results in grey box models and represents the final completion of the investigation. PoF predictions would follow this same methodology and could derive an estimate of Remaining Useful Life (RUL) (see 6.4.1) with achievement probabilities that with appropriate statistical analysis could be inferred as a new failure distribution for the RUL-period.

These new and groundbreaking techniques are revolutionizing PoF efforts and provide fertile research opportunities. Strategic investment in the entire AI/ML/Model-Based Engineering/Digital Transformation (DT) ecosystem will form the new generation of reliability analysis tools.

For additional insights and guidance, see case studies digitally linked here.

6.3.2 Data Monitoring/Analytics

As mentioned throughout this handbook, many PoF analyses need data or operational truths to generate meaningful results. However, NASA challenges in conducting Data Analytics for Reliability/PoF applications have largely centered around generating the right data and limited access to that data (i.e., silos, restrictions, schema challenges), lack of data understanding (i.e., dependency on humans to explain schema), insufficient processing power (i.e., cost and access), discovery challenges (i.e., algorithms), and difficulties associated with sharing results as captured by Thomas [Thomas, 2019]. Therefore, NASA is leveraging ever-evolving technology to digitally transform its approach to data. NASA's PoF-related DT focus areas are Data Management (DM), Model Based Anything (MBx), data collaboration, process transformation, and AI/ML infusion. [Diventi, 2022]

Real-time monitoring that generates useable data for failure quantification is now a mainstay of many industries like automobile manufactures. These enterprises are using the data to foster improvements in customer satisfaction, operational/logistics intelligence, preventative maintenance, safety, and data analytics. NASA can do the same, as designs are not just optimized for performance but also future mission analysis. Assuring the right data is generated will take collaboration and potentially the use of prognostic simulation tools, or digital twins. When NASA is successful in acquiring the right data and making it available, data analysts will have much more complete data sets for generating failure/PoF probabilities and other metrics. These massive new data sets will allow for analysis and correlation of performance parameters, well before reaching any predefined failure criterion. This can have a significant impact on the ability to make predictions about individual units, as opposed to the population of units.

Data analytics is the discipline that applies logic and mathematics to data to provide insights. Currently, NASA generally relies on humans to both interpret computer-generated data and organize its contents for other humans to quickly comprehend. This can be seen in the mission-control rooms that support NASA operations. However, NASA has not been taking full advantage of technologies/processes such as standardized machine-to-human reading protocols (e.g., Extensible Mark-up Language – XML) and AI/ML applications to gather information, interpret schema, discover relationships, and generate additional PoF/Reliability data. This will need to change to enable all the advantages of PoF/Reliability analyses, so this area is ripe for additional research and technology development (e.g., ultra-high-performance computational resources).

For additional insights and guidance, see case studies digitally linked here.

6.4 Methodology Innovation Infusion

This handbook is focused on the creation of a likelihood estimate(s) based on physics (experimental/empirical or theoretical/deterministic) via existing methods. However, industry, researchers, and academia are constantly evolving and adapting reliability estimation methods based on new capabilities and alternate data. For PoF, this could take many forms, such as using Remaining Useful Life and the concept of digital twins.

For additional insights and guidance, see case studies digitally linked here.

6.4.1 Remaining Useful Life (RUL)

Remaining Useful Life (RUL) is defined as the length of time a device or system is likely to operate from a defined event or time before it requires repair or replacement. RUL, after the start of deterioration, is graphically described as shown in figure 27 [Okoh, 2014] with the y-axis showing normalized health index (Healthy, Caution, Repair, and Failure) and the x-axis showing time.

The three different approaches, as shown in figure 28, for determining the RUL with their relevant modeling approaches are:

- Run-to-Failure (Similarity Models)
- Known Failure Threshold (Degradation Models)
- Lifetime data w/ or w/o covariates (Survival Models)

These three approaches use different modeling (e.g., model-based, analytical/PoF-based, knowledge-based, and hybrid-based simulation/models) independently or in collaboration with ML and require unique statistical analysis and the existence of large data sets of historical system performance that are a function of reliability/physics stressors. RUL estimates can also be derived by combining these approaches.

Similarity models calculate RUL for a given system based on the known behavior of similar systems under similar stress/physics conditions. This is an empirical approach in which time or

time-frequency values of similar system components are used with Auto-Regressive Moving Average, exponential smoothing, or probabilistic hidden Markov statistics (see figure 29) to generate an RUL and the probability of achieving that life. This method is highly observational-data dependent but may be assisted by AI/ML.

Degradation-model estimates are based on precise mathematical models that integrate the concepts of physics and cumulative damage models to predict time until a failure inducing condition. These models would be that of wear (see section 3.2.2), corrosion (see chemical and electromigration sections 4.8 and 4.2), and deformation/fracture (see structural and creep sections 4.6 and 4.6.3). These models can be empirical or deterministic, depending on test and performance data available, and will give accumulation results. Therefore, a failure threshold must be known to generate an RUL using linear or exponential statistical methods. This RUL with appropriate statistical analysis can then be inferred as a new failure distribution for the RUL-period.

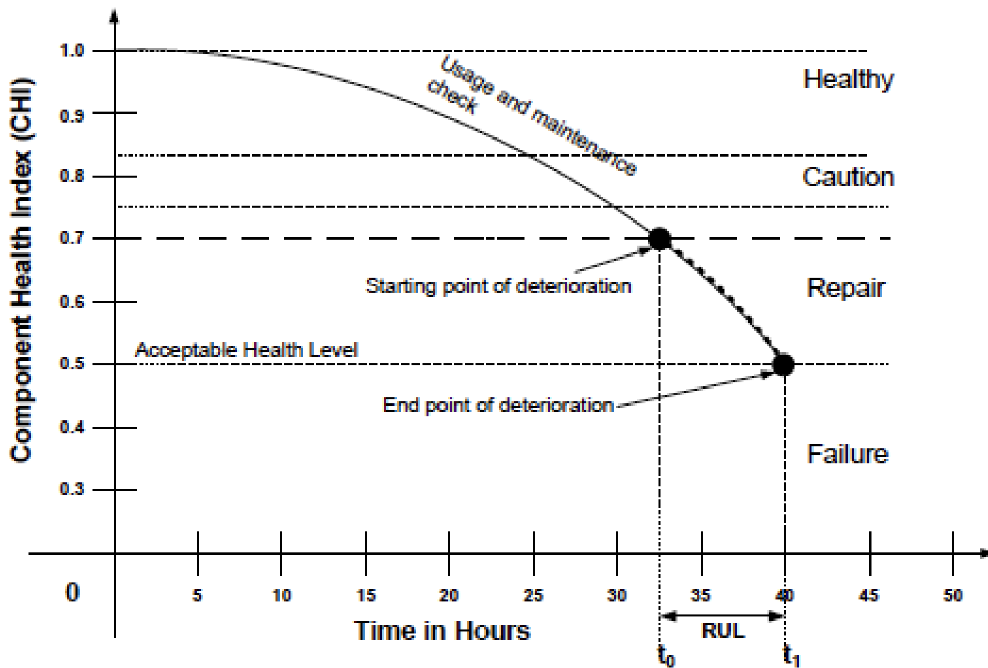

Figure 27. Conceptual Definition of RUL

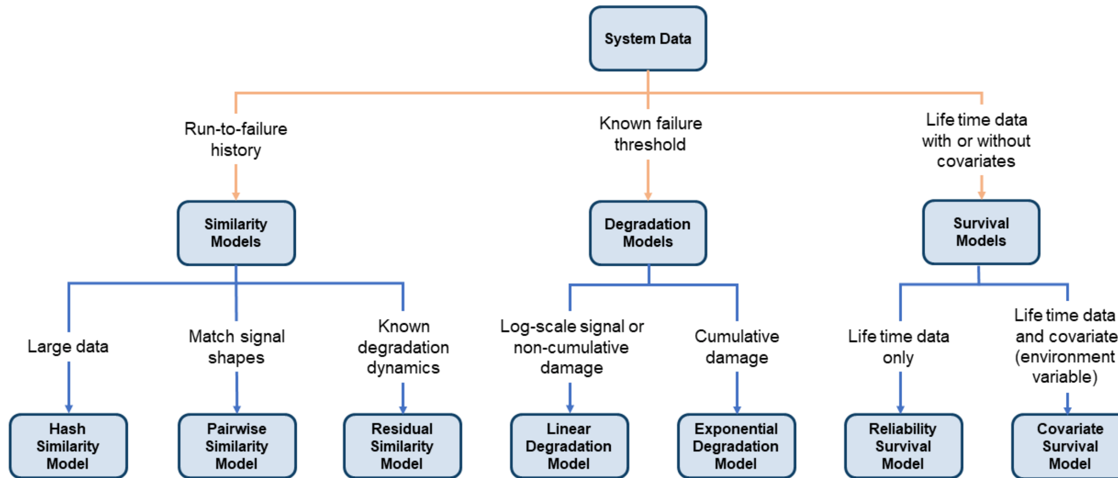

Figure 28. Remaining Useful Life (RUL) systems modeling approaches

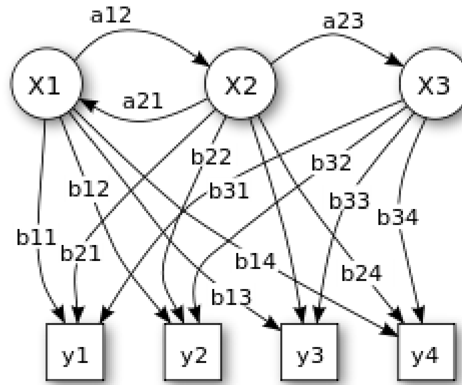

.

Figure 29. Probabilistic parameters of a Hidden Markov

X — states; *y* — possible observations; *a* — state transition probabilities; *b* — output probabilities [W]

Survival models estimate RUL in terms of Mean Time to Failure (MTTF) to RUL-time from the integration of reliability (or the survival of a system beyond the current time (t) to the desired (T) (P(T>t) = 1- F(t)|P(t) = 1-F(t) = S(T>t)) and time-to-event analysis (life expiration with or without covariates). This may require the use of conditional probabilities to factor in the time a system has already been operating, Kaplan-Meier Estimator**,** proportional hazards regression models, and/or Cox Proportional Hazards model to generate a Survival-MTTF (S(T>t)). [Udrescu, 2023] If observed data (e.g., failures and survivals) is used, this may be an empirical analysis or data dependent, but if theoretical physics models are used, then this may be a deterministic analysis and less data dependent. Either way, this MTTF can then be used to infer an RUL failure rate assuming that a constant failure rate (i.e., $\lambda = 1/\text{MTTF}$).

The use of RUL for failure estimation has great potential but is not a common practice and still needs additional research to establish best practices for its use. Therefore, RUL estimation and conversion to failure likelihood is full of fertile research opportunities. For example, State Space Modeling is being researched as way to assist with these efforts. This modeling uses probabilistic

graphical models to describe the dependence between the state variables and the observed measurements. However, great care and research is needed to establish the appropriateness of underlying parameter assumption-making within this approach. [Jianmin, 2011]

For additional insights and guidance, see case studies digitally linked here.

6.4.2 Digital Twin Usage

A digital twin is a digital representation of an intended or actual real-world physical product, system, or process that serves as the effectively indistinguishable digital counterpart of it for practical purposes, for such things as simulation, integration, monitoring, and maintenance. One of the key features of the digital twin is that it is often used in real time and regularly synchronized with the corresponding physical system [Wikipedia-DT, 2023]. Electrical, mechanical, and information systems are able to share and leverage each other's data to constantly improve and understand the final product via AI and ML-assisted physics-based simulations.

Recent literature and NASA studies suggest that creating predictive digital twins can be accomplished by leveraging model-based or interpretable machine learning methods to couple sensor data with physics-based models of the system [Kapteyn, 2020, GSFC, 2019]. These models can be used for senor optimization, failure analysis, safety risks, and more. A library of physics-based models can be used to provide more-representative predictive capabilities. In addition, digital twins can be infused with development-cycle data (e.g., CAD, finite element analysis, life test data, availability), so knowledge is shared across various discipline and mission teams uniformly. This encourages rapid iterations of virtual prototypes that promote common communication platforms across the organization.

These digital twins can also be utilized to virtually simulate in-situ-system conditions by using real-time data ingestion from diagnostic system-level prognostics and on-board sensors. This will enable rapid health evaluation, anomaly investigation, and evolvable monitoring strategies. Alternatively, these same digital twins can be used with simulated data to analyze 'what-if scenarios' and to train operations teams. For example, SpaceX is a well-documented case study of the using digital twins [Carlos, 2021]. In 2022, SpaceX is launching Falcon 9s at the rate of one every 6.4 days. United Launch Alliance, on the other hand, has a launch rate of one every 64 days over the past five years. SpaceX uses digital twins to assist flight controllers with monitoring telemetry, including trajectory, loads, and system-health indicators, and to enable more successful, reliable, and safe SpaceX vehicle operations and development.

Digital twins can evolve, or be trained if AI/ML enabled, with monitoring data and new failure-signatures knowledge to enable analyst-agnostic, accurate, and efficient reliability predictions and system-performance risk identification. Therefore, continued advancement of digital twin capabilities is needed.

For additional insights and guidance, see case studies digitally linked here.

Appendix A. Definitions

Defect – A defect is a characteristic of an item that does not meet specifications. For example, a chip in a paint surface could be a product defect. Defects do not always render an item unusable for its intended purpose.

Defective – A defective item has one or more defects that renders an item unsuitable for its intended use.

Deterministic – Deterministic analysis involves the study of underlying physical processes to predict future behavior.

Displacement Damage Dose (DDD) – the mean energy deposited in a device region by radiation that goes into atomic displacements divided by the mass of the region. One common unit is MeV/g.

Empirical – Empirical analysis studies past data in order to make predictions about future behavior using statistical techniques.

Failure – A failure is an event or condition where a component or system exhibits a fault that causes it to fail to perform its intended function.

Fault – A fault is an event or condition where a component or system does not meet specified behavior. A fault may or may not be a failure.

Linear Energy Transfer (LET) - a measure of the ionizing energy deposited per unit length as an energetic particle travels through a material. The common LET unit is $MeV{\cdot}cm^2/mg$ of material.

Model – A model is an abstract representation of a component, subsystem, or system which allows the study of the item’s processes and responses.

Non-Ionizing Energy Loss (NIEL) - a measure of the energy loss per unit path length due to atomic displacements as a particle traverses a material. The common NIEL unit is $MeV{\cdot}cm^2/g$ of material.

Non-recoverable SEE –single event effects without mitigation or protection schemes.

Physics of Failure – Physics of Failure is an approach to estimating component (and system) lifetime by analyzing the underlying physical mechanisms of failure.

Recoverable SEE – non-destructive single event effects.

Reliability – Reliability is the probability that a component or system will perform its intended function for a specified duration under stated usage and environmental conditions.

Single Event Burnout (SEB) - An event in which a single energetic-particle strike through a high electric field induces a localized high-current state in the device, resulting in catastrophic device

failure or in permanent degradation that is usually characterized by a significant increase in leakage current that exceeds the manufacturer's maximum specification.

Single Event Functional Interrupt (SEFI) - a condition that causes loss of device functionality due to a change induced in a critical portion of a device, commonly a control structure, configuration file, or mode register. It generally requires a device reset or a re-initialization to resume normal device operations, but for many devices, a power cycle is necessary to initiate a full device reset to resume normal operations. A device undergoing a SEFI may simply be non-responsive or may have a sustained high-current state as it is no longer operating as designed.

Single Event Gate Rupture (SEGR) - an event in which a single energetic-particle strike results in a breakdown and subsequent conducting path through the gate oxide of a MOSFET, MOS capacitor, or floating-gate memory. An SEGR is manifested by an increase in gate leakage current and can result in either the permanent degradation or the complete failure of the device.

Single Event Latchup (SEL) - a condition that may cause device failure due to a single event induced high current state associated with the turn-on of a real or parasitic thyristor that creates a short circuit between two power supply rails. A SEL may or may not cause permanent device damage but requires power cycling of the device to resume normal device operations. In addition, SEL that appear recoverable may suffer hidden degradation and must be evaluated for latent damage (device does not fail from the immediate single particle event, but reliability is degraded, and premature failure may occur).

Single Event Transient (SET) – a temporary glitch or deviation from expected operation caused by one particle, with a subsequent return to normal operating behavior.

Single Event Upset (SEU) - a change of state induced by an energetic particle such as a cosmic ray or proton in a device, such as a bit flip in memory. These are "soft" errors in that a reset or rewriting of the device will usually return the device to normal behavior thereafter.

Single Hard Error (SHE) - a SEU that causes a permanent change to the operation of a device. An example is a stuck bit in a memory device.

Single-Bit Upset (SBU) and Multiple Bit Upset (MBU) – a distinction between events that upset a single circuit node (like a memory cell) and those that upset multiple nodes (or memory cells) at once.

Threshold LET (LET_{th}) - the maximum LET at which no SEE is observed.

Total Ionizing Dose (TID) – the mean energy deposited by ionizing radiation in a device region divided by the mass of the region. This is often given in units of rad(Si), where 1 rad(Si) = 100 erg deposited per gram of silicon.

Appendix B: Case Study Chart

Section of PoF Handbook	Case Study Title	Link
3.0 Empirical Methods		
3.1 Empirical Reliability Approach	*TBS - Please consider submitting a case study for inclusion*	
3.2 Statistical Modeling Analysis		
3.2.1 Exponential	*TBS - Please consider submitting a case study for inclusion*	
3.2.2 Weibull	- A General Reliability Model for Ni-BaTiO3-Based Multilayer Ceramic Capacitors	https://ntrs.nasa.gov/api/citations/20140008978/downloads/20140008978.pdf
	- Effect of High-Temperature Storage in Vacuum, Air, and Humid Conditions on Degradation of Gold/Aluminum Wire Bonds in PEMs	https://ntrs.nasa.gov/api/citations/20070016662/downloads/20070016662.pdf
3.2.3 Normal	- Reliability Analysis of Aero-Equipment Components Life Based on Normal Distribution Model	https://ieeexplore.ieee.org/document/8740448
3.2.4 Lognormal	- An Investigation of the Electrical Short Circuit Characteristics of Tin Whiskers	**https://ntrs.nasa.gov/api/citations/20130011768/downloads/20130011768.pdf**
	- New Approach to Total Dose Specification for Spacecraft Electronics	https://ntrs.nasa.gov/api/citations/20170004853/downloads/20170004853.pdf
3.2.5 Binomial	*TBS - Please consider submitting a case study for inclusion*	
3.2.6 Bayesian Statistical Interference	- GOES-T GSFC Magnetometer Reliability Model	https://meta.gsfc.nasa.gov/IntelexLogin/Intelex/Application/SCMSConfigMan/ModernProjLibInventory/DefaultView/SCMSConfigMan_DocumentsSCMSObject/View/a668a2c5-98a6-4d39-82a6-9cb4fa857c9f

Section of Pof Handbook	Case Study Title	Link
3.2.6 Bayesian Statistical Interference	- EOS Aqua Extended Mission Reliability Study Report Revision C -Bayesian Approach for Reliability Assessment of Sunshield Deployment on JWST	https://meta.gsfc.nasa.gov/IntelexLogin/Intelex/Application/SCMSConfigMan/ModernProjLibInventory/Forms/SCMS_DocDetail/View/0d22ecd2-508a-42e7-911b-fb7956609eb5 https://ntrs.nasa.gov/api/citations/20130009067/downloads/20130009067.pdf
3.3 Peck's Temperature-Humidity Relationship Prediction	- An Evaluation of Effects of Molding Compound Properties on the Reliability of Ag Wire Bonded Components	https://ieeexplore.ieee.org/abstract/document/7999992
3.4 Accelerated Performance Analysis	*TBS - Please consider submitting a case study for inclusion*	
3.4.1 Arrhenius	- Degradation of Leakage Currents and Reliability Prediction for Tantalum Capacitors -Improving Reliability of High Power Quasi-CW Laser Diode Arrays Operating in Long Pulse - Damage Propagation Modeling for Aircraft Engine Prognostics - A Thermal Runaway Failure Model for Low-Voltage BME Ceramic Capacitors with Defects	https://ntrs.nasa.gov/citations/20160001192 https://ntrs.nasa.gov/api/citations/20060048507/downloads/20060048507.pdf https://ntrs.nasa.gov/api/citations/20090029214/downloads/20090029214.pdf https://ntrs.nasa.gov/api/citations/20170003045/downloads/20170003045.pdf
3.4.2 Inverse Power	*TBS - Please consider submitting a case study for inclusion*	

Section of PoF Handbook	Case Study Name	Link
3.4.3 Coffin-Manson	- Damage Propagation Modeling for Aircraft Engine Prognostics - X-43A Rudder Spindle Fatigue Life Estimate and Testing	https://ntrs.nasa.gov/api/citations/20090029214/downloads/20090029214.pdf https://ntrs.nasa.gov/api/citations/20050136675/downloads/20050136675.pdf
3.4.4 Zhurkov Equation	*TBS - Please consider submitting a case study for inclusion*	
3.4.5 Palmgren	- Analysis and Life Testing for Design of Cryogenic Bearing Assemblies on the James Webb Space Telescope Optical Telescope Element	https://www.researchgate.net/publication/267595987_Analysis_and_Life_Testing_for_Design_of_Cryogenic_Bearing_Assemblies_on_the_James_Webb_Space_Telescope_Optical_Telescope_Element
3.4.6 Eyring Modeling	- Damage Propagation Modeling for Aircraft Engine Prognostics	https://ntrs.nasa.gov/api/citations/20090029214/downloads/20090029214.pdf
4.0 Deterministic Methods		
4.1 What Are Deterministic Methods?	*TBS - Please consider submitting a case study for inclusion*	
4.2 Electromigration in Electrical and Electronic Components	*TBS - Please consider submitting a case study for inclusion*	
4.2.1 Metals	*TBS - Please consider submitting a case study for inclusion*	
4.2.2 Migration	*TBS - Please consider submitting a case study for inclusion*	
4.2.3 The Fluctuation-Dissipation Theorem	*TBS - Please consider submitting a case study for inclusion*	
4.2.4 Viscous Drag and Brownian Motion	*TBS - Please consider submitting a case study for inclusion*	
4.2.5 Electromigration in Interconnection Traces and Vias in Integrated Circuits	*TBS - Please consider submitting a case study for inclusion*	

Section of PoF Handbook	Case Study Name	Link
4.3 Thermal Physics of Failure	*TBS - Please consider submitting a case study for inclusion*	
4.3.1 Thermal Failure Mechanisms	- Temperature cycling and fatigue in electronics	https://www.researchgate.net/publication/306135282_Temperature_cycling_and_fatigue_in_electronics
4.3.2 Thermally Induced Failure Likelihood	- Thermal barrier coating life prediction model development	https://ntrs.nasa.gov/api/citations/19890003549/downloads/19890003549.pdf
	- A Thermal Runaway Failure Model for Low-Voltage BME Ceramic Capacitors with Defects	https://ntrs.nasa.gov/api/citations/20170003045/downloads/20170003045.pdf
	-Analysis of thermomechanical fatigue of unidirectional titanium metal matrix composites	https://ntrs.nasa.gov/api/citations/19910022363/downloads/19910022363.pdf
	-Comparison of experimental and theoretical thermal fatigue lives for five nickel-base alloys	https://ntrs.nasa.gov/api/citations/19720016935/downloads/19720016935.pdf
4.3.3 Thermal Failure Uncertainties	*TBS - Please consider submitting a case study for inclusion*	
4.4 Fluid (Pipe Flow)	*TBS - Please consider submitting a case study for inclusion*	
4.5 Electromagnetics (Wave Optics, Ray Optics, AC/DC	- Inferring the Probability Distribution of the Electromagnetic Susceptibility of Equipment from a Limited Set of Data	https://ieeexplore.ieee.org/document/8485108

Section of PoF Handbook	Case Study Name	Link
4.5 Electromagnetics (Wave Optics, Ray Optics, AC/DC	- Probability of EMC Failure and Sensitivity Analysis With Regard to Uncertain Variables by Reliability Methods	https://hal.archives-ouvertes.fr/hal-01116322/document
4.6 Structural Analysis Modeling		
4.6.1 Fatigue Analysis	- NESC Bellow Material Compatibility - Model-Based Failure Assessment of Sounding Rocket Mission PWAs - X-43A Rudder Spindle Fatigue Life Estimate and Testing - Micromechanics-Based Progressive Failure Analysis of Composite Laminates Using Different Constituent Failure Theories -Resolution of a Reflector Shroud Fatigue Failure	https://nasa.sharepoint.com/teams/Reliability930/Shared Documents/RM Training Development Area/Physics of Failure Handbook/Version 1/Fatigue Analysis NESC Bellows Material Compatiblity Assessment.pdf https://nasa.sharepoint.com/teams/Reliability930/Shared Documents/RM Training Development Area/Physics of Failure Handbook/Version 1/Case Study MB-Failure Assessment of Rocket Mission PWAs.pdf https://ntrs.nasa.gov/api/citations/20050136675/downloads/20050136675.pdf https://aims.asu.edu/wp-content/uploads/2019/07/Micromechanics-based-progressive-failure-analysis-of-composite-laminates-using-different-constituent-failure-theories.pdf https://ntrs.nasa.gov/api/citations/20180007283/downloads/20180007283.pdf
4.6.2 Damage Tolerance (Fracture) Analysis	- GEDI RTA Fracture Analysis - Analysis of Space Shuttle Flight Hardware Crack or Crack-Like Defect Data	https://ipdtdms.gsfc.nasa.gov/documentation/index.cfm?id=39474&type=1 https://nasa.sharepoint.com/teams/Reliability930/Shared Documents/RM Training Development Area/Physics of Failure Handbook/Version 1/SSMA-08-005.pdf
4.6.3 Creep	*TBS - Please consider submitting a case study for inclusion*	
4.7 Acoustics	*TBS - Please consider submitting a case study for inclusion*	

Section of PoF Handbook	Case Study Name	Link
4.8 Chemical (Batteries and Fuel Cells, Electrodeposition, Chemical Reactions)	- An Investigation of the Electrical Short Circuit Characteristics of Tin Whiskers -Reliability of Radioisotope Stirling Convertor Linear Alternator	https://ntrs.nasa.gov/api/citations/20130011768/downloads/20130011768.pdf https://ntrs.nasa.gov/api/citations/20060012337/downloads/20060012337.pdf
4.9 Radiation Physics of Failure in Semiconductors		
4.9.1 Total Ionizing Dose	-Statistical Methods for Large Flight Lots and Ultra-high Reliability Applications	https://ntrs.nasa.gov/api/citations/20050210085/downloads/20050210085.pdf
4.9.2 Total Non-Ionizing Dose/Displacement Damage Dose	-New Approach to Total Dose Specification for Spacecraft Electronics	https://ntrs.nasa.gov/api/citations/20170004853/downloads/20170004853.pdf
4.9.3 Single Event Effects	- Single-Event Transient Case Study for System Level Radiation Effects Analysis	https://ntrs.nasa.gov/citations/20210010826
4.9.4 Analysing Radiation-Induced Failure Modes	*TBS - Please consider submitting a case study for inclusion*	
4.9.5 Instantaneous Radiation Failures (Single Event Effects)	*TBS - Please consider submitting a case study for inclusion*	
4.9.6 Likelihood of Radiation Induced Failure Summary	*TBS - Please consider submitting a case study for inclusion*	
5.0 Formulating Comprehensive Results From Individual PoF Findings		
5.1 Aggregation Approach	*TBS - Please consider submitting a case study for inclusion*	
5.2. Inclusive Relationship Finding Aggregation	*TBS - Please consider submitting a case study for inclusion*	

Section of PoF Handbook	Case Study Name	Title
5.3. Complementary Relationship Finding Aggregation	*TBS - Please consider submitting a case study for inclusion*	
5.4 Interrelated Relationship Finding Aggregation	*TBS - Please consider submitting a case study for inclusion*	
5.5 Aggregation Assistance	*TBS - Please consider submitting a case study for inclusion*	
6.0 The Evolution of the Physics of Failure		
6.1 NASA Path Forward	*TBS - Please consider submitting a case study for inclusion*	
6.2 Technology Support	*TBS - Please consider submitting a case study for inclusion*	
6.3 Advanced Technology Infusion		
6.3.1 Artificial Intelligence (AI), Machine Learning (ML)	*TBS - Please consider submitting a case study for inclusion*	
6.3.2 Data Monitoring/ Analytics	*TBS - Please consider submitting a case study for inclusion*	
6.4 Methodology Innovation Infusion		
6.4.1 Remaining Useful Life (RUL)	*TBS - Please consider submitting a case study for inclusion*	
6.4.2 Digital Twin Usage	*TBS - Please consider submitting a case study for inclusion*	https://ntrs.nasa.gov/api/citations/20170007965/downloads/20170007965.pdf

Appendix C. References

Arrhenius, S. (1903). Development of the theory of electrolytic dissociation. Nobel Lecture.

ASTM (2018). Standard Guide for the Measurement of Single Event Phenomena (SEP) Induced by Heavy Ion Irradiation of Semiconductor Devices, (ASTM-F1192).

ASTM (2019). Standard Test Method for Strain-Controlled Fatigue Testing (ASTM-E606).

ASTM (2019). Test Method for Measurement of Initiation Toughness on Surface Cracks Under Tension and Bending (ASTM-E2899).

ASTM (2020). Standard Test Method for Measurement of Fracture Toughness (ASTM-E1820).

ASTM (2021). Standard Practice for Conducting Force Controlled Constant Amplitude Axial Fatigue Tests of Metallic Materials. Accessed March 30 2023. https://www.astm.org/e0466-15.html

Battelle Memorial Institute (2020). Metallic Materials Properties Development and Standardization (MMPDS-15).

Carlos, Juan (2021). "SpaceX: Enabling Space Exploration through Data and Analytics," Accessed March 30 2023. https://d3.harvard.edu/platform-digit/submission/spacex-enabling-space-exploration-through-data-and-analytics/.

Clyde, M., et al. (2021). Bayesian Inference. An Introduction to Bayesian Thinking, A Companion to the Statistics with R Course. Coursera.

Coffin, L. F. (1954). The Problem of Thermal Stress Fatigue in Austenitic Steels. Special Technical Publication, American Society for Testing and Materials: 31.

Collins, J. A. (1981). Failure of Materials in Mechanical Design: Analysis Prediction Prevention. New York, John Wiley & Sons.

Collins, J. A., et al. (2010). Mechanical Design of Machine Elements and Machines, 2nd Edition. New York, John Wiley & Sons.

Cooper, S. (1988). General Fracture Control Plan for Payloads Using the STS, NASA.

Defense, U. S. D. o. (1991). Reliability Prediction of Electronic Equipment, MIL-HDBK-217F.

Delsero Engineering Solutions (2015). Accessed March 29 2023. https://www.desolutions.com/blog/2014/10/temperature-cycling-testing-coffin-manson-equation/.

Dezfuli, H., et al. (2009). Bayesian Inference for NASA Probabilistic Risk and Reliability Analysis

DiVenti, A. and Sood, B., Kalia, P. and Sheldon, D. "Infusing Big Data as part of a NEW Physics of Failure (PoF) Framework," 2022 Annual Reliability and Maintainability Symposium (RAMS), Tucson, AZ, USA, 2022, pp. 1-7, doi: 10.1109/RAMS51457.2022.9893984. (https://ieeexplore.ieee.org/document/9893984).

Einstein, A. (1905). Eine Neue Bestimmung der Moleküldimensionen. Bern, Universität Zürich. Ph.D.

ESCIES (European Space Components Information Exchange System). (2014). Single Event Effects Test Method and Guidelines. ESCIES. Accessed March 30 2023. http://escies.org/escc-specs/published/25100.pdf

Eyring, H. (1935). "The Activated Complex in Chemical Reactions." Journal of Chemical Physics 3(2): 107-115.

Feinberg, A. A. and Windom, A. (1996). "Connecting Parametric Aging to Catastrophic Failure Through Thermodynamics." IEEE Transactions on Reliability 45(1).

Feynman, R. P. (1963). The Feynman Lectures on Physics, Addison-Wesley.

Fischer, K., et al. (2016). New Approaches for Reliability Assessment of Mechanical Systems and Parts (Part 1 - Methodology). 14th European Conference on Spacecraft Structures, Materials and Environmental Testing.

Frenkel, J. (1946). Kinetic Theory of Liquids, Oxford University Press.

Glenn., S. "Jeffreys Prior / Jeffreys Rule Prior: Simple Definition." Accessed February 16 2021, from https://www.statisticshowto.com/jeffreys-prior/.

Heard, N.A., P. R.-D. (2018). "Choosing between methods of combining p -values." Biometrica 105(1).

Heard, N.A. ,P. R.-D. (2018). "Choosing between methods of combining p-values." Biometrica 105(1): 239-246.

Hennigh, Oliver, et al. "NVIDIA SimNet™: An AI-accelerated multi-physics simulation framework." *International Conference on Computational Science*. Springer, Cham, 2021.

Hillman, C., et al. (2020). "Prediction Fatigue of Solder Joints Subjected to High Number of Power Cycles." Accessed July 17 2020. https://www.dfrsolutions.com/predicting-fatigue-of-solder-joints.

Hodson, R. F., et al. (2021). Avionics Radiation Hardness Assurance (RHA) Guidelines, NASA.

IBM, “What Is Strong AI?” Accessed Feb 2023. https://www.ibm.com/cloud/learn/strong-ai#:~:text=Weak%20AI%2C%20also%20known%20as,to%20solve%20for%20new%20problems.

Jianmin, Zhao and Tianle, Feng. "Remaining useful life prediction based on nonlinear state space model." 2011 Prognostics and System Health Management Conference, Shenzhen, 2011, pp. 1-5, doi: 10.1109/PHM.2011.5939528. https://ieeexplore.ieee.org/document/5939528.

JEDEC (2010). JEDEC JEP 122F, Failure Mechanisms and Models for Semiconductor Devices. Accessed March 30 2023.https://www.jedec.org/standards-documents/docs/jep-122e.

JEDEC (2013). Test Standard for the Measurement of Proton Radiation Single Event Effects in Electronic Devices. Accessed March 30 2023.https://www.jedec.org/standards-documents/docs/jesd234.

JEDEC (2017). Test Procedure for the Management of Single-event Effects in Semiconductor Devices from Heavy Ion Irradiation. Accessed March 30 2023. https://www.jedec.org/standards-documents/docs/jesd-57.

Kapteyn, M. and Willcox, K. (2020). “From Physics-Based Models to Predictive Digital Twins via Interpretable Machine Learning,” https://arxiv.org/pdf/2004.11356.

Ladbury, R. (2017). Strategies for SEE Hardness Assurance: From Buy-It-And-Fly-It to Bullet Proof. 2017 IEEE Nuclear and Space Radiation Effects Conference (NSREC).

Lienig, J. and Thiele, M. (2018). Fundamentals of Electromigration-Aware Integrated Circuit Design. Cham, Switzerland, Springer.

Lindsey, N.J., Alimardani, M., Gallo, L.D. (2019). “Reliability Analysis of Complex NASA Systems with Model-Based Engineering” (NASA-TM-20200000582)" GSFC Risk & Reliability Branch, Greenbelt, MD, USA.

Manson, S. S. (1953). Behavior of materials under conditions of thermal stress. Heat Transfer Symposium, Ann Arbor, Michigan.

Márquez, Fausto and García, Pedro (2008). "Binary Decision Diagrams applied to Fault Tree Analysis," 2008 4th IET International Conference on Railway Condition Monitoring, Derby, 2008, pp. 1-5, doi: 10.1049/ic:20080314.

Matic, Z. and Sruk, V. (2008). The Physics-of-Failure approach in reliability engineering. IEEE International Conference on Information Technology Interfaces.

Meeker, W. Q. and Escobar, L.A. (1998). "Pitfalls of accelerated testing." IEEE Transactions on Reliability 47(2): 114 - 118.

Miner, M. A. (1945). "Cumulative damage in fatigue." Journal of Applied Mechanics 12: 149-164.
Miner provided a modern formalism and discussion of Palmgren's work and updated to include new material results.

M. Kapteyn, K. Willcox, "From Physics-Based Models to Predictive Digital Twins via Interpretable Machine Learning", https://arxiv.org/pdf/2004.11356

Modarres, M., et al. (2017). Probabilistic Physics of Failure Approach to Reliability, Scrivener Publishing.

NASA (2004). Risk Classification for NASA Payloads.

NASA (2012). NASA Space Flight Program and Project Management Requirements (Updated w/Change 18), NASA.

NASA (2019). NASA-STD-5009, Nondestructive Evaluation Requirements for Fracture-Critical Metallic Components.

Nikfarjam, M. (2020). Simulation Based Reliability Assessment of Printed Circuit Boards, Goddard Space Flight Center/MEI Company.

Norris, K. C. and A. H. Landzberg (1969). "Reliability of Controlled Collapse Interconnections." IBM Journal of Research and Development 13(3): 266-271.

Okoh, C., R. Roy, J. Mehnen, L. Redding. (2014). Overview of Remaining Useful Life Prediction Techniques in Through-life Engineering Services. 6th Conference on Industrial Product-Service Systems.

Palmgren, A. G. (1924). "Die Lebesdauer von Kugellagern [Life Length of Roller Bearings]." Zeitschrift des Vereines Deutscher Ingenieure 68(14): 339-341.

Peck, D. S. (1986). Comprehensive Model for Humidity Testing Correlation. 24th International Reliability Physics Symposium.

Petersen, E. (2011). Single Event Effects in Aerospace, Wiley.

Poivey, C. (2017). Total Ionizing and Non-Ionizing Dose Radiation Hardness Assurance. Nuclear and Space Radiation Effects Conference Short Course. New Orleans, LA.

Reliability Analytics Toolkit. Accessed March 29 2023. https://reliabilityanalyticstoolkit.appspot.com/binomial_probability_of_success.

Sachin Date (2021). "Time Series Analysis, Regression, and Forecasting," Accessed February 2023. https://timeseriesreasoning.com/contents/survival-analysis/.

Schenkelberg, F. (2020). "Introduction to Physics of Failure Models." Accessed July 17 2020. https://accendoreliability.com/introduction-physics-of-failure-models/.

Shigley, J. E. and C. R. Mischke (1989). Mechanical Engineering Design, 5th Edition. New York, McGraw-Hill Co.

Thomas, Brian et al. (2019). "Infrastructural Components to Enable AI and Machine Learning at NASA."

Tobias, P. A. and D. C. Trindade (1995). Applied Reliability, Second Edition. New York, Chapman & Hall/CRC.

Udrescu (2020). "Silviu-Marian Udrescu and Max Tegmark, "AI Feynman: A physics-inspired method for symbolic regression," Science Advances, Vol. 6, No. 16, 6, DOI: 10.1126/sciadv.aay2631, https://advances.sciencemag.org/content/6/16/eaay2631.

Varde, P. (2010). Physics-of-failure based approach for predicting life and reliability of electronics components. BARC Newsletter. 313: 313.

V. Vasudevan and Fan, Xuejun. (2008). "An acceleration model for lead-free (SAC) solder joint reliability under thermal cycling," 58th Electronic Components and Technology Conference, Lake Buena Vista, FL, USA, 2008, pp. 139-145, doi: 10.1109/ECTC.2008.4549960.

White, Bernstein, "National Aeronautics and Space Administration Microelectronics Reliability: Physics-of-Failure Based Modeling and Lifetime Evaluation." https://nepp.nasa.gov/files/16365/08_102_4_%20JPL_White.pdf.

Wikipedia. Accessed February 2023. https://en.wikipedia.org/wiki/Digital_twin.

Wikipedia-HM. Accessed February 2023. https://en.wikipedia.org/wiki/Hidden_Markov_model, https://upload.wikimedia.org/wikipedia/commons/8/8a/HiddenMarkovModel.svg.

Wikipedia. Accessed February 2023. https://en.wikipedia.org/wiki/Machine_learning.

Willard, J., et al. (2020). "Integrating Physics-Based Modeling With Machine Learning: A Survey."

Young, W. C., Roark, R. J., & Budynas, R. G. (2002). "Roark's Formulas for Stress and Strain." McGraw-Hill Europe.

Zhu, M. and A. Y. Lu (2004). "The Counter-intuitive Non-informative Prior for the Bernoulli Family." Journal of Statistics Education 12(2).

Zhurkov, S. N. (1965). "Kinetic Concept of the Strength of Solids." International Journal of Fracture Mechanics 1(4).

Appendix D. Acronyms

AC	critical crack size
ADC	Analog-Digital Converter
AI	Artificial Intelligence
AND	logical AND
ASET	analog single-event transient
BARC	Bhabha Atomic Research Centre
BEOL	Back End of Line
BJT	bipolar junction transistor
CAD	Computer Aided Design
CCD	Charge Coupled Device
CDF	cumulative density function
C&DH	command and data handling
CIS	CMOS image sensors
CMOS	complementary metal oxide semiconductor
CPU	central processing unit
CRÈME96	Cosmic Ray Effects on Micro-Electronics (software)
CTE	charge transfer efficiency
DC	direct current
DDD	displacement damage dose
DRAM	dynamic random-access memory
DSEE	destructive single event effects
DSET	digital single-event transient
EDAC	error detection and correction
EEE	electrical, electronic, and electromechanical
ELDRS	enhanced low dose-rate sensitivity
ESCC	european space components coordination
FDIR	fault-detection-isolation-and-recovery
FMECA	Failure Modes, Effects, and Criticality Analysis
FOM	figure of merit
FPGA	Field Programmable Gate Array
FS	factor of safety
GCR	galactic cosmic rays
GEDI	Global Ecosystem Dynamics Investigation
GEO	geosynchronous
GNC	Guideance Navigation and Control
GOES	Geostationary Operational Environmental Satellite
GSFC	Goddard Space Flight Center
HDBK	handbook
HNC	hardness noncritical

HQ	Headquarters
IBM	International Business Machines
IC	integrated circuit
IEEE	Institute of Electrical and Electronics Engineers
ISS	International Space Station
JFET	junction gate field effect transistor
JPL	Jet Propulsion Laboratory
JSC	Johnson Space Center
LET	linear energy transfer
MATLAB	MATrix LABoratory
MBU	multiple-bit upset
MCU	multiple-cell upset
MEI	Millennium Engineering and Integration
MIL	military
ML	machine learning
MLCC	multi-layer ceramic capacitor
MMPDS	Metallic Materials Properties Development and Standardization
MODIS	Moderate Resolution Imaging Spectroradiometer
MOS	metal oxide semiconductor
MOSFET	metal oxide semiconductor field effect transistor
MTTF	mean time to failure
NDSEE	non-destructive single event effects
NEPAG	NASA Electronic Parts Assurance Group
NESC	NASA Engineering Safety Center
NIEL	non-ionizing energy loss
NMOS	N-type metal oxide semiconductor
NPR	NASA Procdural Requirements
NSREC	Nuclear and Space Radiation Effects Conference
NTSP	NASA Technical Standards Program
OR	logical OR
OSMA	Office of Safety and Mission Assurance
PDE	partial differential equations
PDF	probability density function
PIXL	Planetary Instrument for X-ray Lithochemistry
PKA	primary knock-on atom
PMAD	Radiation-Hardened CubeSat Power Management & Distribution
PWA	printed wiring assemblies
PWM	pulse-width modulator
RDM	radiation design margin
RH	relative humidity
RHA	radiation hardness assurance

RPP	rectangular parallelepiped
RTA	Receiver Telescope Assembly
RUL	remaining useful life
SBU	single-bit upset
SEB	single-event burnout
SEDR	single-event dielectric rupture
SEE	single-event effect
SEECA	single-event effect criticality analysis
SEFI	single-event functional interrupt
SEGR	single-event gate rupture
SEL	single-event latchup
SEP	solar energetic particles
SET	single-event transient
SEU	single-event upset
SN	stress life curve
SRAM	static random-access memory
STD	standard
STS	Space Transportation System
TBD	to be determined
TID	total ionizing dose
TNID	total non-ionizing dose
TST	transition state theory
UAI	use as is